



# DIPLOMARBEIT

Titel der Diplomarbeit

Plectin's role in cytoskeletal remodelling in endothelial cells

angestrebter akademischer Grad

Magistra der Naturwissenschaften (Mag. rer.nat.)

Verfasserin / Verfasser:	Daniela Halak
Matrikel-Nummer:	0201552
Studienrichtung (lt. Studienblatt):	Molekulare Biologie Diplomstudium A490
Betreuerin / Betreuer:	Prof. Dr. Gerhard Wiche
Wien, am Feb. 27, 08	

*Meinen Eltern*

## Danksagung

Die folgende Diplomarbeit wurde im Zuge meiner Arbeit am Institut für molekulare Zellbiologie an der Universität Wien verfasst. Ich möchte mich bei Herrn Univ. Prof. Dr. Gerhard Wiche für die Bereitstellung eines Arbeitsplatzes, die interessante Themenstellung und die freundliche Unterstützung bedanken.

Besonderer Dank gilt meiner Betreuerin Dr. Mag. Selma Osmanagic-Myers, die mich an ihrem Projekt teilhaben ließ. Danke für die ständige Diskussionsbereitschaft, freundschaftliche Betreuung und die Durchsicht dieser Arbeit.

Zudem möchte ich mich bei meinen Kollegen, die mir nie ihre Hilfe verweigert haben, für die nette und anregende Arbeitsatmosphäre bedanken.

Mein aufrichtiger Dank gilt meinen Eltern, ohne die mein Studium nicht möglich gewesen wäre. Ihr hattet immer Vertrauen in meine Berufswahl und habt mich in meinen Entscheidungen bestärkt. Danke für euren Zuspruch und euer Verständnis, besonders am Beginn meines Studienlebens und natürlich auch für die großzügige finanzielle Unterstützung.

Besonders möchte ich mich bei meinen Freunden und bei meinem Bruder Johannes Halak, die mir alle mit viel Motivation zur Seite gestanden sind, für die nötige Ablenkung und die aufbauenden Worte bedanken.

## Summary

Plectin, a multi-domain protein of extraordinary large size, is known to connect cytoskeletal filament systems. Furthermore, plectin is supposed to be a scaffolding platform for signalling molecules. In this thesis plectin's eventual role in regulating endothelial cell (EC) function was investigated.

Two different endothelial cell lines were used for analysis. Briefly, cells derived from kidneys and lungs of plectin<sup>+/+</sup> and plectin<sup>-/-</sup> mice were immortalized by polyoma middle T infection. The middle T antigen causes cell proliferation and specifically ECs gain proliferation advantage over other cells (Williams et al., 1988). Thorough characterization of these cell lines revealed that EC markers are expressed in both plectin<sup>+/+</sup> and plectin<sup>-/-</sup> ECs, although the total amounts of eNOS, caveolin and VE-cadherin are reduced in plectin<sup>-/-</sup> ECs. Data obtained from cell fractionation experiments showed that caveolin, eNOS and VE-cadherin are increased in membrane fractions of plectin<sup>-/-</sup> cells compared plectin<sup>+/+</sup> ECs at the expense of the cytoskeleton fractions.

Measurement of extracellular nitric oxide (NO) demonstrated that plectin<sup>-/-</sup> ECs produce less NO compared to plectin<sup>+/+</sup> ECs. Moreover, plectin<sup>-/-</sup> cells show reduced levels of total eNOS and reduced activity of eNOS.

Mechanical stimuli like shear stress resulting from blood pressure and flow modulate functions of ECs by activating mechano-sensors on the cell membrane. These in turn activate different signalling pathways modulating the activation state and the expression of different proteins (Chien, 2006). Shear-stressed plectin<sup>+/+</sup> and plectin<sup>-/-</sup> ECs were analysed by immunofluorescence microscopy and immunoblotting. In response to fluid shear stress an upregulation of eNOS and caveolin was observed in both plectin<sup>+/+</sup> and plectin<sup>-/-</sup> ECs, although to a lesser extent in plectin<sup>-/-</sup> cells. Furthermore, shear stress-induced VE-cadherin cluster formation was significantly reduced in plectin<sup>-/-</sup> compared to plectin<sup>+/+</sup> ECs. Based on these data, it is suggested that in ECs plectin plays a major role as a regulator of EC key molecules like eNOS and VE-cadherin. Furthermore, an eventual involvement of plectin in sensing and / or responding to fluid shear stress was observed.

## Zusammenfassung

Plectin ist ein außergewöhnlich großes Protein mit vielen Bindungsdomänen, welches die Cytoskelettfilamentsysteme miteinander verbindet. Weiters stellt Plectin eine Plattform für Signalmoleküle dar. Im Zuge dieser Diplomarbeit wurde die Rolle von Plectin in Endothelzellen näher betrachtet.

Zwei unterschiedliche Endothelzelllinien wurden für die durchgeführten Experimente verwendet. Nieren- und Lungenzellen von wildtyp Plectin<sup>+/+</sup> und knock-out Plectin<sup>-/-</sup> Mäusen wurden mittels Polyoma middle T Infektion immortalisiert. Das middle T Antigen verursacht Zellproliferation und bewirkt einen Wachstumsvorteil von Endothelzellen gegenüber anderen Zelltypen (Williams et al., 1988). Eine genaue Charakterisierung dieser Zelllinien ergab, dass Endothelzell-spezifische Markerproteine in Plectin<sup>+/+</sup> und Plectin<sup>-/-</sup> Zellen exprimiert werden, jedoch wurden reduzierte Mengen von eNOS, Caveolin und VE-Cadherin in Plectin<sup>-/-</sup> Zellen gefunden. Zellfraktionierungen zeigten, dass Caveolin, eNOS und VE-Cadherin in Plectin<sup>-/-</sup> Zellen in der Membranfraktion angereichert sind, während sie in der Cytoskelettfraktion reduziert sind.

Messungen von extrazellulärem Stickstoffoxid (NO) zeigten, dass Plectin<sup>-/-</sup> Endothelzellen weniger NO produzieren als Plectin<sup>+/+</sup> Zellen. Weiters, wurden in Plectin<sup>-/-</sup> Zellen reduzierte Mengen von Gesamt-eNOS und eine verringerte Aktivität von eNOS nachgewiesen.

Mechanische Reize, wie vom Blutfluss oder Blutdruck verursachte Scherkräfte, beeinflussen die Funktionen von Endothelzellen durch das Aktivieren von Mechanosensoren an der Zellmembran. Diese Mechanosensoren wiederum aktivieren verschiedene Signalwege, welche die Aktivierung und die Expression verschiedener Proteine beeinflussen (Chien, 2006). Plectin<sup>+/+</sup> und Plectin<sup>-/-</sup> Zellen wurden Scherkräften ausgesetzt und durch Immunofluoreszenzmikroskopie und Immunoblots analysiert. Eine erhöhte Expression von eNOS und Caveolin wurde als Antwort auf Scherkräfte in Plectin<sup>+/+</sup> und Plectin<sup>-/-</sup> Zellen festgestellt, jedoch in geringerem Maße in Plectin<sup>-/-</sup> Zellen. Des Weiteren, war die Scherkraft-induzierte VE-Cadherin Clusterbildung in Plectin<sup>-/-</sup> im Vergleich zu Plectin<sup>+/+</sup> Zellen stark reduziert.

Diese Daten weisen darauf hin, dass Plectin, durch die Regulation von Endothelzell-spezifischen Molekülen, wie eNOS und VE-Cadherin eine wichtige Rolle in Endothelzellen spielt. Weiters, wurde eine eventuelle Beteiligung von Plectin an der Erkennung und / oder an der Antwort auf Scherkräfte in Endothelzellen beobachtet.

<b>1. Introduction</b>	<b>13</b>
<b>1.1. The Cytoskeleton</b>	<b>13</b>
1.1.1. Actin filaments	13
1.1.2. Intermediate filaments (IFs)	14
1.1.3. Microtubules (MTs)	15
<b>1.2. Cytolinker proteins / Plakin family</b>	<b>16</b>
<b>1.3. Plectin – a prototype cytolinker</b>	<b>18</b>
<b>1.4. Plectin and endothelial cells</b>	<b>21</b>
<b>2. Materials and Methods</b>	<b>24</b>
<b>2.1. Common buffers</b>	<b>24</b>
<b>2.2. Mammalian cell culture methods</b>	<b>25</b>
2.2.1. General instructions for different Endothelial cell (EC) lines	26
2.2.2. Thawing of cells	26
2.2.3. Freezing of cells	26
2.2.4. Passaging of cells	27
2.2.5. Isolation of primary endothelial cells (ECs)	27
2.2.6. Immortalization of Endothelial Cells by Polyoma middle T Infection	29
2.2.7. Virus producing cells (GP+E-86)	30
2.2.8. Endothelial cell transfection with FuGENE	31
<b>2.3. Protein methods</b>	<b>32</b>
2.3.1. Lysis of cells	32
2.3.2. SDS-polyacrylamide gel electrophoresis (PAGE)	32
2.3.3. Coomassie staining	33
2.3.4. Ponceau S staining	33
2.3.5. Immunoblotting	33
2.3.6. Quantification of Immunoblotting by Quantiscan software	34
2.3.7. Cell fractionation (digitonin – based method)	35
2.3.8. Immunofluorescence microscopy	36
<b>2.4. Measurement of NO release by 4,5-diaminofluorescein (DAF-2) application</b>	<b>37</b>
2.4.1. Cell culture	37
2.4.2. Preparation of the assay	38
2.4.3. Assay performance	38
<b>2.5. DNA Methods</b>	<b>39</b>
2.5.1. Bacterial strain and growth medium	39
2.5.2. Preparation of bacterial freezer stocks	39
2.5.3. Preparation of KCM competent cells	39
2.5.4. Transformation of bacteria	40
2.5.5. Midi Preparation	40
2.5.6. DNA Isolation from murine tails and toes	41
2.5.7. Polymerase Chain Reaction (PCR) genotyping	42
2.5.8. Agarose gel electrophoresis	42
<b>2.6. Flow Assays using parallel flow chamber</b>	<b>43</b>
2.6.1. Cell cultivation	43
2.6.2. Flow chamber setup	43
<b>3. Aims of thesis</b>	<b>45</b>
<b>4. Results</b>	<b>46</b>
<b>4.1. Characterization of pT Endo cell line</b>	<b>46</b>
<b>4.2. Generation of the endothelial cell line DH-1</b>	<b>48</b>
<b>4.3. Characterization of DH-1 cell line</b>	<b>50</b>

---

<b>4.4. Plectin Isoform expression in endothelial cells</b>	<b>54</b>
<b>4.5. Measurement of NO production</b>	<b>55</b>
<b>4.6. Ser<sup>1177</sup> and Thr<sup>495</sup> Phosphorylation of eNOS</b>	<b>56</b>
<b>4.7. Cell fractionation of endothelial cells</b>	<b>58</b>
<b>4.8. Angiogenesis – Matrigel assay</b>	<b>60</b>
<b>4.9. Effects of shear stress on plectin<sup>+/+</sup> and plectin<sup>-/-</sup> endothelial cells</b>	<b>61</b>
4.9.1. Effects of shear stress on protein levels and localization of eNOS, vimentin and plectin	62
4.9.2. Effects of shear stress on protein levels and localization of caveolin-1 and tubulin	69
4.9.3. Effects of shear stress on protein levels and localization of VE-cadherin and actin	73
4.9.4. Effects of shear stress analyzed by immunoblotting	77
<b>5. Discussion</b>	<b>80</b>
<b>6. References</b>	<b>86</b>



## List of Tables

Tab. 1. Separating gel and Stacking gel solutions in ml	32
Tab. 2. Primary antibody solutions used for immunoblotting	33
Tab. 3. Secondary antibody solutions used for immunoblotting	34
Tab. 4. Primary antibodies used in immunofluorescence microscopy	36
Tab. 5. Fluorescence-labeled secondary antibodies used in immunofluorescence microscopy	36
Tab. 6. Plectin rod ko PCR	41
Tab. 7. PCR protocol for plectin rod ko PCR	41
Tab. 8. Mean values $\pm$ S. D. of cell fractionation experiments of pT Endo cells	57
Tab. 9. Mean values $\pm$ S. D. of cell fractionation experiments of DH-1 cells	58

## Table of Figures

Fig. 1. Schematic diagram of plakin family members	15
Fig. 2. Schematic structure of plectin	20
Fig. 3. Schematic overview of plectin isoforms generated by alternative splicing	21
Fig. 4. Schematic picture of arterial wall	22
Fig. 5. Schematic picture of flow chamber	43
Fig. 6. EC marker expression in pT Endo cells	46
Fig. 7. Analysis of mouse genotype using plectin rod PCR	47
Fig. 8. Structure of retrovirus vector N-TK-mT	48
Fig. 9. Structure of plasmids pgag-polgpt and penv	48
Fig. 10. Phase-contrast images of DH-1 cells, at the beginning phases of immortalization and after PECAM-1 sorting	49
Fig. 11. Phase-contrast images of primary plectin <sup>+/+</sup> and plectin <sup>-/-</sup> ECs	49
Fig. 12. EC marker expression in DH-1 cells	51
Fig. 13. Immunofluorescence microscopy using anti-plectin antiserum #46 and mAb to VE-cadherin in plectin <sup>+/+</sup> and plectin <sup>-/-</sup> of DH-1 cells	52
Fig. 14. Immunofluorescence microscopy using anti-plectin antiserum #46 and mAb to VE-cadherin of plectin <sup>+/+</sup> and plectin <sup>-/-</sup> mixed cultures of DH-1 cells	52
Fig. 15. Immunofluorescence microscopy using anti-plectin antiserum #46 and mAb to eNOS of plectin <sup>+/+</sup> and plectin <sup>-/-</sup> mixed cultures of DH-1 cells	53
Fig. 16. Plectin isoform expression in DH-1 and pT Endo cells	53

---

Fig. 17.	Measurement of NO production in pT Endo cells n=3 (A), DH-1 cells n=2 (B) and primary ECs isolated from kidneys or lungs (C)	55
Fig. 18.	eNOS phosphorylation status of plectin <sup>+/+</sup> and plectin <sup>-/-</sup> DH-1 cells	56
Fig. 19.	Cell fractionation of pT Endo cells	58
Fig. 20.	Cell fractionation of DH-1 cells	59
Fig. 21.	Phase-contrast images of plectin <sup>+/+</sup> and plectin <sup>-/-</sup> DH-1 cells grown on matrigel	60
Fig. 22.	Immunofluorescence microscopy of eNOS in plectin <sup>+/+</sup> and plectin <sup>-/-</sup> pT Endo cells under static conditions and after 1 h of fluid shear stress	63
Fig. 23.	Immunofluorescence microscopy of eNOS and plectin in plectin <sup>+/+</sup> and plectin <sup>-/-</sup> DH-1 mixed cultures under static conditions, after 1 h and 6 h of shear stress	64
Fig. 24.	Immunofluorescence microscopy of eNOS and vimentin in plectin <sup>+/+</sup> and plectin <sup>-/-</sup> DH-1 cells under static conditions (A) and after 1 h (B), 6 h (C) and 24 h (D) of fluid shear stress	65f
Fig. 25.	Immunofluorescence microscopy of VE-cadherin and vimentin in plectin <sup>+/+</sup> plectin <sup>-/-</sup> pT Endo cells under static conditions (A) and after 1 h (B) of fluid shear stress	67
Fig. 26.	Immunofluorescence microscopy of caveolin-1 in plectin <sup>+/+</sup> and plectin <sup>-/-</sup> pT Endo cells under static conditions and after 1 h of fluid shear stress	69
Fig. 27.	Immunofluorescence microscopy of caveolin-1 and tubulin in plectin <sup>+/+</sup> and plectin <sup>-/-</sup> DH-1 cells under static conditions (A) and after 1h (B), 6h (C), and 24 h (D) of fluid shear stress	70f
Fig. 28.	Immunofluorescence microscopy of VE-cadherin and actin in plectin <sup>+/+</sup> and plectin <sup>-/-</sup> DH-1 cells under static conditions (A) and after 1 h (B), 6 h (C) and 24 h (D) of fluid shear stress	74f
Fig. 29.	Immunofluorescence microscopy of VE-cadherin and plectin in plectin <sup>+/+</sup> and plectin <sup>-/-</sup> DH-1 mixed cultures under static conditions and after 1 h of fluid shear stress	76
Fig. 30.	eNOS protein levels in pT Endo cells	77
Fig. 31.	Caveolin (A), eNOS (B) and VE-cadherin (C) protein levels in DH-1 cells	77
Fig. 32.	VE-cadherin protein levels in pT Endo cells	78

## Abbreviations

A23187	Calcium Ionophore A23187
ABD	Actin binding domain
AMP	Adenosine monophosphate
AMPK	AMP-activated protein kinase
APS	Ammonium persulfate
BPAG1	Bullous pemphigoid antigen 1
BSA	Bovine serum albumin
Ca <sup>2+</sup>	Calcium
CaCl <sub>2</sub>	Calcium chloride
cDNA	Complementary DNA
CH domain	Calponin homology domain
CO <sub>2</sub>	Carbon dioxide
C-terminal	Carboxy-terminal
DAF-2	4,5-diaminofluorescein
ddH <sub>2</sub> O	Double distilled water
DMEM	Dulbecco's modified eagle's medium
DMSO	Dimethyl sulfoxide
DNA	Deoxy ribonucleic acid
dNTPs	Deoxynucleotide triphosphates
DTT	Dithiothreitol
E. coli	Escherichia coli
EBS (-MD)	Epidermolysis bullosa simplex (in association with muscular dystrophy)
ECs	Endothelial cells
ECGS	Endothelial cell growth stimulant
EDTA	Ethylenediamine tetraacetic acid
eNOS	Endothelial nitric oxide synthase
F- actin	Filamentous actin
FCS	Fetal calf serum
G- actin	Globular actin
G	Gauche
GC domain	Globular carboxy-terminal domain
GFP	Green fluorescent protein
GFAP	Glial fibrillary acidic protein
GN domain	Globular amino-terminal domain
h	Hour(s)
HBSS	Hank's Balanced Salt Solution

---

HCl	Hydrochloridic acid
HEPES	4-(2-hydroxyethyl)-1-piperazineethanesulfonic acid
HRPO	Horse radish peroxidase
IFs	Intermediate filaments
K <sub>2</sub> HPO <sub>4</sub>	Dipotassium hydrogen phosphate
KCl	Potassium chloride
kDa	Kilodaltons
KH <sub>2</sub> PO <sub>4</sub>	Potassium dihydrogen phosphate
LB	Luria broth
L-Glu	L-Glutamin
L-NAME	NG-monomethyl-L-arginine
LTR	Long terminal repeat
mAb	Monoclonal antibody
MACF	Microtubule-actin crosslinking factor
MAPs	Microtubules associated proteins
Mg <sup>2+</sup>	Magnesium
MgCl <sub>2</sub>	Magnesium chloride
MgSO <sub>4</sub>	Magnesium sulfate
min	minute(s)
mRNA	messenger RNA
MTOC	Microtubule organizing centers
mT	middle T gene
MTs	Microtubules
N <sub>2</sub>	Nitrogen
Na <sub>2</sub> EDTA·H <sub>2</sub> O	Ethylenediamine tetraacetic acid disodium salt
Na <sub>2</sub> HPO <sub>4</sub>	Disodium hydrogen orthophosphate
Na <sub>3</sub> VO <sub>4</sub>	Sodium orthovanadate
NaCl	Sodium chloride
NaN <sub>3</sub>	Sodium acide
NaOH	Sodium hydroxide
NF-H	Neurofilament high
NF-L	Neurofilament low
NF-M	Neurofilament mid
nm	Nanometers
NO	nitric oxide
N-terminal	Amino terminal
OD600	Optical density at 600 nm
P/S	Penicillin/Streptomycin
PBS	Phosphate-buffered saline
PBS-T	PBS containing 0,05 % Tween-20

---

PCR	Polymerase chain reaction
PEG 3350	Polyethylene glycol electrolyte solution
PIP <sub>2</sub>	Phosphatidylinositol-4,5-bisphosphate
PIPES	1,4-Piperazinebis (ethansulfonic acid)
PKA	cAMP-dependent protein kinase
PKC	Protein kinase C
Plectin <sup>+/+</sup>	Plectin wildtype
Plectin <sup>-/-</sup>	Plectin knock-out
PMA	Phorbol 12-myristate-13 acetate
Polybrene	1,5-dimethyl-1,5-diazaundecamethylene polymethobromide
RACE PCR	Rapid amplification of cDNA ends
RACK 1	Receptor for activated C kinase 1
rpm	Revolutions per minute
RRX	Rhodamine red-X
SDS	Sodium dodecyl sulfate
SNAP	S-nitroso-N-acetylpenicillamine
TAE	Tris-Acetate-EDTA
TE	Tris-EDTA
TEMED	N,N,N',N'-Tetramethylethylenediamine
Tris	2-amino-2-hydroxymethyl-1,3-propanediol
TK	Thymidine kinase promotor
VE	Vascular endothelial
VEGF	Vascular endothelial growth factor
vWF	Van Willebrand factor

# 1. Introduction

## 1.1. *The Cytoskeleton*

The cytoskeleton is a dynamic three-dimensional network which spans the cytoplasm. A vast variety of cell functions is based on this organized filament system. The cytoskeleton is essential for maintenance of cell shape, cell orientation and cell polarity as well as for migration and signal transduction. It is involved in fundamental cell mechanics like mitosis and cytokinesis. The intracellular transport, organelle motility and many other processes such as phagocytosis and endocytosis are dependent on this filament network. There are three types of filament systems: actin filaments, intermediate filaments (IFs) and microtubules.

### 1.1.1. **Actin filaments**

Actin filaments, also termed F- (filamentous) actin or microfilaments, are two-stranded  $\alpha$ -helical structures. Those flexible polymers are composed of monomeric actin proteins, called G- (globular) actin and have a diameter of 5 – 9 nm. Although actin filaments are expressed throughout the cell they are found at the cell cortex with the highest density. They can form different types of cell surface projections such as microvilli, filopodia and lamellipodia. The actin cytoskeleton is found in nearly all types of eukaryotic cells and plays a significant role in a variety of cellular mechanisms like providing mechanical strength, spatial organization of the cytoplasm, transmitting internal stresses and signals. Actin filaments are interacting with various proteins like profilin (regulating actin filament polymerization), filamin,  $\alpha$ -actinin and fimbrin (filament cross-linking), or proteins like tropomyosin and cofilin that are responsible for filament stabilization and destabilization, respectively. By providing a structural framework, the actin skeleton contributes to cell-cell (tight junctions, adherens junctions) and to cell-matrix (focal adhesions) junctions. Tight junctions

(TJs) formed by claudins, occludin and zonula occludens (ZO) family members serve as permeability barriers. ZO-2 and ZO-3 proteins as well as occludin interact directly with actin. Adherens junctions (AJs) are formed between two neighboring cells and help to maintain tissue integrity. Cadherins constitute the major adhesive component of AJs and are connected to the actin cytoskeleton via p120,  $\alpha$ - and  $\beta$ -catenins. Focal adhesions (FAs) allow cells to bind to the extracellular matrix via integrins. The intracellular part of integrins is connected to the actin cytoskeleton by vinculin,  $\alpha$ -actinin, talin or filamin.

### 1.1.2. Intermediate filaments (IFs)

IFs have a diameter of 10 nm and are composed of IF subunits which are  $\alpha$ -helical rods that assemble to rope-like structures. IFs have a central  $\alpha$ -helical rod domain flanked by globular amino and carboxylic acid termini. IFs are composed of monomer units which form a coiled-coil dimer that self-associates in an anti-parallel arrangement to build up a staggered tetramer. Tetramer units pack together to form a sheet of eight parallel protofilaments that are twisted into a rope-like filament. The helical rod domain is highly conserved in different isoforms, whereas the globular termini differ.

There are various families of IFs, also termed IF proteins that are expressed in a tissue specific manner. One can distinguish between four major types of IF proteins in vertebrate cells:

Type I: Acidic type of epithelial keratins

Type II: Neutral type of epithelial keratins

Type III: Vimentin like IFs:

- Vimentin which is found in many cells of mesenchymal origin
- Desmin which is expressed in muscle cells
- Glial fibrillary acidic proteins (GFAP) which is found in glial cells

Type IV: Neurofilament proteins (NF-L, NF-M, NF-H) which are expressed in neurons.

Type V: Nuclear lamins (Lamins A, B, C) which are involved in the formation of the nuclear lamina that governs the shape of the nucleus.

IFs play an important role in both structural and functional elements of the cytoskeleton. Those highly viscoelastic filaments function as tension-bearing elements maintaining cell shape and rigidity of several organelles, including the nucleus. The IF network contributes to cell-cell (desmosomes) and cell-matrix (hemidesmosomes) junctions. Desmosomes are formed by the connection of cadherin family members (desmoglein, desmocollin) of neighboring cells. The intracellular part of cadherins is connected to the IF cytoskeleton by plakoglobin and desmoplakin (DP). Hemidesmosomes connect integrins of cells with the basal lamina. The intracellular part of integrins is bound via plectin or BP 230 to the IF cytoskeleton. ECs form unique junctions to capillaries, called the complexus adherens junctions (Schmelz et al., 1993). Within these EC specific junctions DP links VE-cadherin to the vimentin intermediate filament network through one of two intermediary armadillo proteins, p0071 (Calkins et al., 2003), or plakoglobin (Venkiteswaran et al., 2002).

These proteins that connect IFs to each other or to other components, thereby determining the shape of IF networks are called intermediate filament associated proteins (IFAPs). Several other IFAPs like fillagrin which is associated with to keratin fibers in epidermal cells or the best characterized IFAP plectin, have been identified to date.

### **1.1.3. Microtubules (MTs)**

Microtubules are long hollow cylinders with a diameter of 25 nm that are involved in many cellular processes like mitosis, cytokinesis and vesicular transport. A microtubule is built from 13 protofilaments, each composed of tubulin subunits. Tubulin itself is formed of two globular proteins ( $\alpha$ -tubulin,  $\beta$ -tubulin). The designated minus end of the microtubule is always connected with a MTOC (microtubule organizing centers) also called the centrosome, from which the nucleation of microtubules is launched. Microtubules are interacting with proteins called microtubule associated proteins (MAPs). High molecular weight proteins (200 – 300 kDa) and *tau*- proteins (40 – 60 kDa) are stabilizing microtubules against depolymerization. Kinesins and dyneins are responsible for the transport of vesicles and organelles along the microtubules.



## **1.2. Cytolinker proteins / Plakin family**

Cytoskeletal networks cooperate to perform many of their functions. Therefore, connector proteins are needed to crosslink cytoskeleton elements to each other. These connector proteins so called cytolinkers or plakins are a group of large (> 200 kDa) proteins that are able to interact with cytoskeleton filament systems and/or junctional complexes. Seven plakin family members have been identified so far: desmoplakin, bullous pemphigoid antigen 1 (BPAG1), microtubule-actin crosslinking factor (MACF), envoplakin, periplakin, epiplakin and plectin. The members of the plakin family are defined by the presence of a plakin domain or a plakin repeat domain. Actin-binding domain (ABD), coiled-coil rod domain, spectin-repeat containing rod and microtubule-binding domain are common in plakins but are not obligatory (Leung et al., 2002) (Fig. 1). Plakin genes often encode differentially expressed splice forms (Yang et al., 1996). These proteins are often affected by autoimmune and inherited diseases that cause tissue fragility and skin blistering (Leung et al., 2002).

The most multifaceted plakin family member is plectin which is discussed in the following chapter.

The desmoplakin gene encodes two alternatively spliced isoforms (DPI, DPII) that both bind via their carboxyl terminus to IFs and connect them with desmosomes (Green et al., 1989; Stappenbeck et al., 1993). Desmosomes are cell-cell adhesion junctions that are abundantly expressed in tissues that experience mechanical stress. Therefore, desmoplakin plays an important role in maintaining cellular strength and integrity (Green et al., 2000).

Bullous pemphigoid antigen 1 (BPAG1) has four known isoforms (BPAG1-a, BPAG1-b, BPAG-1e, BPAG1-n) that exhibit a distinct tissue distribution. These isoforms also originate from one gene which is alternatively spliced at the 5' terminus. BPAG-1b expression is restricted to the heart and the skeletal muscles. (Leung et al, 2001). The two neuronal splice products of BPAG1 gene, BPAG1-a and BPAG1-n (also called dystonin) are expressed especially in the central nervous system and have the potential to link actin and IF networks (Yang et al., 1996). BPAG-1e is expressed at high levels in basal epithe-

lial and muscle cells and links hemidesmosomes to keratin IFs (Guo et al., 1995).

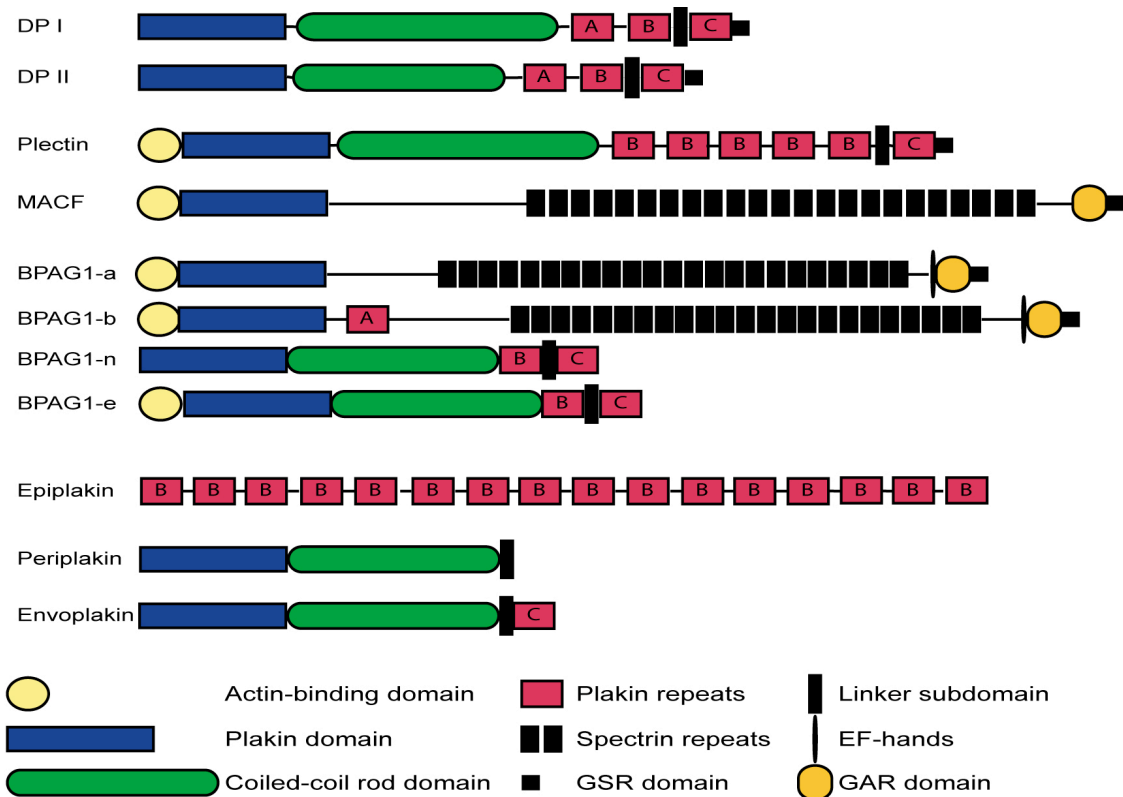


Fig. 1. Schematic diagram of plakin family members. Seven types of functional domains can be found in plakins: actin-binding domain (ABD), plakin domain, coiled - coil rod domain, plakin-repeat domain, spectrin-repeat-containing rod domain, Gas2-related (GAR) domain and glycine-serine-arginine (GSR) domain (modified from Leung et al., 2002).

Microtubule actin cross-linking factor (MACF) also called ACF7 can bind via its amino-terminal ABD to actin. Furthermore, it is bound to microtubules via its carboxyl-terminus, and has the ability to connect both filament systems (Leung et al., 1999; Karakesisoglou et al., 2000). In situ hybridisation revealed that MACF expression is found throughout the mouse embryo with significantly higher expression levels in the nervous system (Leung et al., 1999).

Envoplakin and periplakin are closely related members of the plakin family that are present in complex epithelial tissues like stratified squamous epithelia, mammary gland and bladder, but they can also be found in desmosomes (Ruhrberg et al., 1997; Määttä et al., 2000). Although both proteins share the characteristic plakin domain structure, their C-terminal domains are smaller

than those of the other plakins. Envoplakin and periplakin like no other plakin family members, have the potential to heterodimerize (Ruhrberg et al., 1997).

Epiplakin has an atypical plakin structure because of the missing plakin-and coiled – coil rod domain (Fujiwara et al., 1996). Epiplakin has 16 domains homologous to the B domain in the COOH-terminal region of desmoplakin. It is expressed in a wide range of tissues like brain, epidermis salivary glands and liver. (Fujiwara et al., 2001)

### ***1.3. Plectin – a prototype cytolinker***

Plectin is a versatile cytolinker of extraordinary large size ( $M_r < 500.000$ ) performing a vast variety of functions (for review see Wiche, 1998). It was first identified in high salt/Triton X-100 extracts of rat glioma C6 cells where it associated with IFs (Pytela and Wiche, 1980; Wiche and Baker, 1982). It was shown using immunofluorescence, immunoelectron microscopy as well as immunoblotting that plectin is expressed in many different mammalian cell types and tissues. The highest expression of plectin is found in muscle, stratified and simple epithelia as well as in cells forming the blood brain barrier. Depending on the cell type examined, plectin is localized throughout the cytoplasm, at attachment sites for IFs, or at adherence-type junctions and codistributed with IFs and microtubules (Wiche et al., 1983; Wiche et al., 1984; Wiche, 1989). Furthermore, plectin colocalizes with actin filaments and focal contacts in cultured fibroblast cells (Seifert et al., 1992).

Electron microscopy (Foisner and Wiche, 1987) as well as sequencing of rat plectin cDNA (Wiche et al., 1991) revealed that plectin molecules are dumbbell-shaped 200 nm-long structures consisting of a central rod domain flanked by large globular domains (Fig. 2). A highly conserved ABD which consists of calponin-homology (CH) domains, is found at the N-terminal domain of plectin (Goldsmith et al., 1997). This ABD is shared with a lot of actin binding proteins like spectrin,  $\alpha$ -actinin and dystrophin. The signalling molecule phosphatidylinositol-4, 5-biphosphate ( $PIP_2$ ) that regulates plectin's binding to actin, also binds to this ABD (Andrä et al., 1998). Furthermore, one or more binding

sites for integrin  $\alpha_6\beta_4$  are found at the N-terminal domain (Reznicek et al., 1998).

The  $\alpha$ -helical coiled-coil rod domain is encoded by exon 31 and spans over 200 nm. The properties of the amino acid sequence indicate that plectin molecules form homodimers via this rod domain. The extraordinary long rod domain allows the connection of two binding partners of plectin over long distances (Wiche et al., 1991).

The C-terminal domain of plectin consists of six long tandem repeats and is encoded by the very large exon 32. These highly conserved repeats share a 19 amino acid residue motif (Wiche et al., 1991). A binding site for vimentin and cytokeratins comprising 50 amino acid residues (Herrmann and Wiche, 1986) (Steinböck et al., 2000) was mapped to a region between repeats 5 and 6 of plectin's GC domain (Nikolic et al., 1996). Plectin is phosphorylated during M-phase of the cell cycle by p34<sup>cdc2</sup> kinase at a unique site (threonine 4542) which is located in its repeat 6 region (Foisner et al., 1996). Another binding site for integrin  $\alpha_6\beta_4$  is found at the C-terminal domain (Reznicek et al., 1998).

Due to its tripartite molecular structure plectin has the ability to bind to a great variety of binding partners. Many of them have been identified so far although their exact binding site is partially not known. The cytoskeletal proteins, MAP 1, MAP 2,  $\alpha$ -spectin and fodrin (Herrmann and Wiche, 1986), as well as the hemidesmosomal  $\beta_4$  integrin (Reznicek et al., 1998) and the desmosome-associated protein desmoplakin (Eger et al., 1997) are known to interact with plectin. Plectin binding partners among the IF protein family are vimentin (Foisner et al., 1988), neurofilament proteins NF 210/160/70, glial fibrillary acidic protein (GFAP), certain skin cytokeratins (Steinböck et al., 2000), desmin (Reipert et al., 1999) and lamin B (Foisner et al., 1991). Several other interaction partners of plectin have been identified, including phosphokinases  $\text{Ca}^{2+}$ /calmodulin-dependent kinase, protein kinase A and C but so far their binding sites at plectin are not known (Steinböck and Wiche, 1999).

Due to plectin's intracellular localization, its large set of binding partners and its extraordinary long rod domain, plectin was supposed to be a scaffolding platform for signalling molecules. It is known that plectin interacts with AMP-

activated protein kinase (AMPK) (Gregor et al., 2006) as well as with Fer kinase (Lunter and Wiche, 2002) and regulates their enzymatic activities.

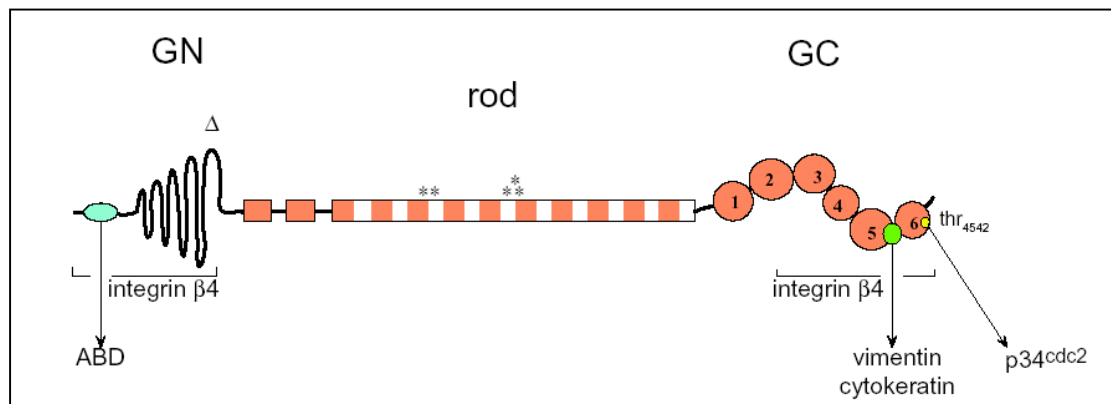


Fig. 2. Schematic structure of plectin. Central rod domain (\* indicate mutations) flanked by the globular terminal domains. ABD and binding site for integrin  $\beta_4$  are located at the globular amino-terminal (GN) domain. IF (vimentin, cytokeratin) and integrin  $\beta_4$  binding sites as well as a phosphorylation site for protein kinase p34<sup>cdc2</sup> are found at the globular carboxy- (GC) domain. (Wiche, 1998)

It is also involved in the reorganization of the actin cytoskeleton by influencing Rho, Rac, and Cdc42 GTPases (Andrä et al., 1998). The hypothesis that plectin is a link between the cytoskeleton and signalling cascades was confirmed by the finding that plectin binds the receptor for activated C kinase 1 (RACK 1) to the cytoskeleton and thereby influences protein kinase C (PKC) signalling (Osmanagic-Myers and Wiche, 2004). Furthermore, plectin is involved in Erk-MAP kinase signalling and affects cellular stress response and migration (Osmanagic-Myers et al., 2006).

Analysis of plectin cDNA from human (Liu et al., 1996), rat (Wiche et al., 1991) and mouse (Andrä et al., 1997) revealed that plectin gene consists of 32 exons extending over 32 kb of DNA. It is localized to the telomeric region of the long arm of chromosome 8 (8q24) (Liu et al., 1996; McLean et al., 1996). Although alternatively splice products are found in some plakin family members, the complexity of 5' transcripts from plectin gene was not expected. So far 16 alternatively first plectin exons have been identified by screening a plectin-primed cDNA library (Elliott et al., 1997) and RACE PCR analysis (Fuchs et al., 1999). 11 of these first coding exons (1 – 1j) splice into the common downstream exon 2 (Fuchs et al., 1999). Two additional exons (2 $\alpha$  and 3 $\alpha$ ) are spliced into the ABD and three non-coding exons precede exon 1c (Fig. 3).

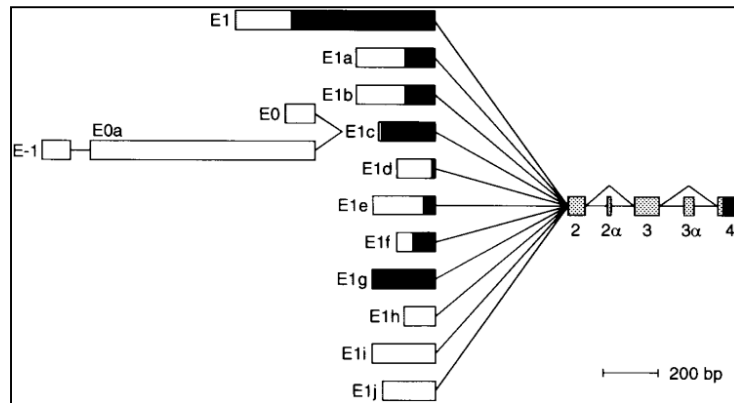


Fig. 3. Schematic overview of plectin isoforms generated by alternative splicing at the 5'-end of the plectin gene. (Fuchs et al., 1999)

Patients suffering from epidermolysis bullosa simplex (EBS) combined with muscular dystrophy (EBS-MD) lack expression of plectin (Gache et al., 1996; McLean et al., 1996). EBS-MD is an autosomal recessive disease characterized by severe skin blistering associated with late onset of muscular dystrophy and in some cases respiratory stridor, respiratory distress and urethral strictures (Mellerio et al., 1997; Dang et al., 1998). By now 22 different mutations in the plectin gene have been identified, most of them causing a frameshift or a premature stop codon in plectin mRNA. (Nakamura et al., 2004)

An autosomal dominant form of EBS, EBS-Ogna was mapped to the same telomeric region of chromosome 8 as the plectin gene. EBS-Ogna is a skin blistering disease resulting from a missense mutation in exon 31 of the plectin gene (Koss-Harnes et al., 2002).

To investigate the relation between plectin and EBS-MD plectin deficient mice were generated. Homozygous plectin deficient mice showed severe skin blistering and abnormalities of muscle, a phenotype corresponding to that observed in EBS-MD patients (Andrä et al., 1997).

#### **1.4. Plectin and endothelial cells**

The endothelium is a thin layer of cells that line the interior surface of blood vessels (Fig. 4). ECs are selective filters that regulate the passage of gases,

fluid and various molecules across their membranes. By secreting biochemical substances like nitric oxide (NO), reactive oxygen species (ROS) or glutathione ECs control the vascular homeostasis. Furthermore, these specialized cells play a role in regulating leukocyte, platelet and red cells functions.

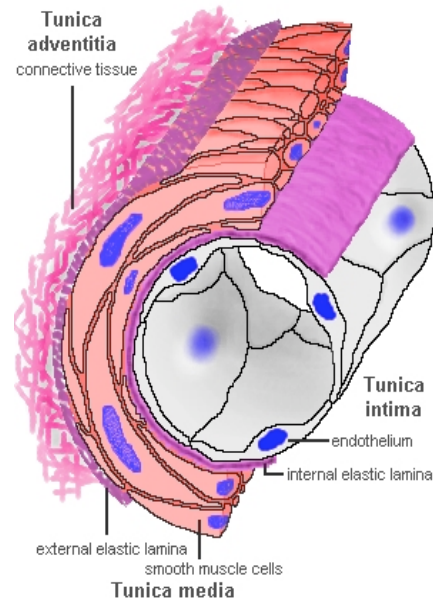


Fig. 4. Schematic picture of arterial wall. *Tunica intima* comprises the endothelium, the associated connective tissue and beneath the internal elastic lamina. *Tunica media* is formed by circumferential smooth muscle, connective tissue and external elastic lamina. *Tunica adventitia* consists mainly of connective tissue fibers.

In this diploma thesis the EC markers eNOS, VE-cadherin and van Willebrand factor were of particular interest.

The endothelial nitric oxide synthase (eNOS), also known as nitric oxide synthase 3 (NOS 3), is constitutively expressed in ECs and generates L-citrulline and NO by oxidizing L-arginine (Wyatt et al., 2004). NO, the endothelium-derived relaxing factor regulates vascular homeostasis and prevents formation of atherosclerotic lesions (Harrison et al., 2006).

Vascular endothelial (VE)-cadherin is a member of the cadherin family, a group of  $\text{Ca}^{2+}$ -dependent cell-cell adhesion molecules (Venkiteswaran et al., 2001). Cadherins are associated to microfilament network by a complex of  $\beta$ -catenin, plakoglobins and  $\alpha$ -catenin. This interaction of cadherins with the cytoskeleton is required for the formation and maintenance of the restrictive endothelial monolayer (Iyer et al., 2003). VE-cadherin is important for tissue

morphogenesis, cell adhesion and intercellular junction assembly. It is known to play a role in regulation of their growth, survival, migration and proliferation (Venkiteswaran et al., 2001). Although VE-cadherin function is not essential for the assembly of a primitive capillary plexus (vasculogenesis), subsequent maturation, branching and remodelling (angiogenesis) is depending on endothelial apoptosis regulated by VE-cadherin (Gory-Fauré et al., 1999).

Another important molecule synthesized in ECs is van Willibrand factor (vWF). It is essential for the blood clotting reaction (haemostasis). vWf deficient patients suffer from pseudohaemophilia an inherited disease resulting in impaired blood clotting and therefore excessive internal or external bleedings (Sadler, 1998).

An indication that plectin might play a role in the regulation of the vascular system and in the development of vascular diseases was given by patients suffering from Epidermolysis bullosa acquisita (EBA). This subepidermal bullous autoimmune disease with autoantibodies against type VII collagen and plectin is characterized by erythematous macules, hypertension and angina pectoris (Buijsrogge et al., 2005). Interestingly, no bleedings have been reported in other EBS variants like Dowling Meara or the Knoeber subtype, resulting from a mutation in keratin 14 or 5, respectively (Coulombe et al., 2002). Although no abnormalities of the vascular system in EBS-MD patients have been reported so far plectin deficient mice develop severe skin blistering particularly at the upper and lower extremities often accompanied by bleedings. This type of bleeding might be an evidence for a perturbation of vascular system.



## 2. Materials and Methods

### 2.1. Common buffers

*TE:*

Tris-HCl            10 mM  
EDTA                1 mM  
pH 8,0

*1 x PBS:*

NaCl                 150 mM  
KH<sub>2</sub>PO<sub>4</sub>/Na<sub>2</sub>HPO<sub>4</sub> 10 mM  
pH 7,4

*PBS-T:*

PBS containing 0,05 % Tween-20

### 2.2. Mammalian cell culture methods

*ECGS (Endothelial cell growth stimulant):*

Biomedical Technologies; Cat. no. BT-203

50 mg were diluted in 10 ml PBS (5 mg/ml), aliquoted and freezed at -20 °C.

*Heparin Sodium:*

Sigma; Cat. no. H3393; 180 U/ml

Heparin Sodium is diluted 1:250 to a final concentration of 25 mg/ml with PBS and stored at room temperature.

*DMEM (Dulbecco's Modified Eagle's Medium):*

DMEM  
FCS                            10 %  
Penicillin/Streptomycin (P/S) 100 U/100 mg/ml  
L-Glutamin                    2 mM

*Base Medium:*

DMEM  
HEPES                        25 mM  
FCS                            20 %  
P/S                             100 U/100 mg/ml  
L-Glutamin                    2 mM

*Complete Culture (CC) Medium:*

Base Medium  
Heparin Sodium                    100 µg/ml  
ECGS                                100 µg/ml  
Non essential amino acid (Invitrogen; Cat. no. 11140050) 1 mM  
Sodium pyruvate (Invitrogen; Cat. no. 11360-039) 1 mM

*Trypsin/EDTA:*

Trypsin                    500 mg/l  
EDTA (Na-salt)         0,2 %  
Sterilized by filtration.

*Gelatine coated dishes:*

For primary endothelial cells and DH-1 cells plates were coated with 2 % gelatine solution type B (Sigma; Cat. no. G-1393) supplemented with P/S (1:100). pT Endo cells were grown on dishes coated with 1 % gelatine solution type B (diluted in PBS) with the addition of 1:100 P/S. All dishes were coated with gelatine over night at 37°C and washed prior to usage with PBS.

### 2.2.1. General instructions for different Endothelial cell (EC) lines

**Primary ECs** isolated from either lungs or kidneys of plectin<sup>+/+</sup> and plectin<sup>-/-</sup> mice (line 29)

**DH-1 ECs** isolated from lungs of plectin<sup>+/+</sup> and plectin<sup>-/-</sup> mice (line 29); immortalized by Polyoma middle T infection. In these mice the plectin gene was inactivated by disruption of rod-encoding exon 31 (Andrä et al., 1997).

**pT Endo ECs** isolated from kidneys of plectin<sup>+/+</sup> and plectin<sup>-/-</sup> mice (line 29); immortalized by Polyoma middle T infection; generated in 1999 by K. Andrä.

Primary ECs and DH-1 ECs were treated the same way. Centrifugation was always preformed at 1 700 rpm using Heraeus Megafuge. For cultivation CC medium was used, while using base medium for short periods of incubation.

pT Endo cells were centrifuged at 1 000 rpm using Heraeus Megafuge and cultivated in DMEM supplemented with 10 % FCS, 100 U/100 mg/ml P/S an 2 mM L-Glu.

### 2.2.2. Thawing of cells

After thawing cells in a 37°C warm-waterbath these were transferred into a 15 ml tube and mixed with 9 ml of the appropriate medium. Cells were harvested by centrifugation for 3 min using Heraeus Megafuge. Pellet was resuspended in adequate medium and cells were seeded on gelatine-coated plates. Cells were cultivated at 37 °C and 5 % CO<sub>2</sub>.

### 2.2.3. Freezing of cells

Cells were washed with PBS, trypsinised and centrifuged for 3 min using Heraeus Megafuge. The pellet was dissolved in 90 % FCS + 10 % DMSO. After transfer into cryotubes cells were kept at -80°C and, after at least 24 h, stored in liquid nitrogen.

### 2.2.4. Passaging of cells

When cells got confluent they were washed with PBS. After incubation with Trypsin/EDTA for 3 – 10 min at 37°C detached cells were mixed with appropriate medium and collected by centrifugation for 3 min using Heraeus Megafuge. The pellet was dissolved in adequate medium and cells were seeded in the desired ratio on gelatine-coated plates.

### 2.2.5. Isolation of primary endothelial cells (ECs)

*Washing buffer:*  
PBS without Ca<sup>2+</sup> and Mg<sup>2+</sup>  
BSA 0,1 %  
EDTA 2 mM  
pH 7,4

#### 1. Precoating of anti-rat IgG Dynal beads:

An aliquot of Dynal M-450 sheep anti-rat immunoglobulin IgG magnetic beads (Dynal, Cat.no. 110.35) was resuspended in 1 ml of washing buffer and placed on the magnetic separator (Dynal MPC-S) for 1 min. Supernatant was removed and this washing step was repeated 3 times. After the last washing step beads were resuspended in the original volume of washing buffer. 2,5 µg of purified rat anti-mouse PECAM-1 (CD31, clone MEC13,3; 0,5 mg/ml concentration, Pharmingen; Cat. no. 557355) or rat anti-mouse ICAM-2 (CD102, clone 3C4; 0,5 mg/ml concentration, Pharmingen; Cat. no. 553326) were added for every 50 µl of magnetic beads and rotated end over end at 4°C overnight. On the

next day washing was repeated 4 times. After resuspending the beads in the original volume of washing buffer they were stored at 4°C.

## 2. Dissection:

The 1 - 2 day old mice were decapitated and the legs were pinned down with needles. The abdomen was sprayed with 70 % ethanol. Starting from the anterior part, the abdomen was opened by scissors. Lungs and kidneys were excised with forceps and scissors. Organs dissected were placed into a 50 ml tube containing 10 ml of ice-cold base medium.

## 3. Tissue dissociation:

### *Collagenase solution:*

Hank's Balanced Salt Solution (HBSS, Invitrogen; Cat. no. 14025050) containing 0,2 mg/ml (180 – 200 U/ml) collagenase type I (Gibco; Cat. no. 17100).

Tissues were finely minced by two scalpels, transferred quantitatively into a 50 ml tube containing 5 ml pre-warmed collagenase solution (diluted 1:10 with HBSS) and incubated for 45 min at 37°C with gentle agitation. The duration of collagenase treatment was varied due to different strengths of collagenase from charge to charge. The cell suspension was pressed about 10 times through 27G needle by a 5 ml syringe and filtered through a 70 µm nylon filter. The filter was rinsed with 10 ml of base medium. Cells were pelleted by centrifugation at 400 g for 8 min at 4°C. The supernatant was discarded and the pellet was resuspended in 2 ml of pre-warmed CC medium.

## 4. Primary sorting of primary ECs by PECAM-1

After one day of cultivation cells were washed up to 6 times with PBS to remove non-adherent cells and new CC medium was added. Upon reaching confluency cells were trypsinised and resuspended in 400 µl base medium. The cells were transferred into a 500 µl Eppendorf tube containing 8 µl of PECAM-1 coated Dynal beads. Suspension was rotated end over end at 4°C for 40 min.

The cell suspension was mixed with 1 ml of washing buffer, placed on the magnetic separator for 2 min and supernatant was discarded. This washing step was repeated 3 times to remove unbound cells. After the last washing step cells were resuspended in 2 ml CC medium and seeded on a 3,5 cm gelatine-coated dish. The next day adherent cells were once rinsed with PBS and 2 ml of CC medium were added.

#### 5. Second sorting of primary ECs by ICAM-2

To improve purity primary cells were sorted a second time (second immunobead isolation) at 80 to 90 % confluency (about 7 days after isolation), although it has to be mentioned that the efficiency of this sorting step was very low.

Medium was removed and cells were washed two times with PBS before trypsinisation (3 min at 37°C). Detached cells were transferred into a 15 ml tube containing base medium (2x amount of trypsin added). After centrifugation at 400 g for 3 min cells were resuspended in 400 µl base medium and transferred into a 500 µl Eppendorf tube. 8 – 10 µl ICAM-2-coated beads were added and cells were rotated end over end for 20 min at 4°C. After this incubation step the cell suspension was mixed with 1 ml of washing buffer, placed on the magnetic separator for 2 min and supernatant was discarded. This washing step was repeated 3 times. After the last washing cells were resuspended in 2 ml CC medium and seeded on a 3,5 cm gelatine-coated dish. The next day adherent cells were once washed with PBS and 2 ml of CC medium were added.

#### 2.2.6. Immortalization of Endothelial Cells by Polyoma middle T Infection

*Collagenase Solution:* 0,2 mg/ml (180 – 200 U/ml) Collagenase type I (Gibco; Cat. no. 17100) in HBSS

*G 418 Sulphate:* 800 µg/ml in ddH<sub>2</sub>O (Gibco; Cat. No. 11811-064)

*Polybrene:* Hexadimethrinbromide (Fluka; Cat. no. 52495) in ddH<sub>2</sub>O

Cells were isolated from 1-day old mice (line 29) by following procedure:

Lungs and kidneys got dissected and were kept in 10 ml base medium on ice. The organs got minced finely by two scalpels and digested in 5 ml collagenase solution for 45 min at 37°C. After centrifugation for 8 min at 1 700 rpm (Hereaus centrifuge) the pellet was resuspended in 2 ml CC medium and plated onto a 3,5 cm gelatine-coated dish. The same day the virus producing cells (GP+E-86) were splitted to guarantee a high titer of virus particles in the supernatant.

On the second day of cultivation cells were washed 5 times with PBS to get rid of non-adherent cells and new CC medium was added.

When cells reached a confluency of 50 – 70 % virus transfection was started: Virus particle containing supernatant of GP+E-86 and CC medium were mixed 1:1 and 8 µg/ml polybrene was added. This solution was filtered through a 0,45 µm Nylon filter. The cells were incubated with this mixture at 37°C and 5 % CO<sub>2</sub>. After 4 h the medium was discarded and new CC medium (+ 800 µg/ml G 418) was added. This virus infection was repeated at least 3 times every 24 h.

After infection periods the medium (CC medium + G418) was changed every 3 to 4 days. After 1 or 2 weeks groups of ECs appear while other cells die. ECs can easily be distinguished from other cells by their typical cobblestone morphology. After reaching a relatively high concentration of ECs (after 2-3 weeks), cells were sorted by PECAM-1 sorting and a high purity EC culture was obtained. Addition of G 418 to the CC medium was performed for at least 1 month.

### **2.2.7. Virus producing cells (GP+E-86)**

We got this cell line as a kind gift of the group of Wagner Erwin (Institute of molecular pathology).

Media: DMEM supplemented with 10 % FCS, 100 U/100 mg/ml P/S, 2mM L-Glu

Handling with this virus producing fibroblast cell line was always performed in a special retroviral hood. Thawing, freezing and passaging of cells were exe-

cuted like in basic protocol by taking care of the standard rules for working with retroviruses (see above). Cells were cultivated in 1 % gelatine-coated culture flasks.

### **2.2.8. Endothelial cell transfection with FuGENE**

DMEM supplemented 10 % FCS, 100 U/100 mg/ml P/S, 2mM L-Glu or CC Medium (without heparin)  
DMEM

Cells were seeded on 6 well dishes or 3,5 cm dishes. After reaching a confluency of 50 – 70 % transfection was started.

DMEM was pipetted in a 15 ml Falcon tube and FuGENE reagent was directly added to the medium avoiding contact with the walls of the tube. After mixing carefully Plasmid DNA (1 µg/µl) was added followed by mixing and incubation for 30 min at room temperature. Meanwhile the medium was aspirated and fresh DMEM supplemented with 10 % FCS, 100 U/100 mg/ml P/S and 2mM L-Glu was added. After adding 100 µl DMEM the transfection mix was pipetted slowly on the cells.

The next day new DMEM supplemented with 10 % FCS, 100 U/100 mg/ml P/S and 2mM L-Glu was added to the dishes to get a final volume of 2 ml or 5 ml per 3,5 cm or 6 cm dish, respectively.

24-48 h after transfection cells were fixed by ice-cold methanol for 90 sec and immunostained.

For transfection of DH-1 cells, cells were grown and transfected in CC medium (without heparin).

*Protocol for 3,5 cm dish:*

- 67 µl DMEM
- 2.7 µl FuGENE
- 1.7 µg DNA
- 100 µl DMEM
- 833 µl DMEM + 10 % FCS + P/S + L-Glu or CC-medium (without heparin)

*Protocol for 6 cm dish:*

- 200 µl DMEM
- 8 µl FuGENE
- 5 µg DNA

- 300 µl DMEM
- 2.5 ml DMEM + 10 % FCS + P/S + L-Glu or CC-medium (without heparin)

## **2.3. Protein methods**

### **2.3.1. Lysis of cells**

*2x Sample buffer:*

Tris-HCl, pH 6,8	50 mM
DTT	100 mM
SDS	2 %
Bromphenol blue	0,1 %
Glycerol	10 %

Cells were rinsed with pre-warmed PBS, 150 µl 2x Sample buffer per 3,5 cm dish were added and cells were scraped off with a cell scraper. Lysates were pressed through a 27G needle to get a homogenous solution, heated at 95°C for 3 min and stored at -20°C for short periods or at -80°C for longer intervals.

### **2.3.2. SDS-polyacrylamide gel electrophoresis (PAGE)**

*Running buffer:*

Tris	25 mM
Glycine	250 mM
SDS	0,1 %

*30 % Acrylamide mix:*

Acrylamide	29 g
Bis-Acrylamide	1 g
ddH <sub>2</sub> O	to 100 ml

Separating gel was prepared and overlaid with 96 % ethanol. After polymerization the alcohol was discarded and the stacking gel was poured. Samples mixed with 2x Sample buffer were heated to 95°C for 3 min before loading onto the gel. The gel apparatus was filled with running buffer and gels were run at 20 mA / gel until the marker front reached the bottom of the gel.



	Separating gel			Stacking gel 5 %
	8 %	10 %	12 %	
ddH <sub>2</sub> O	4,6	4,0	3,3	1,4
30 % Acrylamide mix	2,7	3,3	4,0	0,33
1,5 M Tris-HCl (pH 8,8)	2,7	2,5	2,5	
1,5 M Tris-HCl (pH 6,8)				0,25
10 % SDS	0,1	0,1	0,1	0,02
10 % APS	0,1	0,1	0,1	0,02
TEMED	0,006	0,004	0,004	0,002

Tab. 1: Separating gel and Stacking gel solutions in ml (for 10 ml and 2 ml, respectively)

### 2.3.3. Coomassie staining

*Staining solution.*

Coomassie R-250	0,4 %
Acetic acid	10 %
Methanol	45 %

*Destaining solution:*

Acetic acid	10 %
Methanol	30 %

Polyacrylamide gels were incubated for 30 min in staining solution, followed by incubation in destaining solution for 1-2 h (changing the solution every 30 min) until the bands became visible. Gels were dried in the vacuum drier for 2 h at 80°C or scanned and quantified.

### 2.3.4. Ponceau S staining

*Ponceau S solution:*

Ponceau S	0,1 %
Acetic acid	1 %

To perform a reversible staining of proteins, nitrocellulose membranes were stained with Ponceau S solution for 5 min at room temperature and washed with ddH<sub>2</sub>O until the bands became visible. After photographing membranes were completely destained by incubation in PBS-T for 5 – 10 min.

### 2.3.5. Immunoblotting

*Transfer buffer (10x):*

Tris	0,48 M
Glycine	0,4 M
SDS	0,01 %

*Blocking solution:*

5 % non-fat dry milk powder or 4 % BSA in PBS-T

Proteins were separated by SDS-PAGE (see above). The polyacrylamide gel was laid on a nitrocellulose membrane (Schleicher & Scheull). This sandwich was placed between 3MM Whatman filter papers and sponges and was fixed in blotting frames. Transfer was performed in a BioRad Mini Protean II blotting chamber, filled with transfer buffer, over night at 4°C with 25 V. After transfer proteins were detected by Ponceau S staining (see above). The membranes were rinsed with PBS-T, to destain them completely, followed by subsequent blocking of unspecific binding sites by blocking solution for 1 h at room temperature. Antibodies were diluted in PBS-T with 0,02 % NaN<sub>3</sub> and stored at 4°C. After blocking primary antibodies were added for 1 h at room temperature or over night at 4°C. Membranes were washed 3 times for 10 min with PBS-T prior to the incubation with the secondary antibody for 1 h at room temperature. Membranes were washed 3 times for 10 min with PBS-T, incubated with HRP substrate solution (Super Signal West Pico Chemiluminescent Substrate Pierce; Cat. no. 34080) for 5 min and exposed to film (Fuji).

<b>Primary antibodies</b>	<b>dilution</b>
mouse $\alpha$ actin	1: 200
mouse $\alpha$ $\alpha$ -actinin	1: 1 000
mouse $\alpha$ AKT	1: 200
rabbit $\alpha$ caveolin	1: 2 500
rabbit $\alpha$ eNOS	1: 500
rat $\alpha$ ICAM 2	1: 500
rabbit $\alpha$ integrin $\alpha$ 5	1: 500
rabbit $\alpha$ Phospho-Threonin eNOS	1: 2 500
rabbit $\alpha$ Phospho-Serine eNOS	1: 2 500
rabbit $\alpha$ Plectin (#9)	1: 3 000
rabbit $\alpha$ Plectin Exon 1	1: 500
rabbit $\alpha$ Plectin Exon 1a	1: 1 000
rabbit $\alpha$ Plectin Exon 1c	1: 2 000
rabbit $\alpha$ Plectin Exon 1f	1: 300
mouse $\alpha$ Tubulin	1: 1 000
rat $\alpha$ VE-cadherin	1: 500
mouse $\alpha$ Vinuclin	1: 1 000
rabbit $\alpha$ vWF	1: 100

Tab. 2: Primary antibody solutions used for immunoblotting

<b>Secondary antibodies</b>	<b>dilution</b>
goat $\alpha$ mouse HRPO	1: 10 000
goat $\alpha$ rabbit HRPO	1: 10 000
goat $\alpha$ rat HRPO	1: 10 000

Tab. 3: Secondary antibody solutions used for immunoblotting

### 2.3.6. Quantification of Immunoblotting by Quantiscan software

Bands were scanned and quantified using Quantiscan software. Only bands intensities falling in linear range were used for quantification. Tubulin or  $\alpha$ -actinin were used as loading control. The values obtained by the software were plotted against loading control values to obtain absolute values independent on cell confluency.

### 2.3.7. Cell fractionation (digitonin – based method)

*Digitonin buffer:*

Digitonin	0,01 %
PIPES	10 mM
Succrose	300 mM
NaCl	100 mM
MgCl <sub>2</sub>	3 mM
EDTA	5 mM
DTT	0,2 mM
Na <sub>3</sub> VO <sub>4</sub>	1 mM
pH	6,8

*Buffer 2:*

Triton X-100	0,5 %
PIPES	10 mM
Succrose	300mM
NaCl	100 mM
MgCl <sub>2</sub>	3 mM
EDTA	3 mM
DTT	0,2 mM
pH	7,4

To reach a confluency of 80 – 90 % after 1 day,  $200 \cdot 10^4$  cells were seeded on a 10 cm dish. Next day medium was discarded and cells were washed with pre-warmed PBS. Cell culture dishes were placed on ice and cells were scraped off in ice-cold PBS (containing phosphatase inhibitor mix) with a cell scraper. Cells were transferred into a 50 ml tube. After centrifugation at 1.000 rpm for 3 min with Hereaus centrifuge, the pellet was resuspended in 150  $\mu$ l

digitonin buffer and rotated end over end for 10 min at 4°C. After centrifugation at 14 000 rpm for 1 min with Eppendorf centrifuge the supernatant (cytosolic fraction) was transferred into a Eppendorf tube containing 50 µl x Sample buffer, heated at 95°C for 3 min and stored at -20°C. The pellet was resuspended in 150 µl buffer 2 and rotated end over end for 20 min at 4°C. After centrifugation at 14 000 rpm for 1 min with Eppendorf centrifuge the supernatant (membrane fraction) was transferred into a Eppendorf tube containing 50 µl 6x Sample buffer, heated at 95°C for 3 min and stored at -20°C. The pellet (cytoskeleton fraction) was resuspended in 40 µl 8M urea and kept on ice for 30 min. After vortexing this fraction every 10 min 6 µl 6x Sample buffer was added, the mixture was heated at 95°C for 3 min and stored at -20°C.

### 2.3.8. Immunofluorescence microscopy

*Blocking solution:*

2 % BSA + 0,02 % NaN<sub>3</sub>

*Mowiol:*

6 g glycerol and 2,4 g Mowiol (Hoechst) were incubated in 6 ml of ddH<sub>2</sub>O for 2 h. 12 ml of 0,2 M Tris-HCl solution, pH 8,5 were added for 10 min, heated to 50°C and spun for 15 min. The supernatant was stored at -20°C.

Cells were grown on gelatine-coated dishes or on gelatine coated coverslips. Cells were rinsed with pre-warmed PBS, fixed for 90 sec with ice-cold methanol and washed three times with PBS and could be stored in PBS at 4°C. Unspecific binding sites were blocked with blocking solution for 1 h at room temperature. Cells were incubated for 1 h with primary antibodies, diluted in blocking solution. Prior to incubation with the secondary antibody cells were washed 3 times with PBS for 10 min. Cells were incubated with fluorescence-labeled secondary antibody, diluted in PBS, for 1 h at room temperature in darkness. Cells were washed three times with PBS for 10 min and rinsed immediately with ddH<sub>2</sub>O before they were mounted with Mowiol.

Primary antibodies	dilution
mouse α actin	1: 80
rabbit α actin	1: 80
rabbit α caveolin	1: 500

mouse $\alpha$ desmoplakin	1: 10
rabbit $\alpha$ eNOS	1: 100
rabbit $\alpha$ GFP	1: 700
rat $\alpha$ integrin $\alpha$ 6	1: 100
mouse $\alpha$ plectin (10F6)	1: 100
rabbit $\alpha$ plectin (#46)	1: 400
mouse $\alpha$ tubulin	1: 500
rat $\alpha$ VE-cadherin	1: 30
goat $\alpha$ vimentin	1: 800
mouse $\alpha$ vinculin	1: 300
rabbit $\alpha$ vWF	1: 100

Tab. 4: Primary antibodies used in immunofluorescence microscopy.

<b>Secondary antibodies</b>	<b>dilution</b>
donkey $\alpha$ goat Alexa	1: 1 000
donkey $\alpha$ goat Texas Red	1: 100
donkey $\alpha$ mouse Cy 5	1: 800
donkey $\alpha$ mouse RRX	1: 100
donkey $\alpha$ rabbit Cy5	1: 300
donkey $\alpha$ rat Cy2	1: 100
donkey $\alpha$ rat Cy5	1: 300
goat $\alpha$ mouse Alexa	1: 800
goat $\alpha$ mouse Texas red	1: 200
goat $\alpha$ rabbit Alexa	1: 1 000
goat $\alpha$ rabbit Texas red	1: 100
goat $\alpha$ rat Texas red	1: 200

Tab. 5: Fluorescence-labeled secondary antibodies used in immunofluorescence microscopy.

## **2.4. Measurement of NO release by 4,5-diaminofluorescein (DAF-2) application**

Measurement was performed by Christoph Schmidt (Department for Pharmacognosy, University Vienna) by following protocol.

*L-arginine stock solution:*  
100 mM L-arginine in H<sub>2</sub>O

*A23187 stock solution:*  
10 mM A23187 in DMSO; stored at -20°C

*DAF-2 stock solution:*  
5 mM in DMSO, aliquoted and freezed at -80°C

*PBS+Ca<sup>2+</sup>:*

KH <sub>2</sub> PO <sub>4</sub>	1,47 mM
Na <sub>2</sub> HPO <sub>4</sub> • 7 H <sub>2</sub> O	9,57 mM
NaCl	137,00 mM
MgSO <sub>4</sub> • 7 H <sub>2</sub> O	0,49 mM
KCl	2,68 mM

CaCl<sub>2</sub> • 2 H<sub>2</sub>O      0,90 mM

CaCl<sub>2</sub> was solved in 1 l and all other components in another 1 l H<sub>2</sub>O. Both solutions were carefully mixed and pH was adjusted to 7.4. The pH has to be strictly regarded since the fluorescence of the DAF derivatives is pH-dependent.

### **2.4.1. Cell culture**

Cells were seeded in a density of 20 x 10<sup>4</sup> cells per well in 6-well plates. When cells were confluent they were stimulated by PMA 24 h before measurement.

### **2.4.2. Preparation of the assay**

The incubator, the water bath and a drying chamber were warmed up to 37°C. PBS+Ca<sup>2+</sup> (supplemented with 100 µM L-arginine) were prepared and warmed up. The A23187 stock solution was diluted 1:5 in DMSO. DAF-2 stock solution was diluted 1:250 in PBS+Ca<sup>2+</sup> (supplemented with L-arginine) and kept on ice in a light-protected box until use. The fluorescein derivate 4,5-diaminofluorescein (DAF-2) reacts with an oxidation product of NO reaction to DAF-2T, a highly fluorescent triazolofluoresein

### **2.4.3. Assay performance**

All operations with DAF-2 were preformed in a darkened room. And samples are protected from light while being transported to the spectrofluorimeter. NO production was measured in untreated, PMA-treated and L-NAME-treated cells.

Cell supernatant was removed and cells were washed twice in 1 ml PBS+Ca<sup>2+</sup>. Cells were incubated with 2 ml PBS+Ca<sup>2+</sup> (supplemented with L-arginine) for 5 min at 37°C to let them equilibrate with a defined concentration of L-arginine. 1 µl of the diluted A23187 solution and 10 µl of the diluted DAF-2 solution were added. Cells were incubated again for another 5 min at 37°C in darkness. NO released during this time will react with DAF-2 to DAF-2T. Cell

supernatants were transferred into 2 ml plastic caps quickly to assure that the reaction time for all samples will be the same. The fluorescence of cell supernatants was measured in a standard cuvette at an excitation wavelength of 490 nm and an emission wavelength at 515 nm. Wells without cells were measured in order to calculate the DAF-2 auto-fluorescence.

## **2.5. DNA Methods**

### **2.5.1. Bacterial strain and growth medium**

*Bacterial strain:*

E.coli strain XL-2 blue (recA1, endA1, gyrA96, thi-1, hsdR17, supE44, relA1, lac[F'proAB lacIq $\Delta$ M15Tn10 (tetR) Amy CamR] was used for cloning procedures.

*LB (luria broth):*

Bacto-tryptone	10 g
Bacto-yeast extract	5 g
NaCl	10 g

The pH was adjusted to 7,0 with NaOH and ddH<sub>2</sub>O was added to a final volume of 1 000 ml. The medium was autoclaved (20 min at 121°C, liquid cycle). Appropriated antibiotics (ampicillin: 100  $\mu$ g/ml) were added to the medium after cooling down.

To prepare plates, 15 g/l agar was added to the medium before autoclaving after hardening, plates were stored at 4°C.

### **2.5.2. Preparation of bacterial freezer stocks**

0,85 ml bacterial culture were mixed with 0,15 ml glycerol in a screw-cap storage tube. After vortexing the stocks were frozen using liquid N<sub>2</sub> and stored for longer time periods at -80°C.

### **2.5.3. Preparation of KCM competent cells**

*TSS Solution:*

LB	75 ml
PEG 3350	10 g
DMSO	5 ml
1 M MgSO <sub>4</sub>	10 ml
1 M MgCl <sub>2</sub>	10 ml

5 ml LB medium (add antibiotic if cells have antibiotic resistance) were inoculated with a single *E. coli* colony and incubated overnight at 37°C and 220 rpm. 1 ml of overnight culture was added to 100 ml LB medium (without antibiotic) and incubated at 37°C at 220 rpm until an OD<sub>600</sub> of 0,5 – 0,6 was reached. At this point the flask was kept on ice for at least 20 min and cells were collected by centrifugation at 4 000 rpm for 10 min at 4°C. The bacterial pellet was re-suspended in 5 ml of ice-cold TSS solution and incubated on ice for 15 min. The suspension was divided into 100 µl aliquots, which were quickly frozen in liquid N<sub>2</sub> and stored at -80°C.

#### **2.5.4. Transformation of bacteria**

*5x KCM:*

KCl	0,5 M
CaCl <sub>2</sub>	0,15 M
MgCl <sub>2</sub>	0,25 M

sterile filtered, stored at 4°C

Competent *E. coli* cells (prepared with KCM method) were thawed on ice. 1 -80 µl of plasmid DNA were mixed with 20 µl 5x KCM and ddH<sub>2</sub>O were added to a final volume of 100 µl. 100 µl of the cell suspension were mixed with the DNA mixture and incubated for 20 minutes on ice. The suspension was heated for 5 min to 37°C, 1 ml of pre-warmed LB medium was added and incubated for 40 – 60 min at 37°C. The bacteria were plated on a selective medium and left to grow overnight at 37°C.

#### **2.5.5. Midi Preparation**

To perform a Midi preparation the Promega kit Pure Yield Plasmid Midiprep System (Promega; Cat. no. A2495) was used according to manufacturers instructions:



150 ml overnight culture were harvested by centrifugation for 10 min with 5000 g. The supernatant was discarded and the cell pellet was resuspended in 6 ml cell resuspension solution. 6 ml cell lysis solution was added and incubated for 3 min. After adding 10 ml neutralization solution the pellet was mixed carefully and incubated for 3 min at room temperature. After centrifugation for 10 min at 15 000 rpm the DNA was cleaned by a column system. The blue clearing column was placed onto the white binding column and the cell lysate was added to the blue column. After starting vacuum pump and detaching the blue clearing column, 5 ml endotoxin removal wash and 20 ml column wash solution were sucked through the binding column. After 1 min the vacuum was turned off and the binding column was placed into a 50 ml Falcon tube. 600  $\mu$ l nuclease-free water were pipetted onto the column. After 5 min incubation the DNA was eluted by centrifugation at 2 000 g for 5 min.

### 2.5.6. DNA Isolation from murine tails and toes

*Tail buffer:*

Tris-HCl pH 8,0	50 mM
EDTA pH 8,0	100 mM
NaCl	100 mM
SDS	1 %

To isolate DNA from 3 week-old mice, pieces of their tails were cut and following protocol were used. To determine genotype of 10 day-old mice, their toes were used for DNA isolation but only half of the amounts denoted in following protocol were used.

715  $\mu$ l of tail buffer and 35  $\mu$ l proteinase K (10 mg/ml) were added to each sample and shaken by thermomixer overnight at 55°C at level 10. (As toes of 10 day-old mice get digested more quickly, 3 h of incubation were sufficient). After incubation, probes were shaken for 5 min at level 14 and 50  $\mu$ l 5,5 M NaCl were added. Probes were reversed 3 times and shaken for 5 min at level 14. After centrifugation at 14 000 rpm for 10 min with Eppendorf Centrifuge the supernatant was transferred into new Eppendorf tubes containing 500  $\mu$ l isopropanol. DNA precipitated after reversing the samples about 50 times. By centrifugation at 14 000 rpm for 15 min with Eppendorf Centrifuge DNA got

pelleted. The supernatant was discarded and 1 ml of 70 % ethanol was added to the pellet. After centrifugation at 14 000 rpm for 10 min with Eppendorf Centrifuge the alcohol was completely removed. The DNA pellet was dried for 30 min and dissolved in 100  $\mu$ l 10 mM Tris pH 8,0 by thermomixing at 37°C and level 9 overnight. The DNA was stored at 4°C.

### 2.5.7. Polymerase Chain Reaction (PCR) genotyping

To determine the genotype of mice from line 29 plectin rod PCR was performed. DNA was isolated from tails or toes (see above).

Reactions	plectin rod PCR
ddH <sub>2</sub> O	16,25 $\mu$ l
5x PCR Buffer	5 $\mu$ l
dNTPs (10 mM each)	0,5 $\mu$ l
Primer (10 pmol/ $\mu$ l)	0,5 $\mu$ l mPE30/U 0,5 $\mu$ l mPIntr30/L 0,5 $\mu$ l Primer mPle6437L 0,5 $\mu$ l Neo 19
Go TAQ Polymerase (Promega)	0,25 $\mu$ l
DNA template	1 $\mu$ l

Tab. 6: Plectin rod PCR

Following PCR approach was preformed for plectin rod PCR:

Cycles	Temperature	Duration
1 x	94°C	5 min
35 x	94°C	30 sec
	58°C	30 sec
	72°C	2 min
1 x	72°C	7 min
1x	4°C	Ad infinitum

Tab. 7: PCR protocol for plectin rod PCR

Primer 5' to 3' Sequences:

mPE30/U	CAGTGAGACCCTTCGCCGCATG
mPIntr30/L	GTGCTCACATGACACGGAAGGTAC
Neo 19	CATTCAGGACATAGCGTTGG

### 2.5.8. Agarose gel electrophoresis

10x DNA sample buffer:

Urea	4 M
Saccharose	50 % (w/v)
EDTA	1 mM
Brompheel-blue	0,1 % (w/v)

50 x TAE:  
Tris-acetate            400 mM  
Na<sub>2</sub>EDTA·H<sub>2</sub>O        20 mM  
pH 8,2

0,8 – 1,8 % agarose gels were prepared and 8 µl ethidiumbromide were added before pouring the gels to visualize DNA under UV light. Samples were mixed with 1/10 vol. of 10x DNA sample buffer and DNA fragments were separated with 100 V.

## **2.6. Flow Assays using parallel flow chamber**

Rectangular Flow Chamber (for standard microscope slide)  
Glycotech (Maryland, USA; Cat. no. 31-010)

### **2.6.1. Cell cultivation**

Cells were cultured on a microscope slide coated with gelatine. The microscope slide (Fig. 4C) was either put inside a 10 cm dish or a 10 x 10 cm chamber and cells were grown to confluency. One day before flow stress assay was performed medium was changed to avoid detaching of cells.

### **2.6.2. Flow chamber setup**

The incubator and media were warmed to 37°C 1 h prior to beginning flow assay.

The flow system apparatus was assembled by following procedure: flow deck (Fig. 4A) and the chamber gasket (Fig. 4B) were connected by aligning the gasket to the flow deck and pressing the deck on top of the gasket. If static was a problem the flow deck was placed on an antistatic strip prior to installing gasket. The medium inlet and outlet as well as vacuum lines were connected to flow deck. The inlet reservoir was filled with media. The microscope slide was attached to the flow chamber by holding the deck inverted. A small bubble of media was placed on flow path area to avoid air bubbles in the system. Vac-

uum held the slide on the deck. Flow was initiated by connecting peristaltic pump to outlet of the flow chamber at a shear stress rate of 5 dynes/cm<sup>2</sup> for 1 – 24 h.

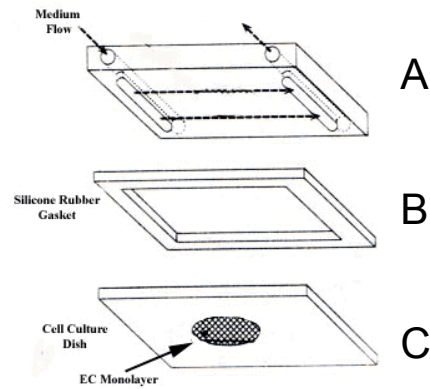


Fig. 5. Schematic picture of flow chamber. (A) flow deck (B) chamber gasket (C) microscope slide with cultured ECs

### 3. Aims of thesis

There are several hints for plectin's involvement in the endothelium and the vascular system. Patients with mutations in basic functions of the plectin gene as well as plectin-deficient mice develop haemorrhagic blisters atypical for other skin blistering diseases. This suggests an altered structural integrity of the endothelium in the absence of plectin. VE-cadherin, a component of adherens junctions, stabilizes EC cell junctions and maintains tissue integrity. Therefore, we wanted to investigate the intracellular distribution and protein levels of VE-cadherin in plectin<sup>+/+</sup> and plectin<sup>-/-</sup> ECs.

Furthermore, an involvement of plectin in regulating vascular function was indicated by treatment of ECs with the nitric oxide (NO) donor SNAP. This resulted in a much more fragile vimentin filament system in plectin<sup>-/-</sup> cells compared to plectin<sup>+/+</sup> cells (Spurny, unpublished data). To further investigate this phenotype extracellular NO had to be examined as well as protein levels and localization of the NO producing enzyme eNOS had to be assessed. eNOS primarily resides in small plasma membrane invaginations called caveolae. The major coat protein of caveolae, caveolin-1 is known to interact with eNOS. Hence, it was important to examine caveolin levels and localization in plectin<sup>+/+</sup> and plectin<sup>-/-</sup> ECs.

NO plays a central role in controlling vascular homeostasis and its production is dramatically influenced by mechanical forces (like shear stress) imposed on the endothelium (Harrison et. al, 2006). Moreover, in response to fluid shear stress cytoskeletal protein and EC protein marker levels are known to be upregulated. After exposure to laminar shear stress plectin levels are also elevated suggesting a role of plectin in strengthening the endothelial cytoskeleton in the face of biomechanical forces (Garcia-Cardena et. al, 2001). The major goal of this thesis was to investigate the effects of fluid shear stress on plectin<sup>+/+</sup> and plectin<sup>-/-</sup> ECs. Eventual differences in protein levels and the localization of eNOS, caveolin and VE-cadherin as well as cytoskeletal proteins were studied in detail by immunofluorescence microscopy and immunoblotting.

## 4. Results

### 4.1. Characterization of pT Endo cell line

Experiments described in this diploma thesis were performed on an endothelial cell line (pT Endo) originally generated by Andrä in 1999. Briefly, cells derived from kidneys of plectin<sup>+/+</sup> and plectin<sup>-/-</sup> mice of line 29 and were immortalized by polyoma middle T infection (Williams et al., 1988). In these mice the plectin gene was inactivated by disruption of rod-encoding exon 31 (Andrä et al., 1997). Those cell line, however, needed a thorough characterization.

First, to confirm that pT Endo cells are indeed ECs and to check their purity, expression of EC markers was evaluated using immunoblotting (Fig. 6). To check if the eventual differences in expression pattern between plectin<sup>+/+</sup> and plectin<sup>-/-</sup> cells were dependent on confluency state of cells, these were lysed after 1, 2 and 3 days of cultivation. On day 1 and 2 of cultivation cells had reached a confluency of ~70 %, and ~90 %, respectively. At day 3 cells were completely confluent.

The expression of three different endothelial cell markers was checked: endothelial nitric oxide synthase (eNOS), vascular endothelial-cadherin (VE-cadherin) and von Willebrand factor (vWf). To confirm the genotype of pT Endo cells the expression of plectin was determined by anti-plectin antiserum #9. Additionally, caveolin-1 (caveolin) expression was checked since this protein is very abundant in ECs. Quantification of protein bands was determined by Quantiscan software (Fig. 6), described in Materials and Methods using tubulin as Quantiscan loading control. As expected plectin was only expressed in plectin<sup>+/+</sup> pT Endo cells confirming the genotype of these cells (Fig. 6A). eNOS was expressed in both plectin<sup>+/+</sup> and plectin<sup>-/-</sup> ECs but its levels were reduced in plectin<sup>-/-</sup> pT Endo cells. The effect appeared to be the strongest at day 1 in a subconfluent state of the cells (Fig. 6B).

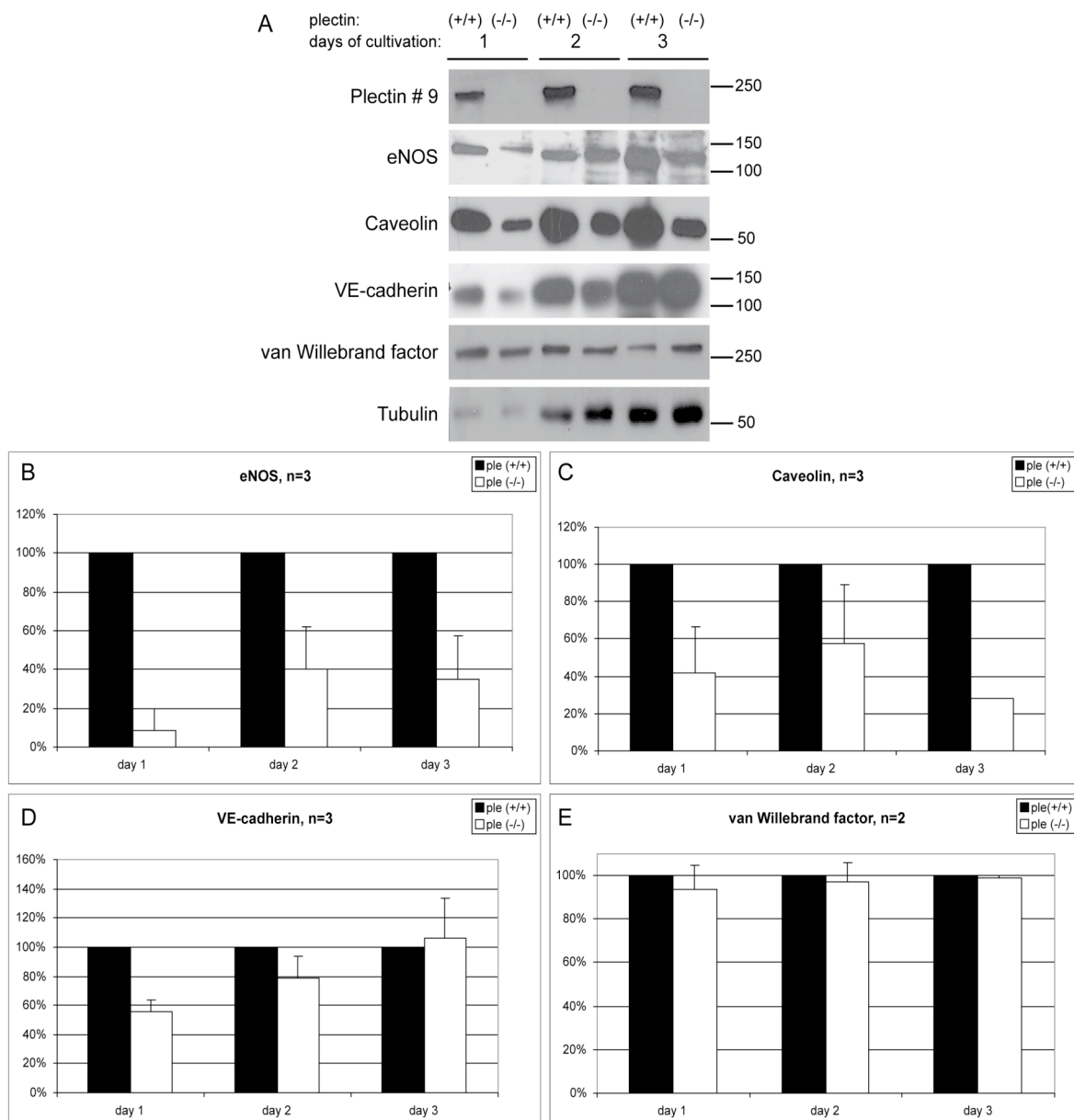


Fig. 6. EC marker expression in pT Endo cells. Plectin<sup>+/+</sup> and plectin<sup>-/-</sup> cells were lysed after 1, 2 and 3 days of cultivation and analysed by immunoblotting using specific primary antibodies and HRP-conjugated secondary antibodies. *Tubulin*: loading control (A). Statistic evaluation of eNOS (B), caveolin (C), VE-cadherin (D) and vWf (E). Blots were scanned and quantified by Quantiscan and standard deviation was calculated. Abbreviations: *n*: number of blots scanned.

Similarly, caveolin levels were reduced in plectin<sup>-/-</sup> pT Endo cells, however, this effect did not depend on confluency state of cells (Fig 6C). VE-cadherin levels were reduced in plectin<sup>-/-</sup> pT Endo cells after day 1 and 2 of cultivation. However, when ECs reached a confluent state (day 3 of cultivation) the expression of VE-cadherin was more or less the same in both plectin<sup>+/+</sup> plectin<sup>-/-</sup> ECs (Fig. 6D). To determine if plectin<sup>-/-</sup> ECs are expressing less of these EC markers because they are less pure than wildtype ECs, vWf expression was

checked. Equal amounts of vWf were found in both plectin<sup>+/+</sup> and plectin<sup>-/-</sup> pT Endo cells (Fig. 6E). Taken together, these results confirm that plectin<sup>+/+</sup> and plectin<sup>-/-</sup> pT Endo cells have the same purity and express EC markers, although the total amounts of eNOS, caveolin and VE-cadherin are reduced in plectin<sup>-/-</sup> ECs.

## 4.2. Generation of the endothelial cell line DH-1

Since pT Endo cell lines were available only at higher passage numbers it was necessary to have another endothelial cell line. Cells were isolated from lungs of plectin<sup>+/+</sup>, plectin<sup>-/-</sup> and heterocygous plectin<sup>+/-</sup> mice of line 29 (Fig. 7).

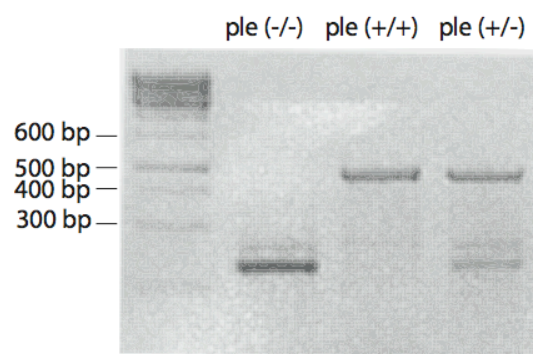


Fig. 7. Analysis of mouse genotype using plectin rod PCR. Lane 1: plectin<sup>-/-</sup>, 350 bp; Lane 2: plectin<sup>+/+</sup>, 950 bp; Lane 3: plectin<sup>+/-</sup>, 350 bp and 950 bp.

When cells reached confluency they were immortalized by the middle T oncogene using a replication-defective selectable retrovirus (N-TKmT). Virus amplification was achieved in the safe packaging cell line (GP+E-86) stably transfected with three plasmids. The *gag* and *pol* genes were on one plasmid (pGag-PolGpt) while the *env* gene was on the other (pEnv) (Fig. 9). The third plasmid contains a neomycin resistance gene ( $\Delta$ neo) and the polyoma middle T oncogene which expression is under the control of the thymidine kinase promoter (Fig. 8) (Markowitz et al., 1988). It is still not exactly known why middle T antigene causes ECs proliferation and why specifically ECs gain proliferation advantage over other cells (Williams et al., 1988).



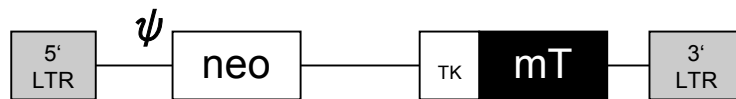


Fig. 8. Structure of retrovirus vector N-TK-mT. Symbols and abbreviations: *neo*, neomycin resistance gene; *LTR*, long terminal repeat; *TK*, thymidine kinase promoter; *mT*, middle T gene;  $\psi$ , packaging signal sequence (Williams et al., 1988).

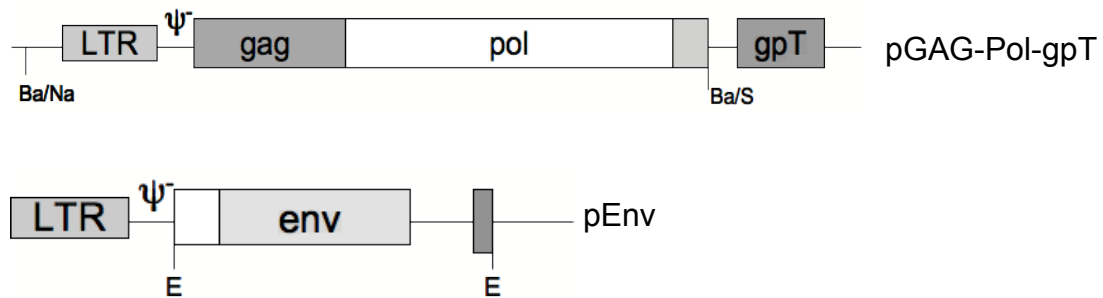


Fig. 9. Structure of plasmids pgag-polgpt and penv. Symbols and abbreviations: thin lines, pBR322 sequences;  $\psi^-$ , deletion of  $\psi$  packaging sequences; *Ba*, BamHI; *E*, EcoRI; *Na*, NaeI; *S*, Scal (adapted from Markowitz et al., 1988).

The presence of the *neo* gene in N-TK-mT enabled the in vitro selection of cells containing the vector by addition of G-418 (neomycin homolog) to the medium. After 1 - 2 weeks of virus application, groups of ECs having cobblestone like morphology appeared while other cells died (Fig. 10). This typical EC morphology was also found in primary ECs cultures (Fig. 11). When ECs reached high density, cells were sorted by platelet-endothelial cell adhesion molecule -1 (PECAM-1). Since PECAM-1 is a cell surface molecule especially found on ECs (Gurubhagavatula I. et al., 1998), ECs of high purity were obtained after this sorting step. This cell line was named DH-1.

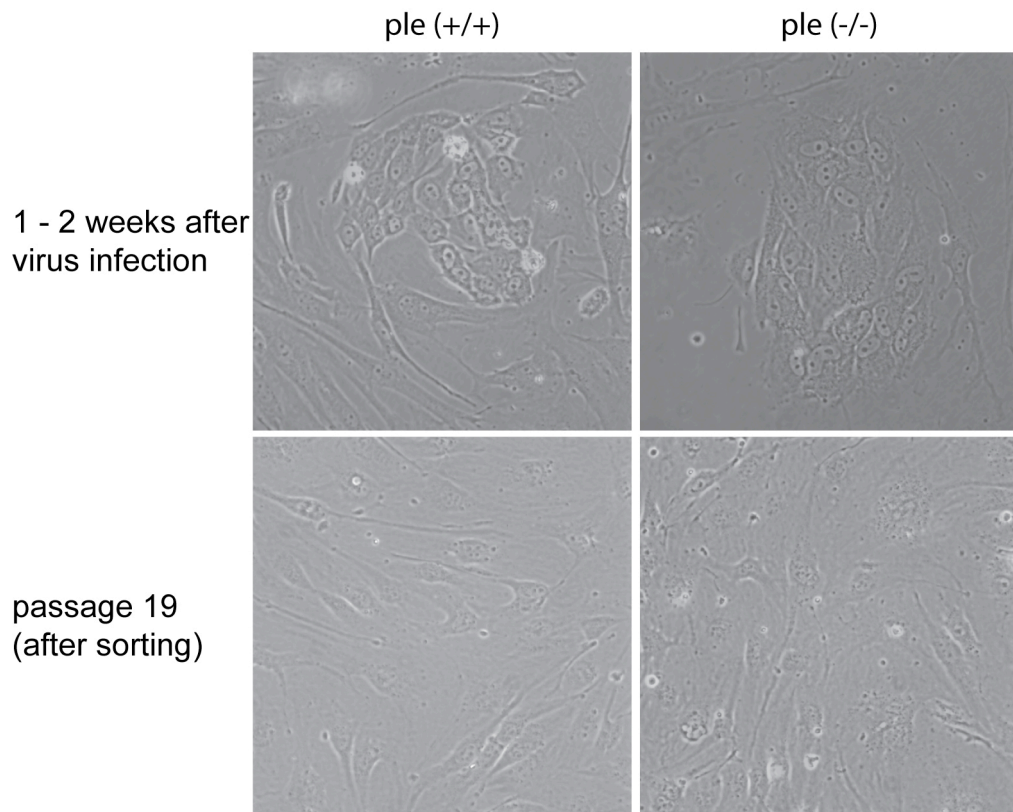


Fig. 10. Phase-contrast images of DH-1 cells, at the beginning phases of immortalization (*1 – 2 weeks after virus infection*) and after PECAM-1 sorting (*passage 19*).

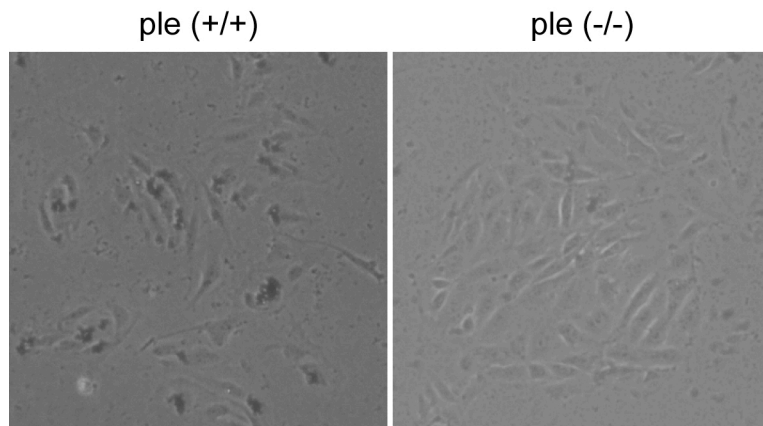


Fig. 11. Phase-contrast images of primary plectin<sup>+/+</sup> and plectin<sup>-/-</sup> ECs.

### **4.3. Characterization of DH-1 cell line**

A detailed characterization of DH-1 cells was indispensable to confirm that these cells are indeed pure ECs. Expression of EC markers was checked using immunoblotting and immunofluorescence microscopy.

Cells were lysed after 1, 2 and 3 days of cultivation and analysed using immunoblotting (Fig. 12). To further confirm the genotype of these cells plectin expression was determined by anti-plectin antiserum #9. As expected, plectin was only expressed in plectin<sup>+/+</sup> ECs (Fig. 12A). DH-1 cells showed more or less the same expression pattern for eNOS, caveolin, VE-cadherin and vWf like pT Endo cells. eNOS and caveolin were expressed in both plectin<sup>+/+</sup> and plectin<sup>-/-</sup> DH-1 cells but the levels were reduced in plectin<sup>-/-</sup> cells irrespectively from confluency state of the cells (Fig. 12B, C). VE-cadherin levels were reduced plectin<sup>-/-</sup> cells after the first two days of cultivation in a subconfluent state of the cells. However, when cells were completely confluent no difference in VE-cadherin expression between plectin<sup>+/+</sup> and plectin<sup>-/-</sup> cells was detectable (Fig. 12D). Like in pT Endo cells equal amounts of vWf were found in both plectin<sup>+/+</sup> and plectin<sup>-/-</sup> DH-1 cells (Fig. 12E).

Taken together, these results confirm that plectin<sup>+/+</sup> and plectin<sup>-/-</sup> DH-1 cells have the same purity and express all EC markers checked. Furthermore, DH-1 cells had more or less the same expression pattern of EC markers as pT Endo cells.

Next, DH-1 cells were fixed in a subconfluent state after 1 day of cultivation and immunofluorescently stained by specific antibodies.

It was already observed that primary plectin<sup>-/-</sup> ECs express less VE-cadherin and form less cell-cell contacts (Osmanagic-Myers, unpublished data). These data could be confirmed in DH-1 cells. In plectin<sup>+/+</sup> DH-1 cells VE-cadherin staining was more prominent and zipper-like structures more pronounced compared to plectin<sup>-/-</sup> cells (Fig. 13). In mixed plectin<sup>+/+</sup> and plectin<sup>-/-</sup> cultures, plectin<sup>-/-</sup> cells grown between plectin<sup>+/+</sup> cells showed a more prominent VE-cadherin staining (Fig. 14). Thus, plectin<sup>+/+</sup> cells seemed to induce VE-cadherin cluster formation in neighboring plectin<sup>-/-</sup> cells. Immunofluorescence microscopy of eNOS was a punctuated and no accumulations were found at the cell periphery. eNOS fluorescence signal was more intense in

plectin<sup>+/+</sup> cells compared to plectin<sup>-/-</sup> cells, although the difference was not that drastic as observed in cell lysates (Fig. 15).

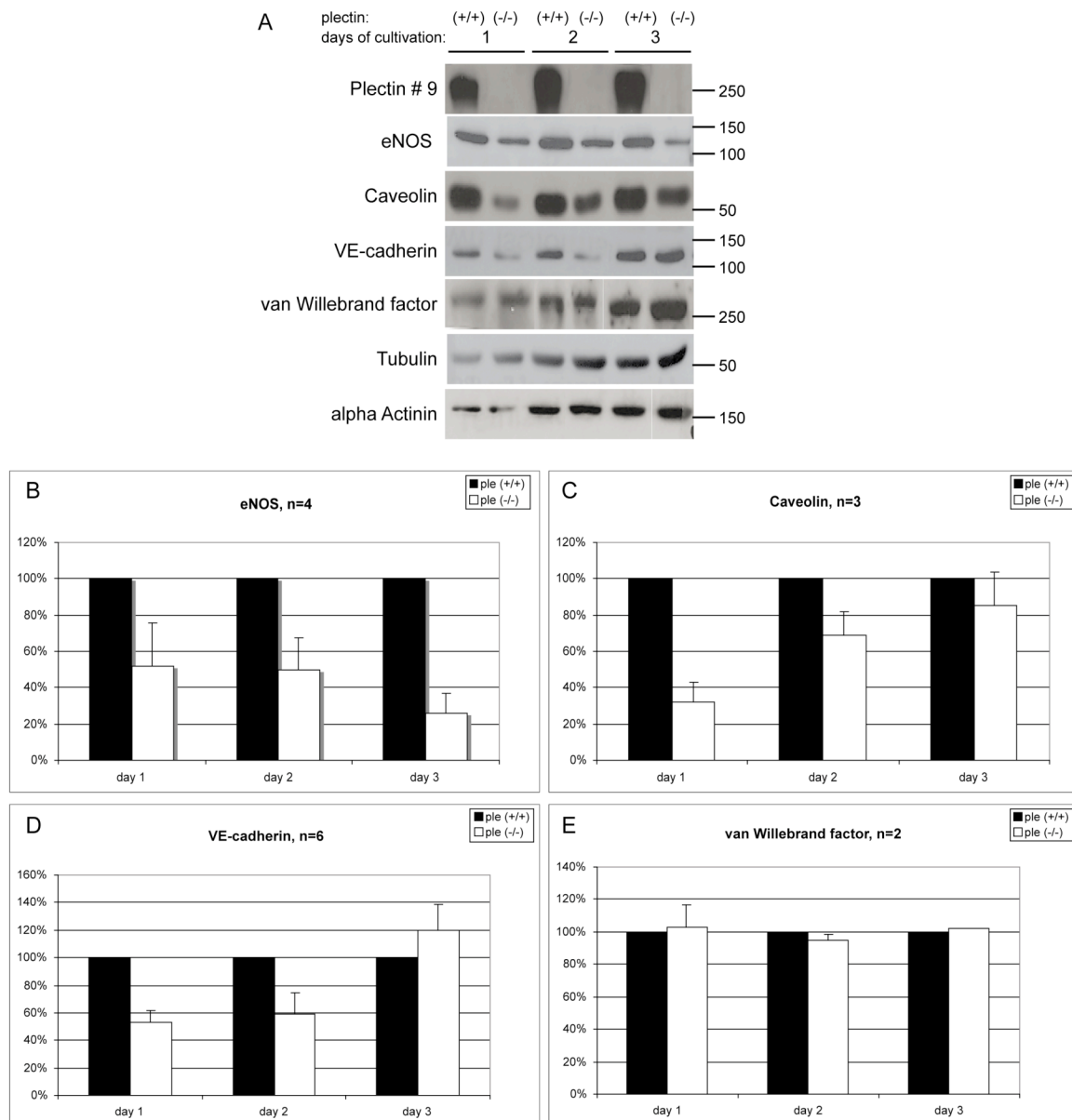


Fig. 12. EC marker expression in DH-1 cells. Plectin<sup>+/+</sup> and plectin<sup>-/-</sup> cells were lysed after 1, 2 and 3 days of cultivation and analysed by immunoblotting using specific primary antibodies and HRP-conjugated secondary antibodies. *Tubulin*: loading control (A). Statistic evaluation of eNOS (B), caveolin (C), VE-cadherin (D) and vWf (E). Blots were scanned and quantified by Quantiscan and standard deviation was calculated. Abbreviations: n: number of blots scanned.

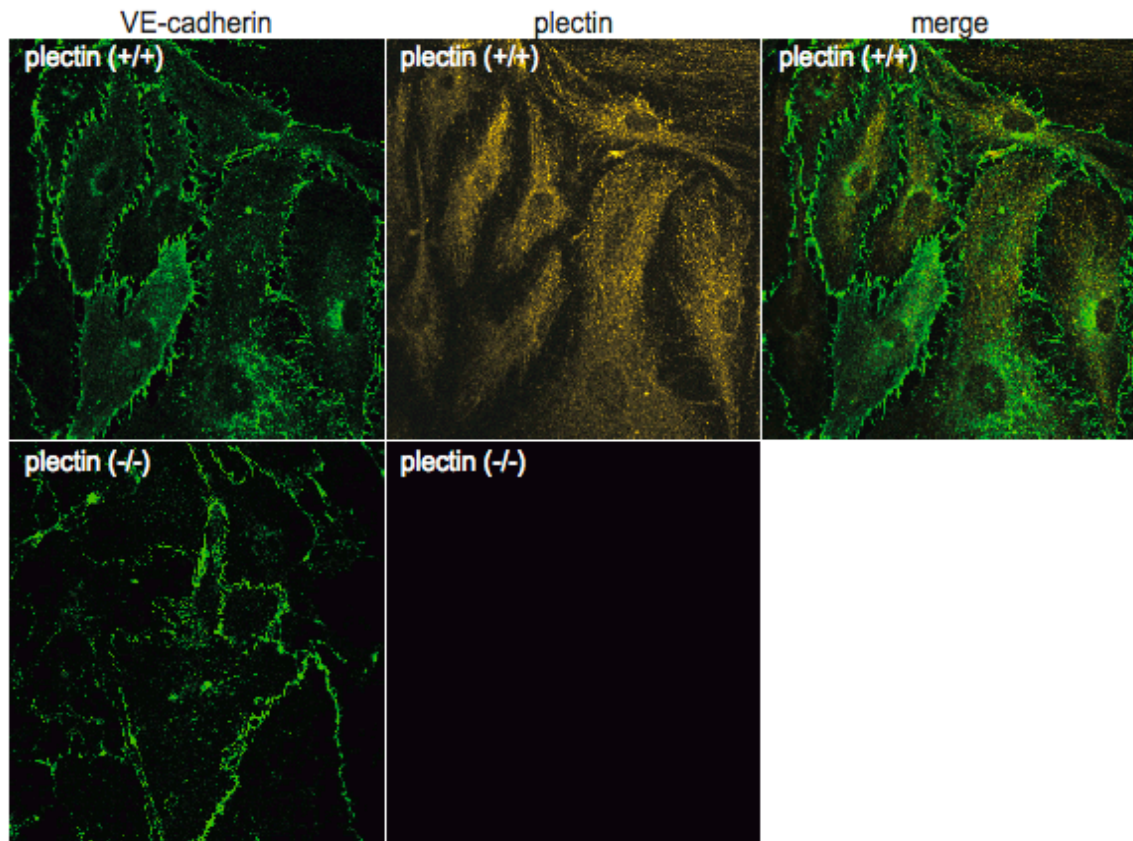


Fig. 13. Immunofluorescence microscopy using anti-plectin antiserum #46 and mAb to VE-cadherin in plectin<sup>+/+</sup> and plectin<sup>-/-</sup> of DH-1 cells.

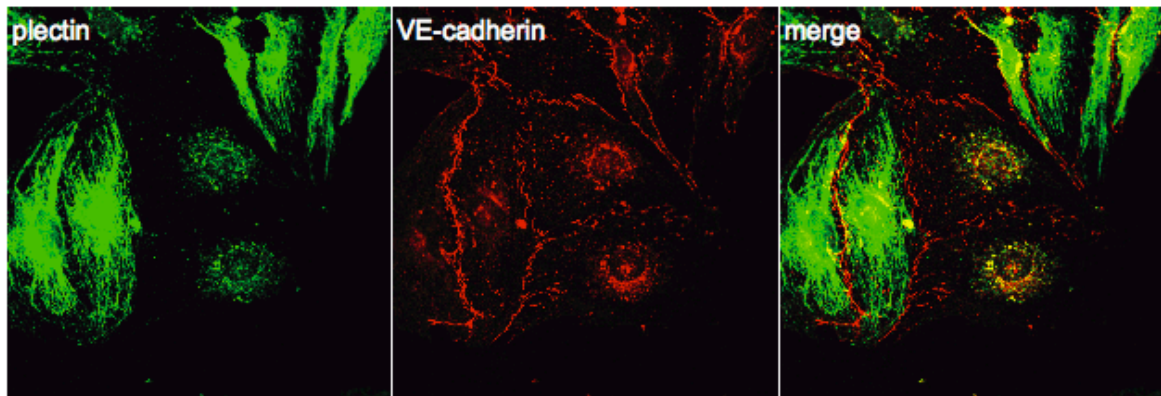


Fig. 14. Immunofluorescence microscopy using anti-plectin antiserum #46 and mAb to VE-cadherin of plectin<sup>+/+</sup> and plectin<sup>-/-</sup> mixed cultures of DH-1 cells.

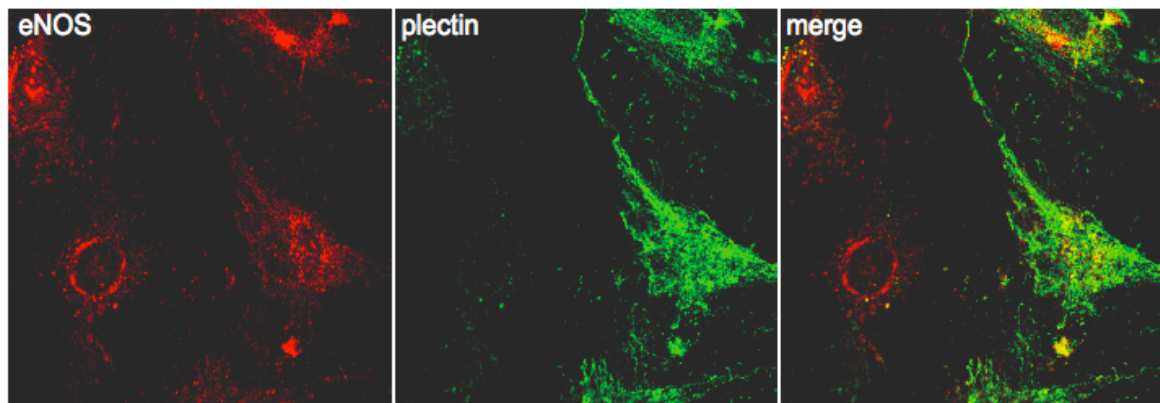


Fig. 15. Immunofluorescence microscopy using anti-plectin antiserum #46 and mAb to eNOS of plectin<sup>+/+</sup> and plectin<sup>-/-</sup> mixed cultures of DH-1 cells.

#### 4.4. Plectin Isoform expression in endothelial cells

Plectin isoform expression in pT Endo cells and DH-1 cells was checked by immunoblotting using specific plectin isoform antibodies. Plectin<sup>+/+</sup> keratinocyte and plectin<sup>+/+</sup> fibroblast lysates were used as positive controls for plectin isoforms 1a and 1c, and isoforms 1 and 1f, respectively. As shown in Fig. 16 DH-1 and pT Endo cells express plectin isoforms 1a and 1.

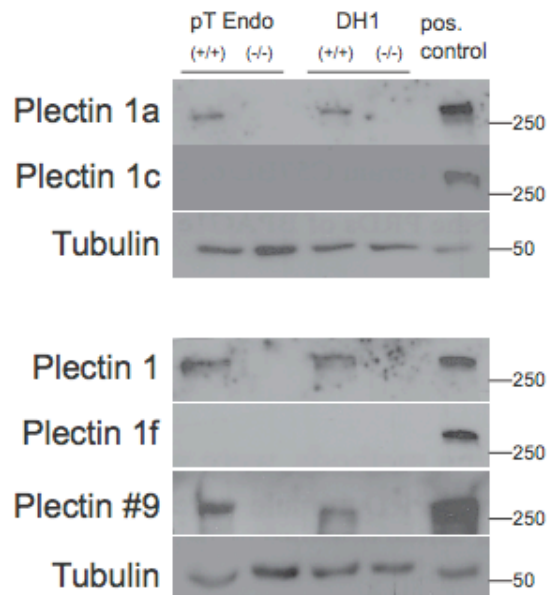


Fig. 16. Plectin isoform expression in DH-1 and pT Endo cells. Plectin<sup>+/+</sup> and plectin<sup>-/-</sup> pT Endo (left column) and DH-1 (middle column) cells were lysed and analysed by immunoblotting using specific plectin-isoform antibodies. *Tubulin*: loading control.

Since only four isoform-specific antibodies were available it would be necessary to perform RNase protection assay to further check the expression of other isoforms in these cell lines. These data indicated that at least plectin isoforms 1a and 1 are expressed in plectin<sup>+/+</sup> cells of both cell lines. Plectin isoforms 1c and 1f are not expressed in these cell lines (Fig. 16)

#### **4.5. Measurement of NO production**

It has already been shown that vimentin filament system of plectin<sup>-/-</sup> pT Endo is much more fragile to SNAP treatment in comparison to that of plectin<sup>+/+</sup> pT Endo cells. Therefore, we wanted to check how plectin<sup>-/-</sup> cells cope with endogenous levels of NO produced by eNOS. DAF-2 based extracellular NO measurement assay (see Material and Methods) was performed in cooperation with the group of Verena Dirsch at the Institute of Pharmacognosy (Vienna). Cells were either left untreated, treated with phorbol-12-myristate-13 acetate (PMA) to induce a maximum eNOS expression or treated with N<sup>G</sup>-monomethyl-L-arginine (L-NAME) to completely inhibit eNOS activity.

In NO production assay performed in pT Endo cells (Fig. 17A) the eNOS activity in untreated plectin<sup>+/+</sup> pT Endo cells was set arbitrary to 100% increasing after PMA treatment to 200 %. In plectin<sup>-/-</sup> pT Endo cells no eNOS activity was detected neither in untreated nor in PMA-treated cells. After treatment with eNOS inhibitor L-NAME eNOS activity was depleted in both cell types (Spurny et al., unpublished data).

Both plectin<sup>+/+</sup> and plectin<sup>-/-</sup> DH-1 cells produced NO, however, plectin<sup>-/-</sup> cells still produced less (~10 %) in comparison to their wildtype counterparts (Fig. 17B). PMA treatment of plectin<sup>+/+</sup> led to a potent increase of eNOS activity to 160 %, whereas in plectin<sup>-/-</sup> DH-1 cells only a slight increase to 98 % was detectable. Treatment with L-NAME led to complete depletion of NO production in both cell types.

NO production measurements were also performed with primary ECs (Fig. 17C) isolated from kidneys and lungs of plectin<sup>+/+</sup> and plectin<sup>-/-</sup> mice. Primary plectin<sup>-/-</sup> ECs isolated from kidneys showed a reduction in NO production in

comparison to plectin<sup>+/+</sup> cells. In ECs isolated from lungs we observed a reversed phenotype, plectin<sup>+/+</sup> ECs were producing less NO than plectin<sup>-/-</sup> ECs. It must be noted, however, that the results of primary ECs were not very reliable due to a very low efficiency of cell isolation.

Together, these findings demonstrated that plectin<sup>-/-</sup> ECs produce less NO in comparison to plectin<sup>+/+</sup> ECs. Furthermore, in contrast to strong eNOS activation observed in plectin<sup>+/+</sup> ECs after PMA treatment only a negligible eNOS activation was observed in plectin<sup>-/-</sup> ECs.

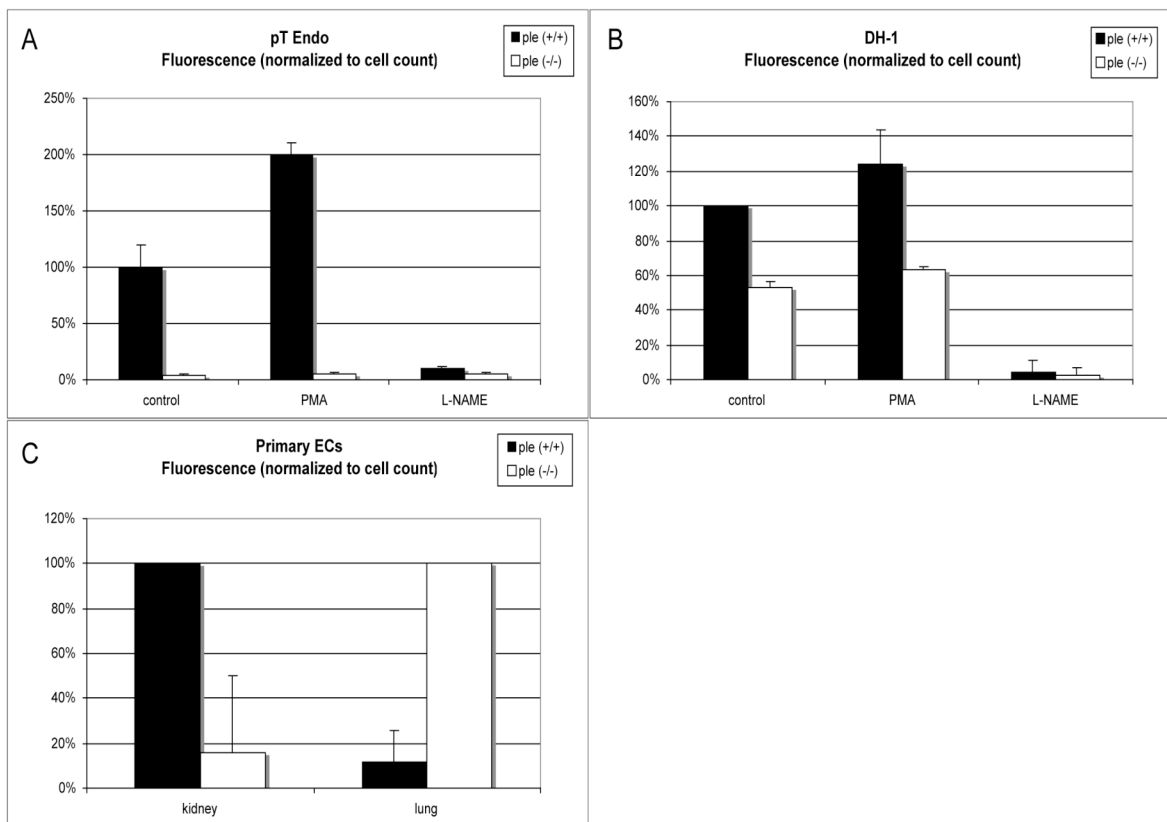


Fig. 17. Measurement of NO production in pT Endo cells  $n=3$  (A), DH-1 cells  $n=2$  (B) and primary ECs isolated from kidneys or lungs (C). Prior to measurement cells were either left untreated (*control*), treated with *PMA* or with *L-NAME*.

#### 4.6. Ser<sup>1177</sup> and Thr<sup>495</sup> Phosphorylation of eNOS

To further investigate if reduced NO production in plectin<sup>-/-</sup> ECs is due to the fact that eNOS is less expressed in these cells immunoblotting using specific phospho-Thr<sup>495</sup> and phospho-Ser<sup>1177</sup> antibodies was performed. The activation



and inactivation status of eNOS were monitored with anti-phospho-Ser<sup>1177</sup> and anti-phospho-Thr<sup>495</sup>, respectively.

eNOS protein levels (see also Fig. 6B and 12B) and activity (Fig. 17) were checked after 1, 2 and 3 days of cell cultivation. Later was particularly of interest since at this day NO production was measured (see Fig.17). Tubulin was used as a loading control.

As shown in Fig. 6A and 12A total eNOS amounts are reduced in plectin<sup>-/-</sup> ECs in comparison to plectin<sup>+/+</sup> ECs after 1, 2, or 3 days of cultivation (Fig. 18A).

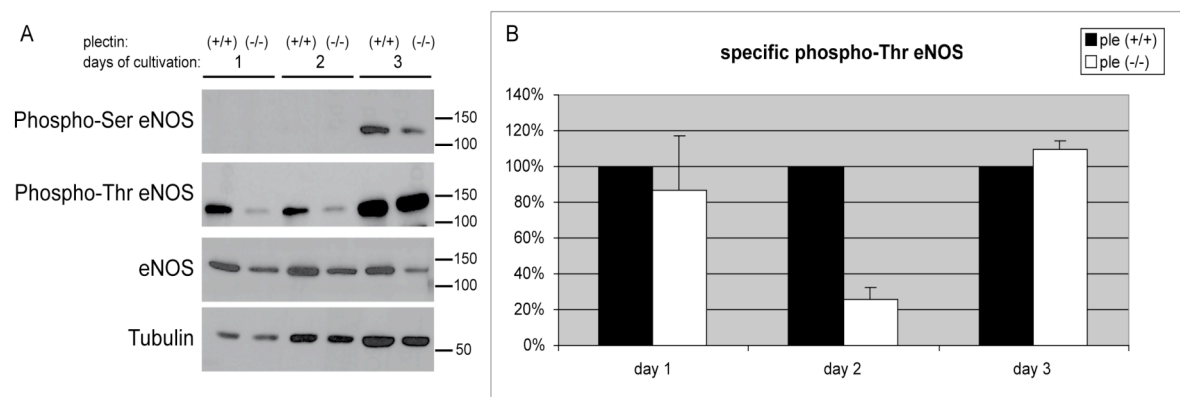


Fig. 18. eNOS phosphorylation status of plectin<sup>+/+</sup> and plectin<sup>-/-</sup> DH-1 cells. Cells were lysed after 1, 2, or 3 days of cultivation and analysed by immunoblotting using specific antibodies against eNOS, P-Ser<sup>1177</sup>, P-Thr<sup>495</sup>. *Tubulin*: loading control (A) Thr<sup>495</sup> phosphorylation at the third day of cultivation calculated by Quantiscan software and plotted against eNOS values. n=2 (B)

At day 1 and 2 no phospho-Ser<sup>1177</sup> could be detected. Only at day 3 Ser<sup>1177</sup> phosphorylation of plectin<sup>+/+</sup> and plectin<sup>-/-</sup> DH-1 cells was observed, however, slightly reduced in plectin<sup>-/-</sup> cells (Fig. 18A). At the first two days of cultivation specific-Thr<sup>495</sup> phosphorylation was reduced in plectin<sup>-/-</sup> cells in comparison to plectin<sup>+/+</sup> cells. At day 3 specific Thr<sup>495</sup> phosphorylation increased ~ 15 % in plectin<sup>-/-</sup> DH-1 cells in comparison to plectin<sup>+/+</sup> cells (Fig. 18B). Specific phospho-Ser<sup>1177</sup> eNOS was slightly decreased, whereas specific phospho-Thr<sup>495</sup> eNOS was significantly increased in plectin<sup>-/-</sup> compared to plectin<sup>+/+</sup> ECs (Fig. 18). Thus, this data indicated that plectin<sup>-/-</sup> DH-1 cells have reduced levels of total eNOS but also less active eNOS.

#### 4.7. Cell fractionation of endothelial cells

Caveolin, eNOS and VE-cadherin show different expression patterns in total lysates of plectin<sup>+/+</sup> and plectin<sup>-/-</sup> pT Endo and DH-1 cells. To check if the localisation of these proteins is influenced by plectin deficiency digitonin-based cell fractionation experiments were performed in both cell types. Cell fractions were analysed by immunoblotting, scanned and quantified by Quantiscan software (see Materials and Methods) followed by statistic evaluation (Tab. 8, 9).

eNOS was found increased in the membrane fraction of plectin<sup>-/-</sup> compared to plectin<sup>+/+</sup> pT Endo cells, with a corresponding reduction in cytoskeleton fraction. A slight increase of eNOS in plectin<sup>-/-</sup> cells compared to plectin<sup>+/+</sup> cells was also detected in the cytosolic fraction (Fig. 19A). Compared to plectin<sup>+/+</sup> cells plectin<sup>-/-</sup> cells show drastic increase of caveolin in membrane fraction at the expense of the cytoskeleton fraction (Fig. 19B). Similar to caveolin and eNOS, VE-cadherin was increased in membrane fraction and reduced in cytoskeleton fraction of plectin<sup>-/-</sup> compared to plectin<sup>+/+</sup> pT Endo cells. In cytosolic fractions no, or very low levels of VE-cadherin were detected (Fig. 19C).

Cell fractionation experiments performed in DH-1 cells resulted in a more or less similar distribution of caveolin, eNOS and VE-cadherin compared to pT Endo cells. The protein levels were increased in membrane fraction of plectin<sup>-/-</sup> cells compared to plectin<sup>+/+</sup> cells with a corresponding reduction in cytoskeleton fraction (Fig. 20). It has to be noted that all of these proteins were found increased in the cytosolic fractions of both plectin<sup>+/+</sup> and plectin<sup>-/-</sup> DH-1 cells, compared to pT Endo cells (compare Fig. 19 with Fig. 20).

	plectin	fractions		
		cytosol	membrane	cytoskeleton
<b>Caveolin</b>	+	2±3	33±4	65±1
	-	1±0	75±14	24±9
<b>eNOS</b>	+	8±8	63±9	29±16
	-	12±7	78±15	10±9
<b>VE-cadherin</b>	+	4±1	26±1	70±1
	-	2±2	48±9	50±11

Tab. 8. Mean values ± S. D. of cell fractionation experiments in pT Endo cells.

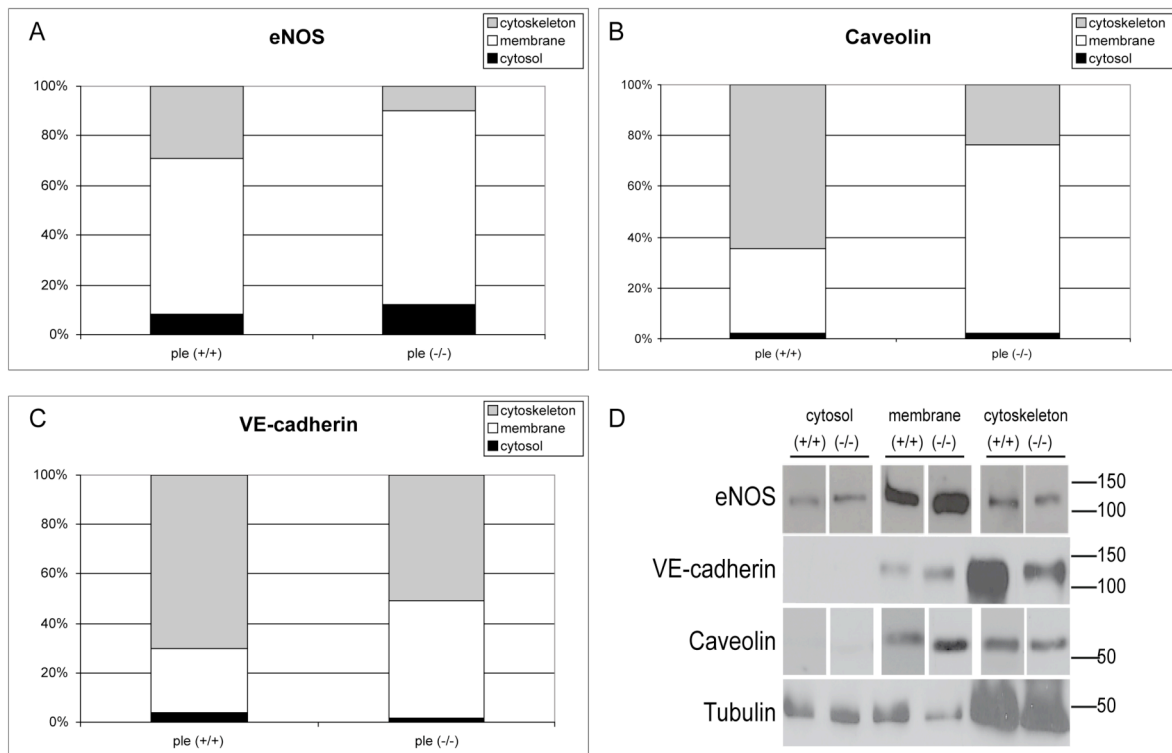


Fig. 19. Cell fractionation of pT Endo cells: Bar digrams showing cytosolic (black), membrane (white) and cytoskeleton (grey) fraction subjected to immunoblotting using specific antibodies against eNOS (A), caveolin (B), and VE-cadherin (C). Representative blot of cell fractions (D) (eNOS: membrane fraction longer exposed; VE-cadherin: same gel; caveolin: same gel; membrane fraction longer exposed; representative tubulin blot); Concentrations: cytosol: membrane: cytoskeleton= 8:8:1. Protein bands (n=5) were scanned and quantified by Quantiscan

In conclusion the data obtained from cell fractionation experiments showed that caveolin, eNOS and VE-cadherin are found increased in membrane fractions and cytosolic fractions of plectin<sup>-/-</sup> cells compared to plectin<sup>+/+</sup> ECs, at the expense of the cytoskeleton fractions.

	plectin	fractions		
		cytosol	membrane	cytoskeleton
<b>Caveolin</b>	+	25±13	13±6	62±25
	-	23±8	46±6	31±15
<b>eNOS</b>	+	20±9	24±16	56±16
	-	21±9	55±1	24±11
<b>VE-cadherin</b>	+	19±7	43±9	38±5
	-	23±4	59±5	17±9

Tab.9. Mean values ± S. D. of cell fractionation experiments in DH-1 cells.

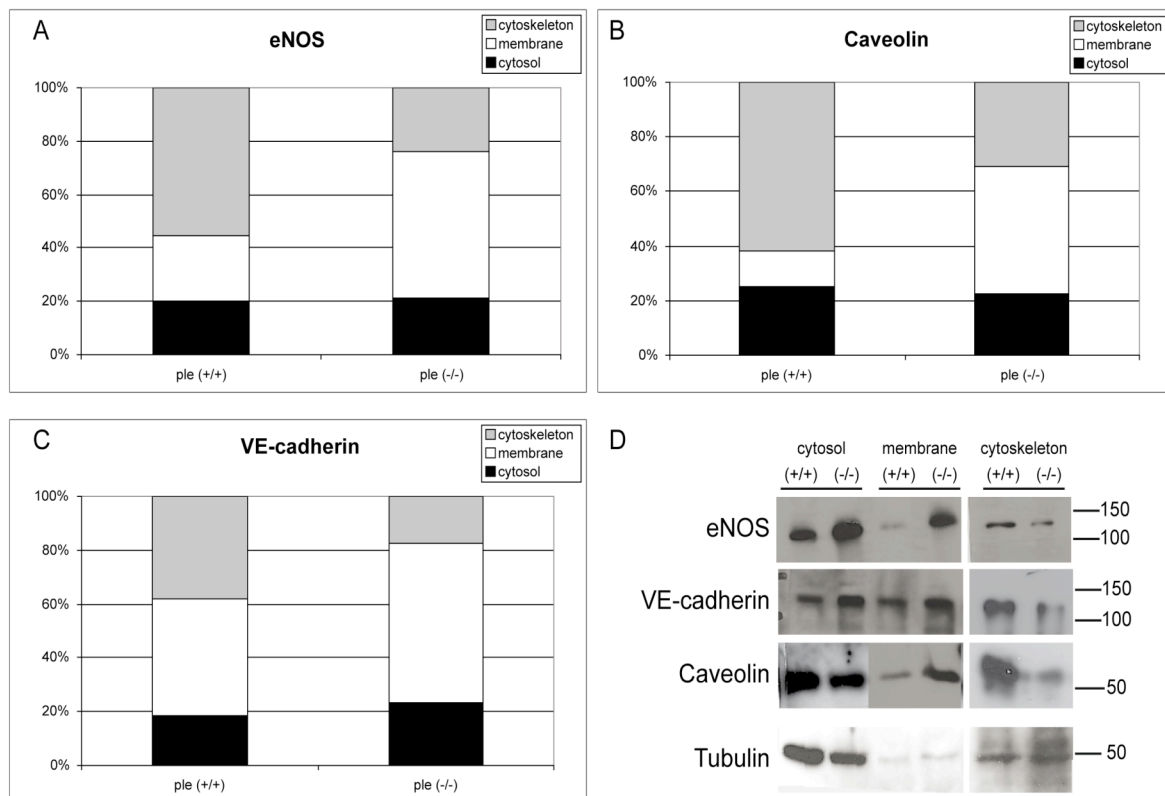


Fig. 20. Cell fractionation of DH-1 cells: Bar digrams showing cytosolic (black), membrane (white) and cytoskeleton (grey) fraction subjected to immunoblotting using specific antibodies against eNOS (A), caveolin (B) and VE-cadherin (C). Representative blot of cell fractions (D) (eNOS: cytosolic and membrane fraction: same gel; VE-cadherin; cytosolic and membrane fraction: same gel; caveolin: cytosolic and cytoskeletal fraction from same gel; tubulin: representative blot; same gel as VE-cadherin). Concentrations: cytosol: membrane: cytoskeleton= 4:2:1. Protein bands (n=4) were scanned and quantified by Quantiscan.

#### 4.8. Angiogenesis – Matrigel assay

ECs play an essential role in angiogenesis. New blood capillaries are formed by sprouting from pre-existing ECs (Speidel, 1933). Matrigel, a basement membrane matrix, is a gelatinous protein mixture secreted by mouse tumor cells. It is known that cloned capillary ECs, cultured in tumour-conditioned medium, form capillary tubes in vitro (Folkman et al., 1980).

Tubing formation of DH-1 cells grown on matrigel for 6 h did not show any differences between plectin<sup>+/+</sup> and plectin<sup>-/-</sup> cells (Fig. 21). This result would need further investigation at shorter growth time or under different conditions to

completely exclude the eventual role of plectin in tubing formation and angiogenesis.

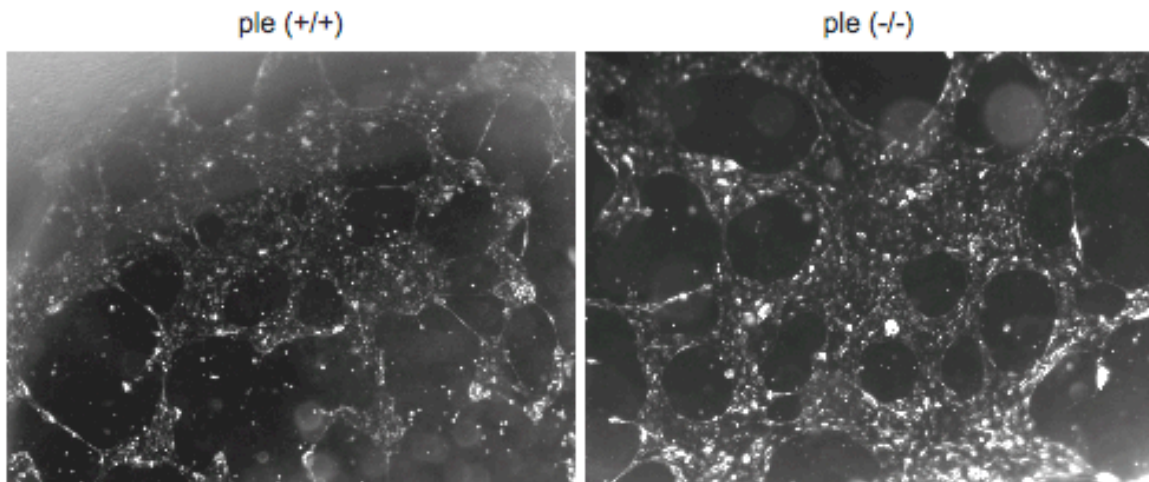


Fig. 21. Phase-contrast images of plectin<sup>+/+</sup> and plectin<sup>-/-</sup> DH-1 cells grown on matrigel.

#### **4.9. Effects of shear stress on plectin<sup>+/+</sup> and plectin<sup>-/-</sup> endothelial cells**

Functions of ECs are modulated by mechanical stimuli (like shear stress resulting from blood pressure and flow) that activate mechano-sensors on the cell membrane. These in turn activate different signalling pathways modulating the activation state and the expression of different proteins (Chien, 2006). Hemodynamic forces lead to a reorientation of cells parallel to the direction of flow. All three cytoskeletal networks adapt their structure in response to shear stress: microtubules IFs elongate with the cell shape, whereas F-actin bundles disassemble, forming aligned stress fibers (Helmke, 2005).

To determine eventual differences in the response of plectin<sup>+/+</sup> and plectin<sup>-/-</sup> ECs to fluid shear stress flow experiments with a flow rate of 5 dynes/cm<sup>2</sup> for 1, 6 and 24 h were performed with both pT Endo and DH-1 cells. After exposure to fluid shear stress, cells were either fixed and immunofluorescently stained or lysed and analysed by immunoblotting. Effects of shear stress on eNOS, cave-

olin, VE-cadherin, plectin and on all cytoskeletal filaments (microtubules, actin and vimentin) were investigated.

#### 4.9.1. Effects of shear stress on protein levels and localization of eNOS, vimentin and plectin

Laminar shear affects endothelial NO production via activating eNOS within seconds and via increasing eNOS mRNA and protein levels within hours after initiation of flow stress (Harrison et. al, 2006).

Immunofluorescence microscopy of eNOS was diffuse and punctated in plectin<sup>+/+</sup> and plectin<sup>-/-</sup> pT Endo and DH-1 cells under control conditions. In response to laminar shear the staining became more prominent in plectin<sup>+/+</sup> cells dependent on the duration of flow. Plectin<sup>-/-</sup> DH-1 cells showed reduced intensity of eNOS compared to plectin<sup>+/+</sup> cells irrespectively to duration of fluid shear stress (Fig. 22, 24).

For better comparison of plectin<sup>+/+</sup> and plectin<sup>-/-</sup> cells the eNOS signal intensity in mixed plectin<sup>+/+</sup> and plectin<sup>-/-</sup> DH-1 cultures were analysed. The staining was weak and punctated under no-flow conditions, however, being slightly more prominent in plectin<sup>+/+</sup> cells. After 1 and 6 h of fluid shear stress the fluorescence signal of eNOS became more intense in both plectin<sup>+/+</sup> and plectin<sup>-/-</sup> cells dependent on the duration of fluid shear stress, but it was still less prominent in plectin<sup>-/-</sup> DH-1 cells. The intensity for eNOS was higher in plectin<sup>+/+</sup> cells, subjected to 6 h of flow than in cells subjected to 1 hour of fluid shear stress (Fig. 23).

Taken together, these shear stress data revealed an eNOS up-regulation in both plectin<sup>+/+</sup> pT Endo and plectin<sup>+/+</sup> DH-1 cells but no up-regulation in plectin<sup>-/-</sup> pT Endo cells and very slight up-regulation in plectin<sup>-/-</sup> DH-1 cells in response to 1, 6 and 24 h of fluid shear stress.

As expected, no colocalization between eNOS and vimentin could be observed under static. However, a slight colocalization was observed when eNOS signal became more intense in plectin<sup>+/+</sup> cells under flow conditions. Under static conditions vimentin network of plectin<sup>+/+</sup> DH-1 cells was more

compact and organized, whereas that of plectin<sup>-/-</sup> DH-1 cells was more flattened and disorganized (Fig. 24A). In response to shear stress plectin<sup>+/+</sup> vimentin network became flattened and cells tried to orientate in the direction of flow (Fig. 24C). Since cell density was very high, plectin<sup>+/+</sup> cells did not manage to re-orientate completely (Fig. 24B, D). Shear stress did not seem to induce the re-orientation of plectin<sup>-/-</sup> DH-1 cells to flow (Fig. 24B, C, D). Vimentin network of plectin<sup>-/-</sup> DH-1 cells stayed more or less disorganized irrespectively to subjection to fluid shear stress.

Similar changes of vimentin network were observed in pT Endo cells. However, more prominent disorganization of vimentin network was observed in plectin<sup>-/-</sup> pT Endo cells in comparison to plectin<sup>+/+</sup> cells. Vimentin staining was filamentous in plectin<sup>+/+</sup> pT Endo under static conditions. In plectin<sup>-/-</sup> pT Endo cells vimentin structure was star-like and progresses reached the cell periphery under no-flow conditions (Fig. 25A). Cell periphery could be nicely detected by VE-cadherin staining. Similar to DH-1 cells, vimentin staining of plectin<sup>+/+</sup> pT Endo cells was more prominent and cells seemed to orientate in the direction of flow while the vimentin network of plectin<sup>-/-</sup> cells did not show drastic changes upon onset of fluid shear stress (Fig. 25B).

Immunofluorescence microscopy of VE-cadherin cells showed a discontinuous pattern at the cell periphery of plectin<sup>+/+</sup> and plectin<sup>-/-</sup> pT Endo cells (Fig. 25A). After exposure to laminar shear the fluorescence signal for VE-cadherin became more intense in plectin<sup>+/+</sup> pT Endo cells, whereas a slight increase was detectable in plectin<sup>-/-</sup> cells (Fig. 25B).

Plectin is known to be up-regulated upon shear stress (Garcia-Carena et al, 2001). Also in plectin<sup>+/+</sup> pT Endo and DH-1 cells an increase of plectin expression was detectable after exposure to laminar shear for 1, 6 and 24 h (data not shown). The most significant increase of plectin was observed after 1 h of fluid shear stress (Fig. 23).

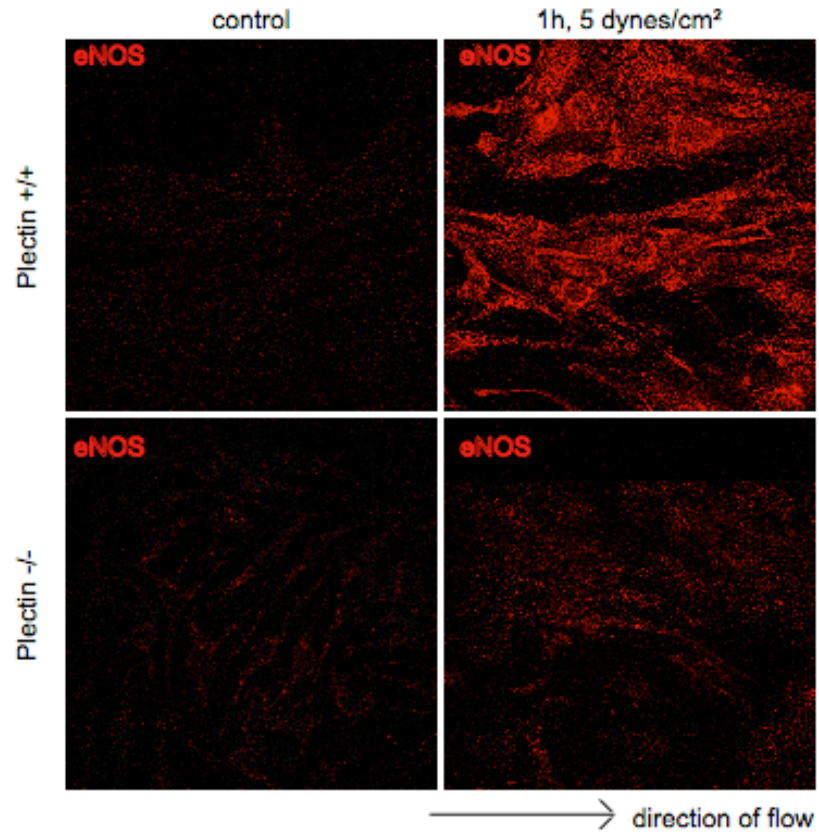


Fig. 22. Immunofluorescence microscopy of eNOS in plectin+/+ and plectin-/- pT Endo cells under static conditions and after 1 h of fluid shear stress (5 dynes/cm<sup>2</sup>). Magnification x 63



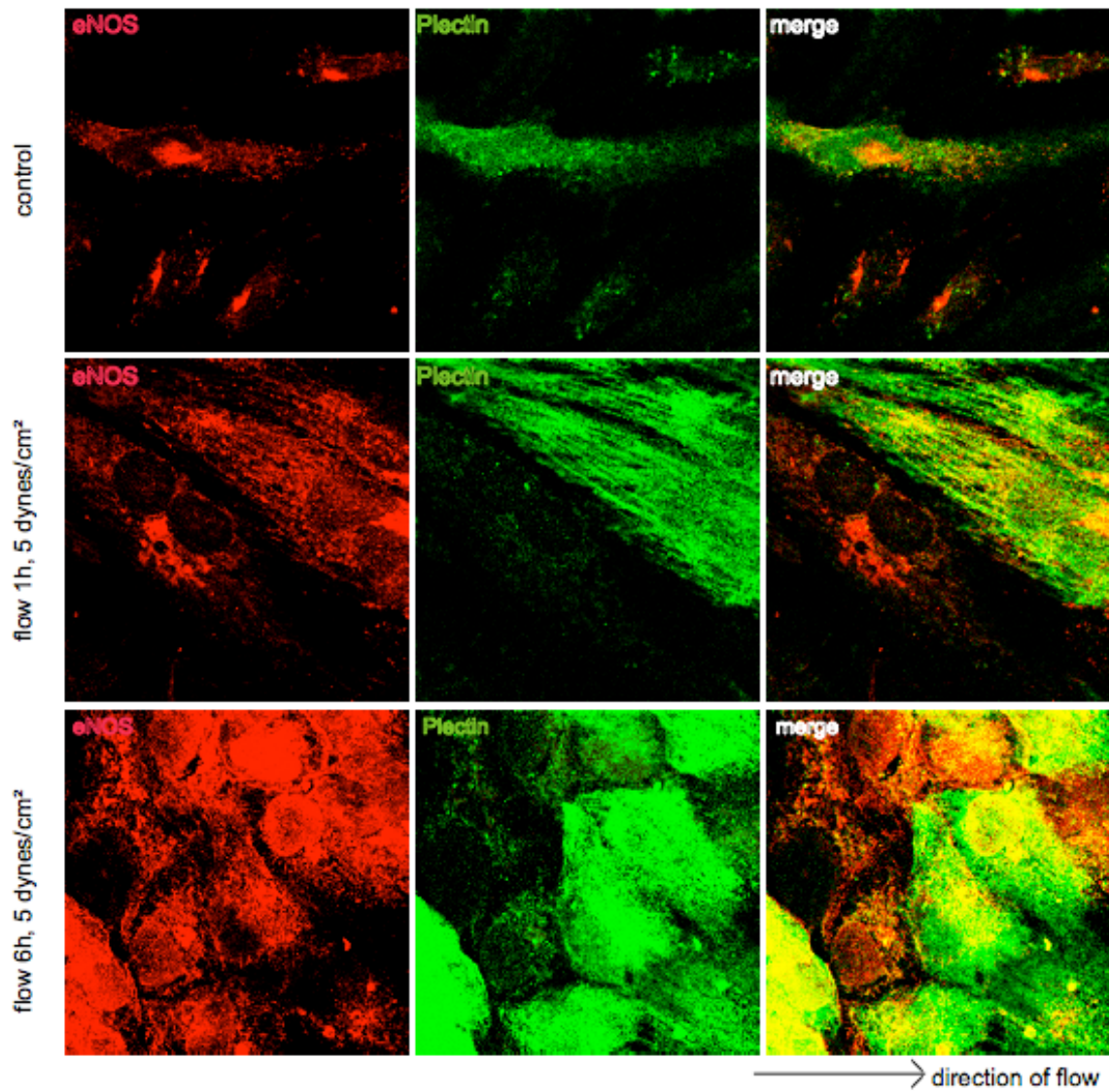


Fig. 23. Immunofluorescence microscopy of eNOS and plectin in plectin<sup>+/+</sup> and plectin<sup>-/-</sup> DH-1 mixed cultures under static conditions, after 1 h and 6 h of fluid shear stress (5 dynes/cm<sup>2</sup>). Magnification x 100

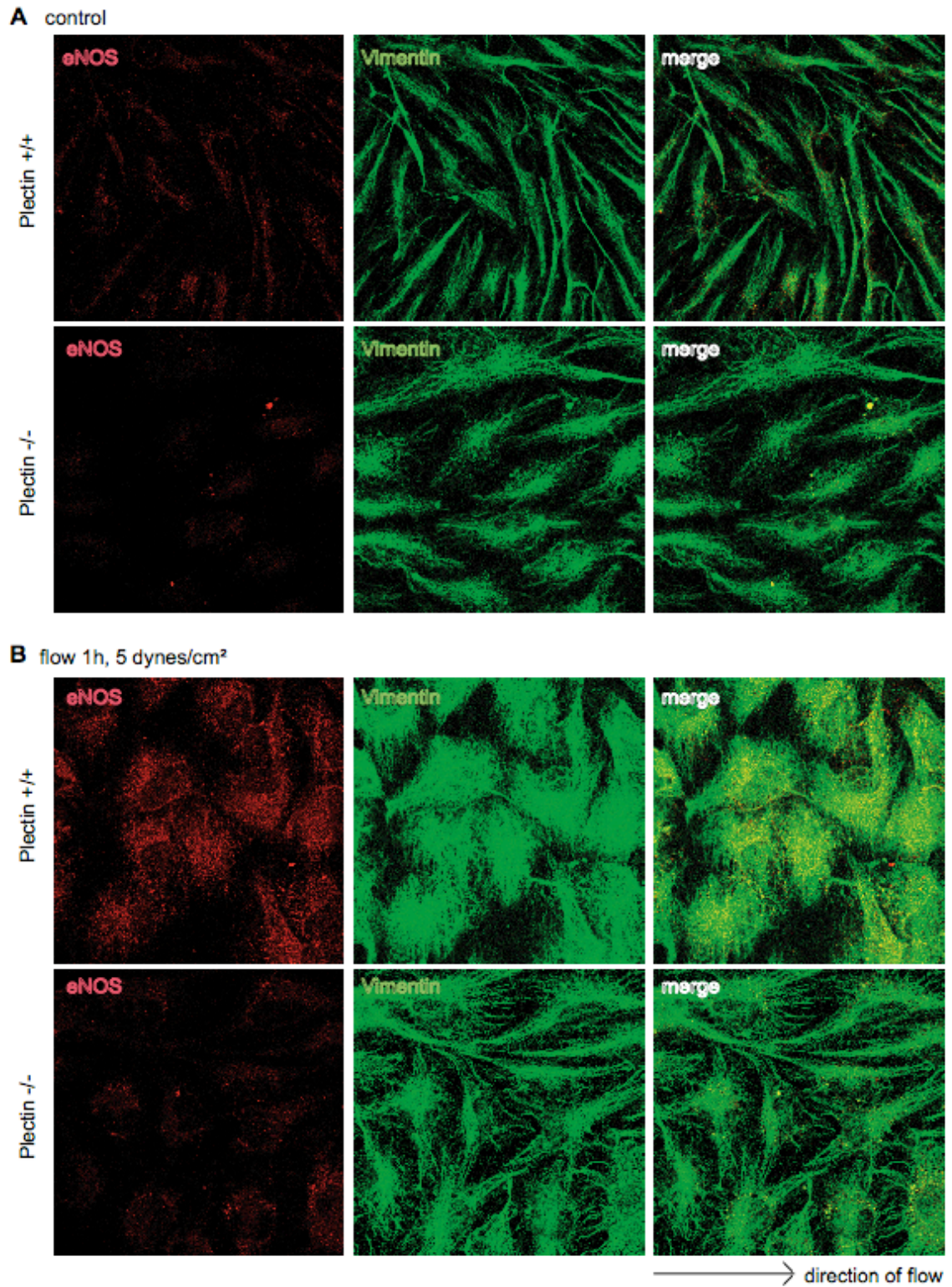


Fig. 24 A, B. Immunofluorescence microscopy of eNOS and vimentin in plectin<sup>+/+</sup> and plectin<sup>-/-</sup> DH-1 cells under static conditions (A) and after 1 h (B), 6 h (C) and 24 h (D) of fluid shear stress. (5 dynes/cm<sup>2</sup>). Magnification x 63

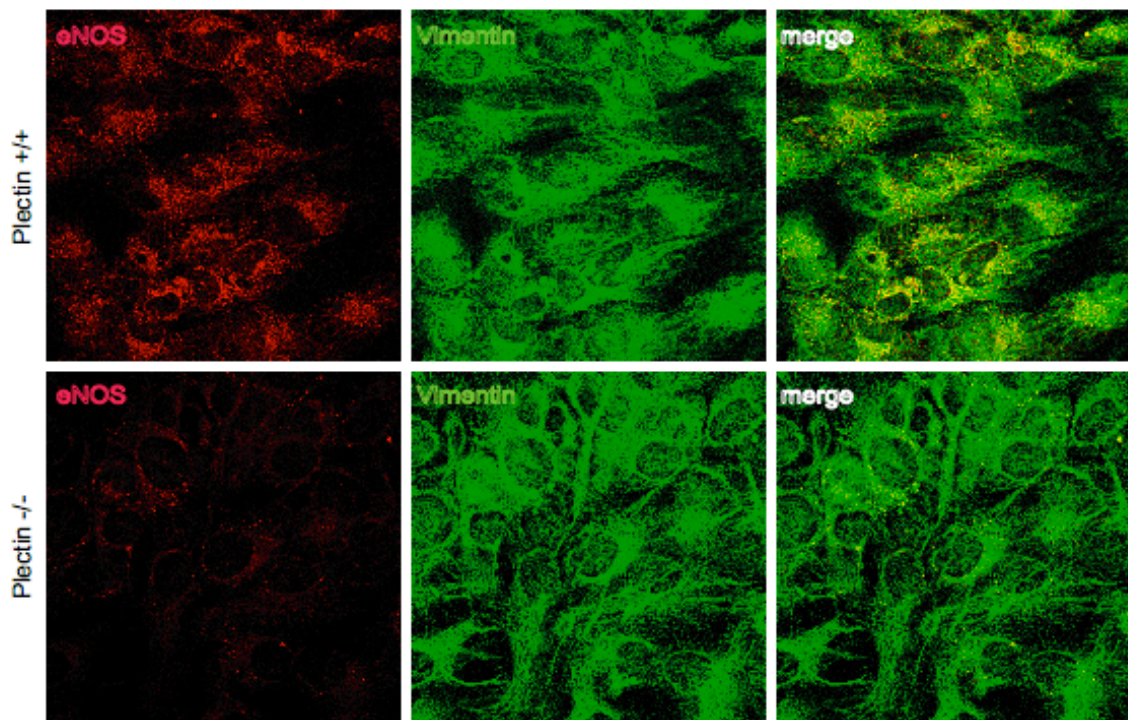
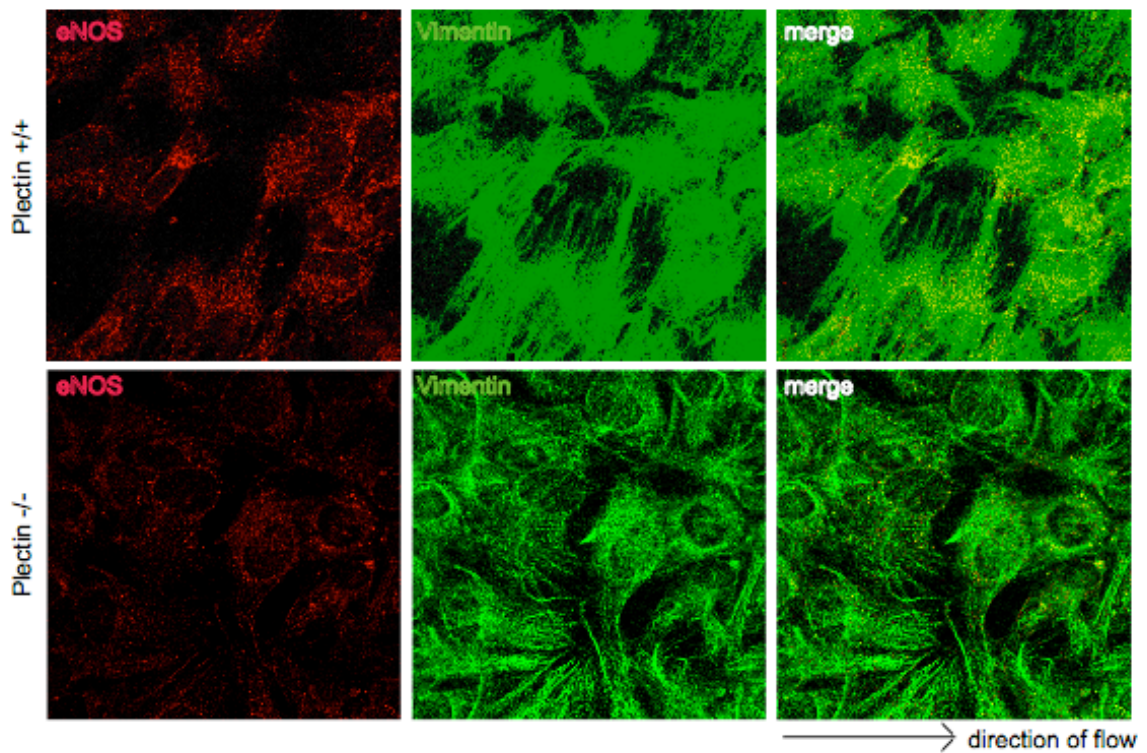
**C** flow 6h, 5 dynes/cm<sup>2</sup>**D** flow 24 h, 5 dynes/cm<sup>2</sup>

Fig. 24 C, D. Immunofluorescence microscopy of eNOS and vimentin in plectin<sup>+/+</sup> and plectin<sup>-/-</sup> DH-1 cells under static conditions (A) and after 1 h (B), 6 h (C) and 24 h (D) of fluid shear stress. (5 dynes/cm<sup>2</sup>). Magnification x 63

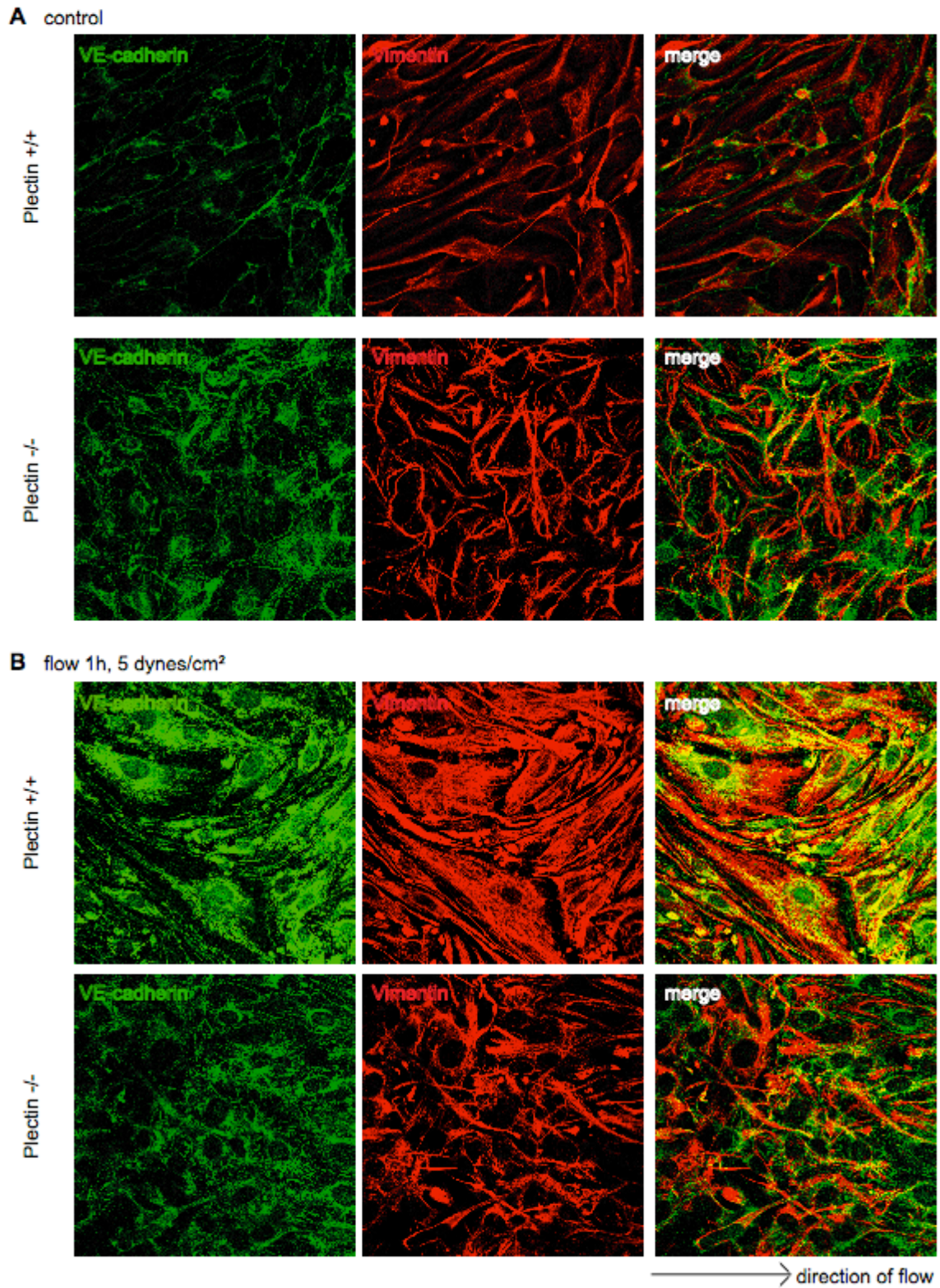


Fig. 25. Immunofluorescence microscopy of VE-cadherin and vimentin in plectin<sup>+/+</sup> and plectin<sup>-/-</sup> pT Endo cells under static conditions (A) and after 1 h (B) of fluid shear stress (5 dynes/cm<sup>2</sup>). Magnification x 63

#### 4.9.2. Effects of shear stress on protein levels and localization of caveolin-1 and tubulin

Exposure to shear stress affects caveolin localization and expression and increases caveolae density. Flow-preconditioned cells expressed a fivefold increase in caveolin compared to no-flow controls (Rizzo et. al, 2003).

Immunofluorescence microscopy of the caveolar coat protein caveolin showed a punctate pattern in plectin<sup>+/+</sup> and plectin<sup>-/-</sup> pT Endo and DH-1 cells under static conditions. However, the fluorescence signal for caveolin was more intense plectin<sup>+/+</sup> pT Endo cells compared to plectin<sup>-/-</sup> cells. After exposure to shear stress caveolin signal intensity increased in both plectin<sup>+/+</sup> and plectin<sup>-/-</sup> pT Endo and DH-1 cells but was still reduced in plectin<sup>-/-</sup> cells (Fig. 26, 27).

After 1 hour of fluid shear stress a slight increase of caveolin signal intensity in plectin<sup>+/+</sup> and plectin<sup>-/-</sup> DH-1 cells was detected (Fig. 27B). After 6 and 24 h caveolin staining was very intense in plectin<sup>+/+</sup> DH-1 cells. Also in plectin<sup>-/-</sup> DH-1 cells an enhancement of the signal was observed, however, less prominent compared to plectin<sup>+/+</sup> DH-1 cells (Fig. 27C, D).

These results showed a slightly reduced intensity for caveolin in plectin<sup>-/-</sup> compared to plectin<sup>+/+</sup> cells in both pT Endo and DH-1 under static conditions. Upon onset of flow stress for 1, 6 and 24 h an up-regulation of caveolin was observed in both cell types although to less extent in plectin<sup>-/-</sup> cells.

After 6 and 24 h of laminar shear stress a colocalization of tubulin and caveolin was observed in both plectin<sup>+/+</sup> and plectin<sup>-/-</sup> cells, however, being more significant in plectin<sup>+/+</sup> DH-1 cells (Fig. 27C, D). Between plectin<sup>+/+</sup> and plectin<sup>-/-</sup> DH-1 cells no obvious difference concerning the microtubule network organization was observed. The tubulin staining in both plectin<sup>+/+</sup> and plectin<sup>-/-</sup> DH-1 was showing a compact and aligned filamentous network under static conditions (Fig. 27A). After exposure to fluid shear stress for 1 and 6 h microtubule network got flattened and widespread in both cell types (Fig. 27B, C). Upon 24 h of shear stress microtubule signal intensity slightly increased in both plectin<sup>+/+</sup> and plectin<sup>-/-</sup> DH-1 cells (Fig. 27D).

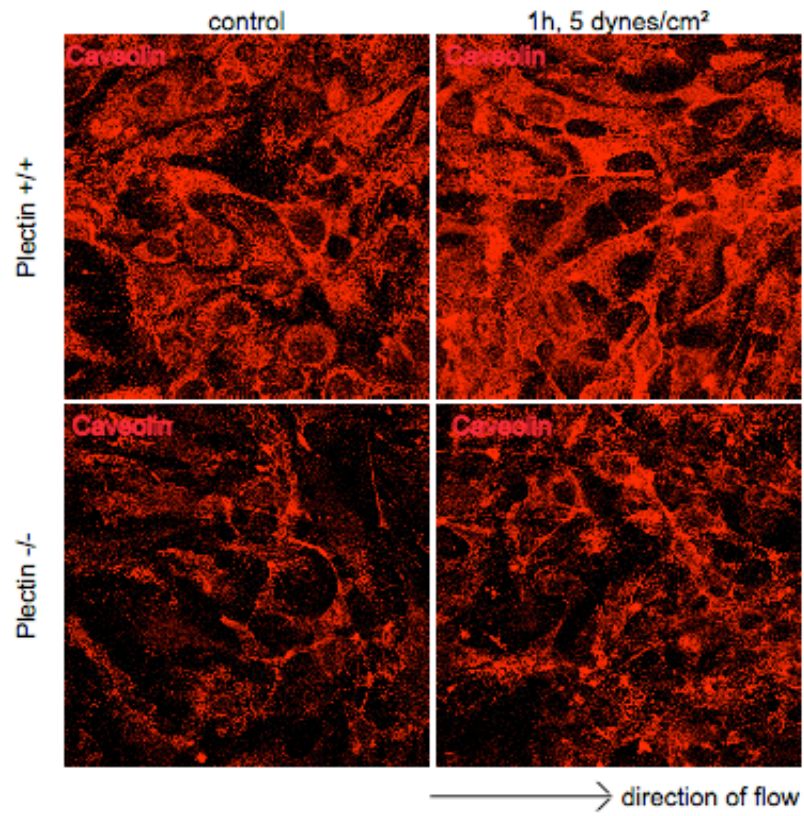


Fig. 26. Immunofluorescence microscopy of caveolin-1 in plectin<sup>+/+</sup> and plectin<sup>-/-</sup> pT Endo cells under static conditions and after 1 h of fluid shear stress (5 dynes/cm<sup>2</sup>). Magnification x 63

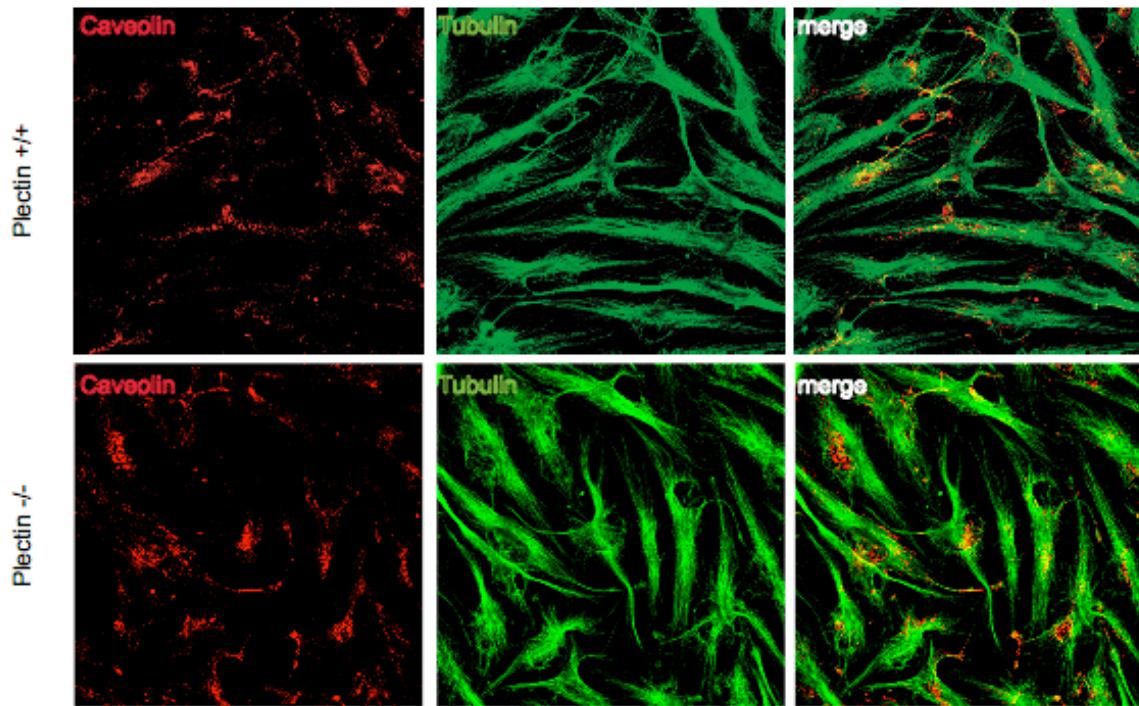
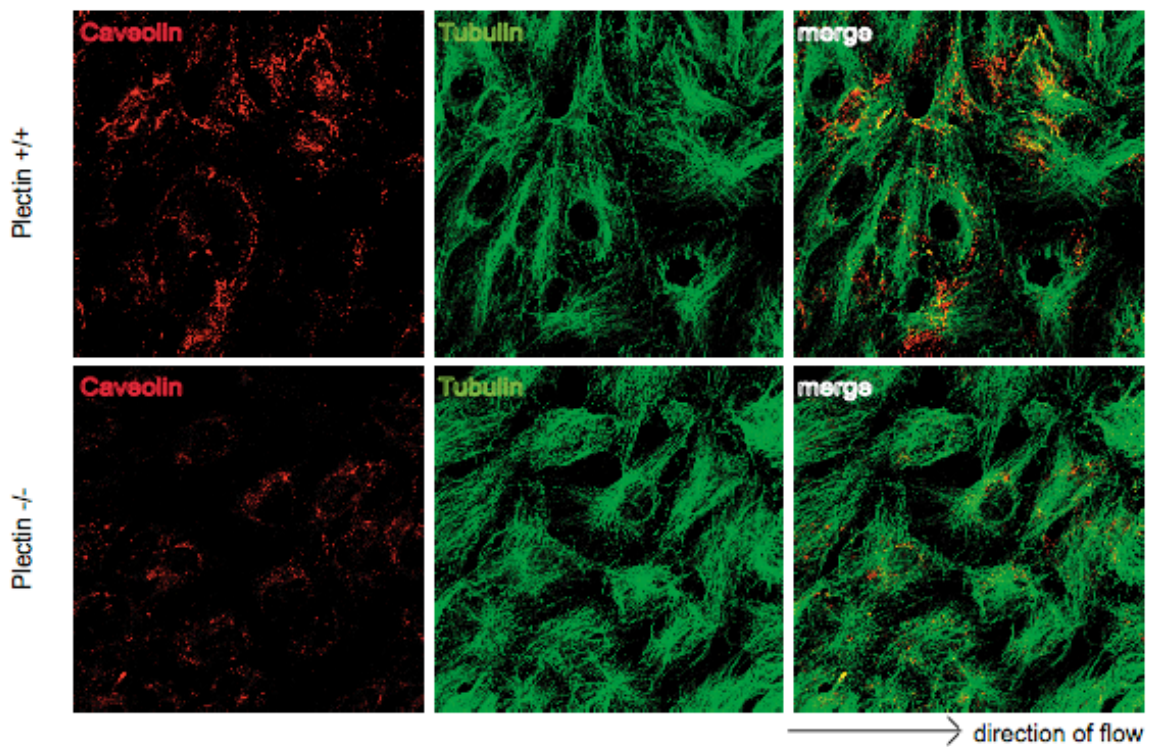
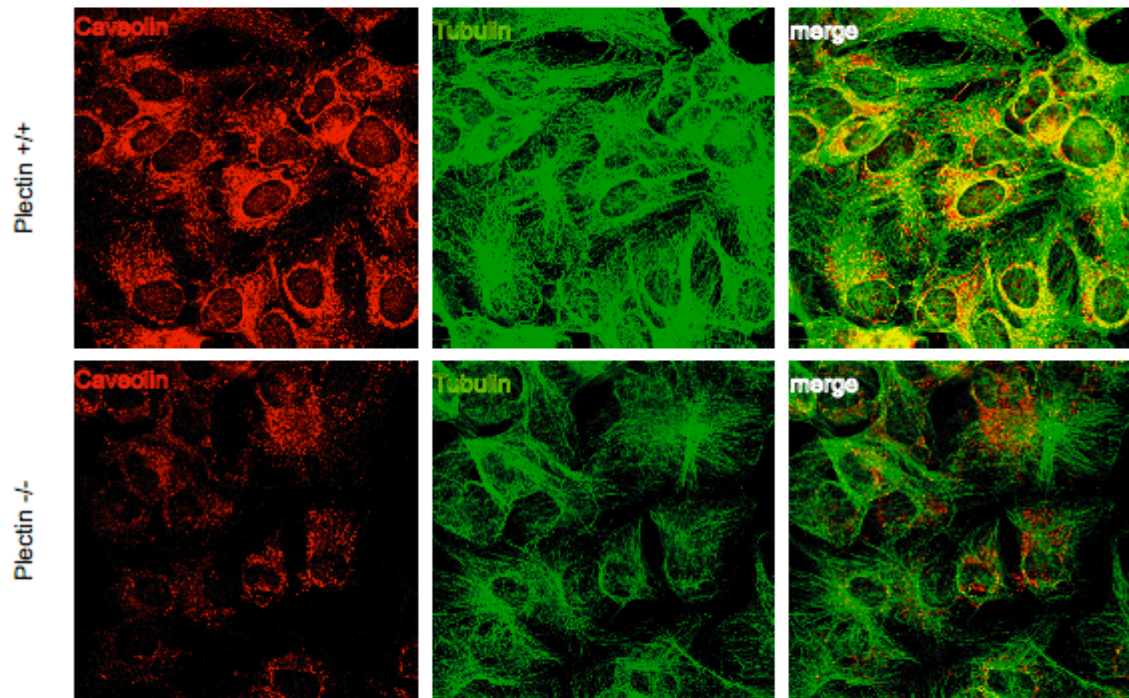
**A** control**B** flow 1h, 5 dynes/cm<sup>2</sup>

Fig. 27 A,B. Immunofluorescence microscopy of caveolin-1 and tubulin in plectin<sup>+/+</sup> and plectin<sup>-/-</sup> DH-1 cells under static conditions (A) and after 1h (B), 6h (C), and 24 h (D) of fluid shear stress (5 dynes/cm<sup>2</sup>). Magnification x 63

**C** flow 6h, 5 dynes/cm<sup>2</sup>



**D** flow 24 h, 5 dynes/cm<sup>2</sup>

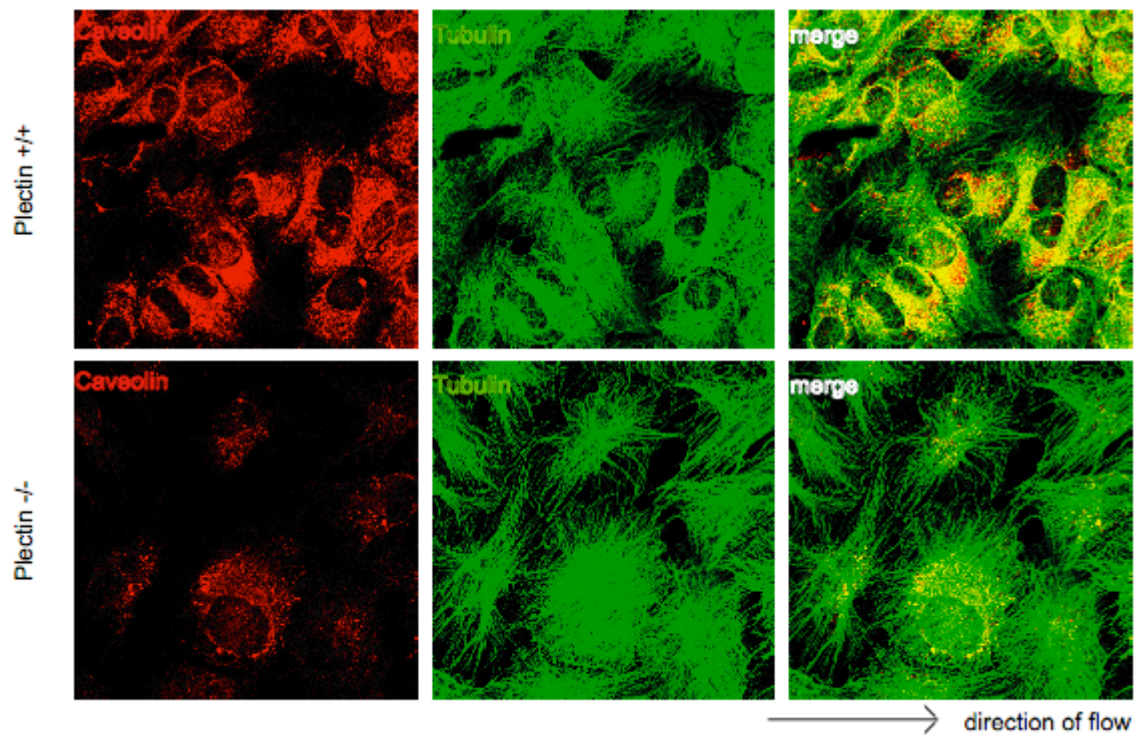


Fig. 27 C,D. Immunofluorescence microscopy of caveolin-1 and tubulin in plectin<sup>+/+</sup> and plectin<sup>-/-</sup> DH-1 cells under static conditions (A) and after 1h (B), 6h (C), and 24 h (D) of fluid shear stress (5 dynes/cm<sup>2</sup>). Magnification x 63



#### 4.9.3. Effects of shear stress on protein levels and localization of VE-cadherin and actin

In response to fluid shear stress VE-cadherin complexes undergo dynamic changes including a coordinated release and reattachment to the actin cytoskeleton (Ukropec et. al, 2002).

As already observed in pT Endo cells, VE-cadherin staining of plectin<sup>+/+</sup> and plectin<sup>-/-</sup> DH-1 cells was predominantly found at the cell periphery under no-flow conditions. In plectin<sup>+/+</sup> cells, patches of VE-cadherin, so called lattice-like structures were observed (Fig. 28A). Ukropec and colleagues observed lattice-like VE-cadherin staining in ECs resulting from overlapping regions of membranes on apposed cells under static conditions. After exposure to fluid shear stress the VE-cadherin staining at the cell borders became more intense in plectin<sup>+/+</sup> DH-1 cells compared to plectin<sup>-/-</sup> cells (Fig. 28B). Upon 1, 6 and 24 h of laminar shear zipper-like character of VE-cadherin complexes became more prominent and increased upon longer exposure to flow in plectin<sup>+/+</sup> DH-1 cells (Fig. 28B, C, D). After 24 h of fluid shear stress these structures were most pronounced in plectin<sup>+/+</sup> cells (Fig. 28D). In plectin<sup>-/-</sup> DH-1 cells those zipper-like structures were less prominent under all conditions (Fig. 28B, C, D).

To confirm the different effect of fluid shear stress on VE-cadherin in plectin<sup>+/+</sup> and plectin<sup>-/-</sup> DH-1 cells mixed cultures were subjected to fluid shear stress under absolute same conditions like confluency and shear stress rate. In mixed plectin<sup>+/+</sup> and plectin<sup>-/-</sup> DH-1 cultures VE-cadherin was more prominent in plectin<sup>+/+</sup> cells. Zipper-like structures were formed between neighboring cells under static conditions (Fig. 29). Upon onset of fluid shear stress VE-cadherin fluorescence signal became slightly more intense in both plectin<sup>+/+</sup> and plectin<sup>-/-</sup> cells, zipper-like character of VE-cadherin complexes got more emphasized, however, being reduced in plectin<sup>-/-</sup> DH-1 cells (Fig. 29).

Taken together, immunofluorescence microscopy of DH-1 and pT Endo cells showed slightly higher levels of VE-cadherin and much more zipper-like VE-cadherin clusters in plectin<sup>+/+</sup> cells in comparison to plectin<sup>-/-</sup> cells after exposure to flow stress. It has to be noted that under static conditions contrary results were observed. The effect was more pronounced in mixed cultures

where plectin<sup>-/-</sup> cells showed reduced levels of VE-cadherin, whereas plectin<sup>+/+</sup> and plectin<sup>-/-</sup> cells showed equal VE-cadherin levels when cultured separately.

Interestingly, co-staining of VE-cadherin and actin showed a nice colocalization after exposure to fluid shear stress in plectin<sup>+/+</sup> cells. Under static conditions no or very little actin stress fibers were found in plectin<sup>+/+</sup> and plectin<sup>-/-</sup> DH-1 cells. Since cells were completely confluent for at least 24 h before subjected to flow stress actin staining was confined to cortical actin. It is known that in post-confluent cells stress fibers are becoming less prominent and a junctional dense peripheral band of F-actin is established (Noria et al., 2004). Cortical actin co-localized with lattice-like VE-cadherin patches in both plectin<sup>+/+</sup> and plectin<sup>-/-</sup> DH-1 cells. Since much more of these patches were found in plectin<sup>+/+</sup> cells this colocalization was more prominent in plectin<sup>+/+</sup> DH-1 cells (Fig. 28A). After exposure to fluid shear stress actin signal intensity became stronger in both plectin<sup>+/+</sup> and plectin<sup>-/-</sup> DH-1 cells. In plectin<sup>-/-</sup> DH-1 cells more actin stress fibers assembled increasing with the duration of fluid shear stress (Fig. 28B, C, D). However, the significant colocalization of cortical actin and VE-cadherin was only found in plectin<sup>+/+</sup> cells and was most pronounced after 6 and 24 h of laminar shear (Fig. 28C, D). Since co-staining of actin and VE-cadherin were only performed in DH-1 cells this phenotype could not be confirmed in pT Endo cells.

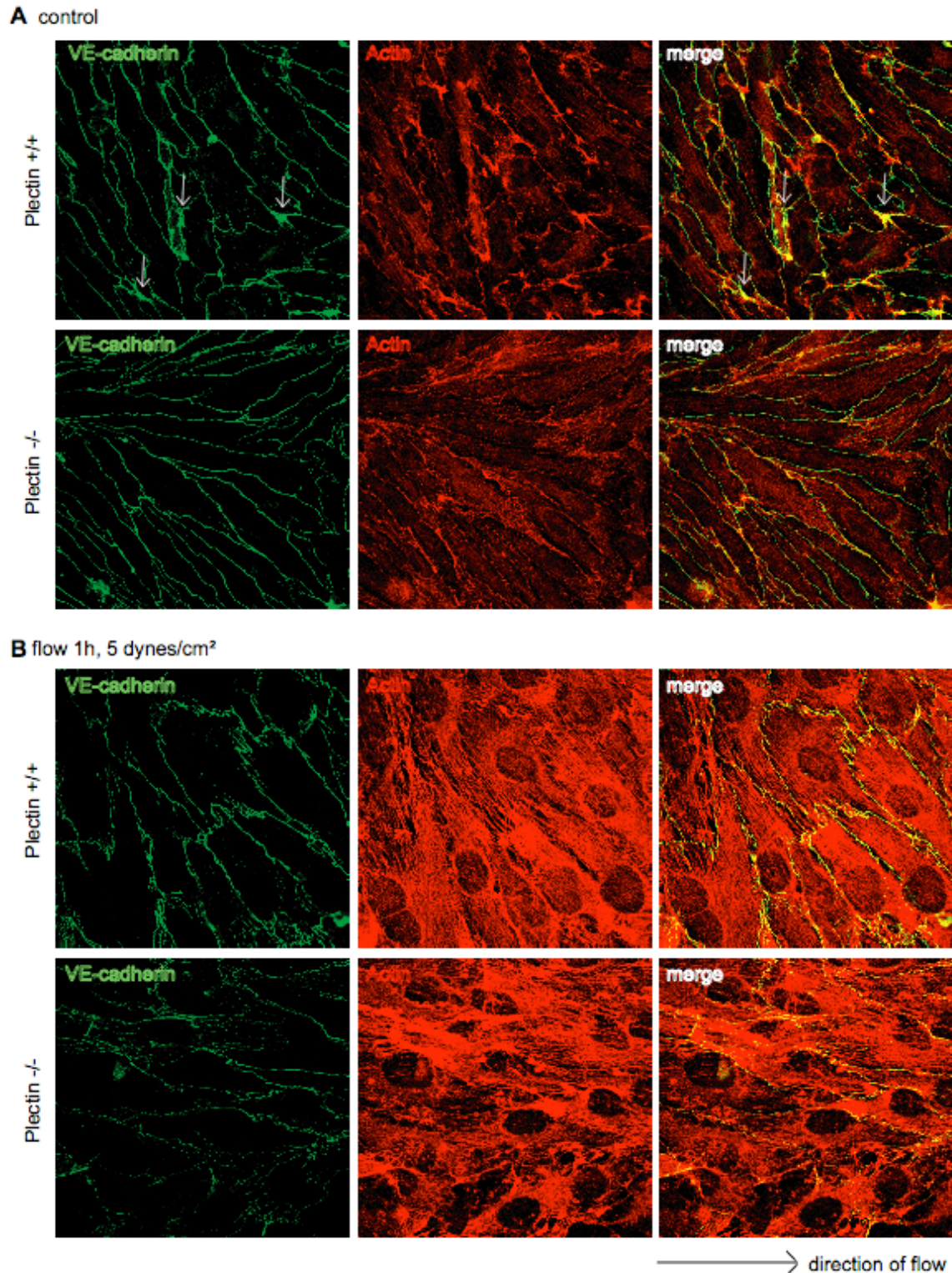
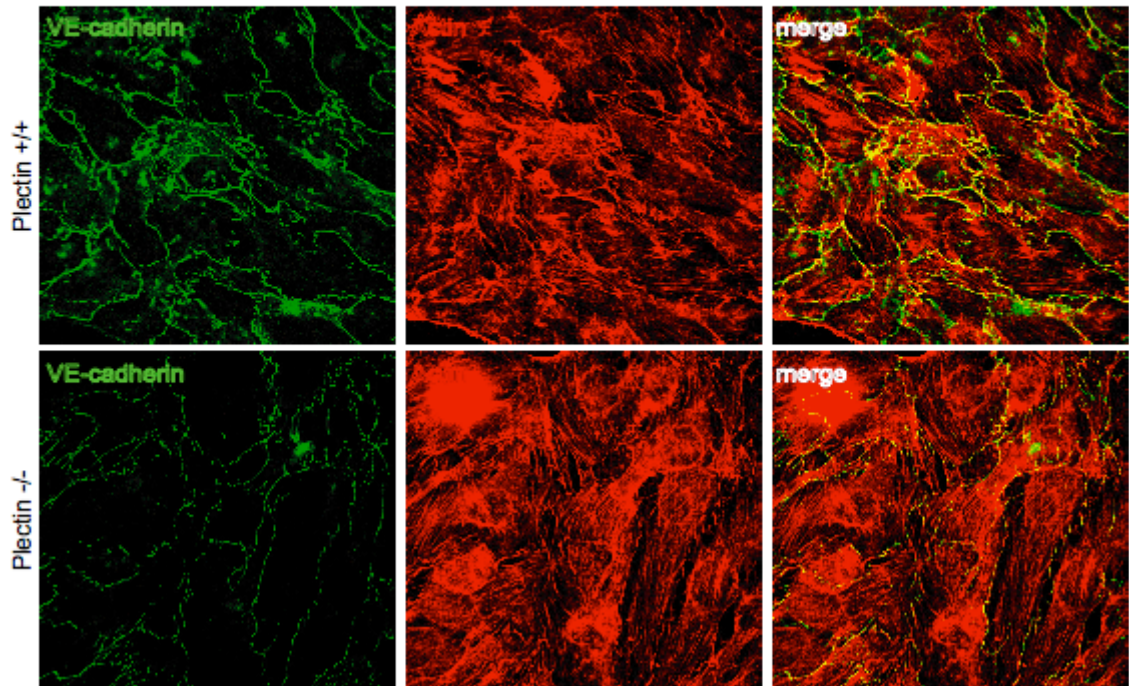


Fig. 28 A, B. Immunofluorescence microscopy of VE-cadherin and actin in plectin<sup>+/+</sup> and plectin<sup>-/-</sup> DH-1 cells under static conditions (A) and after 1 h (B), 6 h (C) and 24 h (D) of fluid shear stress (5 dynes/cm<sup>2</sup>). Arrows indicating zipper-like VE-cadherin patches. Magnification x 63.

**C** flow 6h, 5 dynes/cm<sup>2</sup>



**D** flow 24 h, 5 dynes/cm<sup>2</sup>

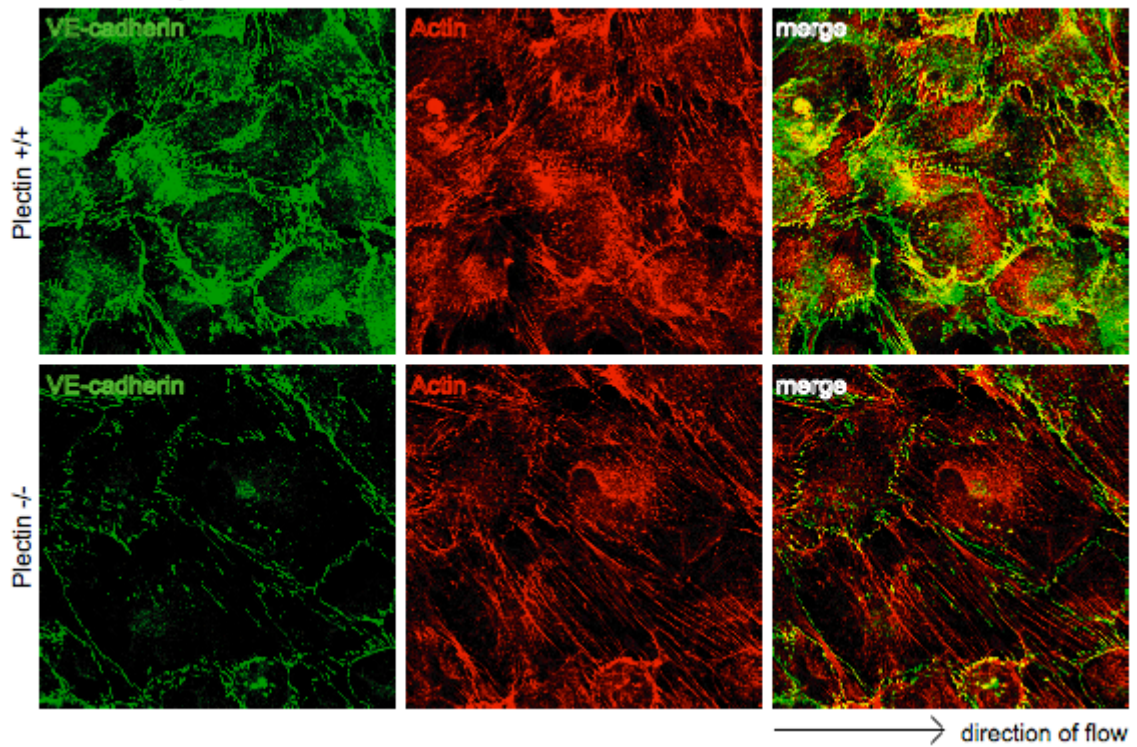


Fig. 28 C, D. Immunofluorescence microscopy of VE-cadherin and actin in plectin<sup>+/+</sup> and plectin<sup>-/-</sup> DH-1 cells under static conditions (A) and after 1 h (B), 6 h (C) and 24 h (D) of fluid shear stress (5 dynes/cm<sup>2</sup>). Magnification x 63

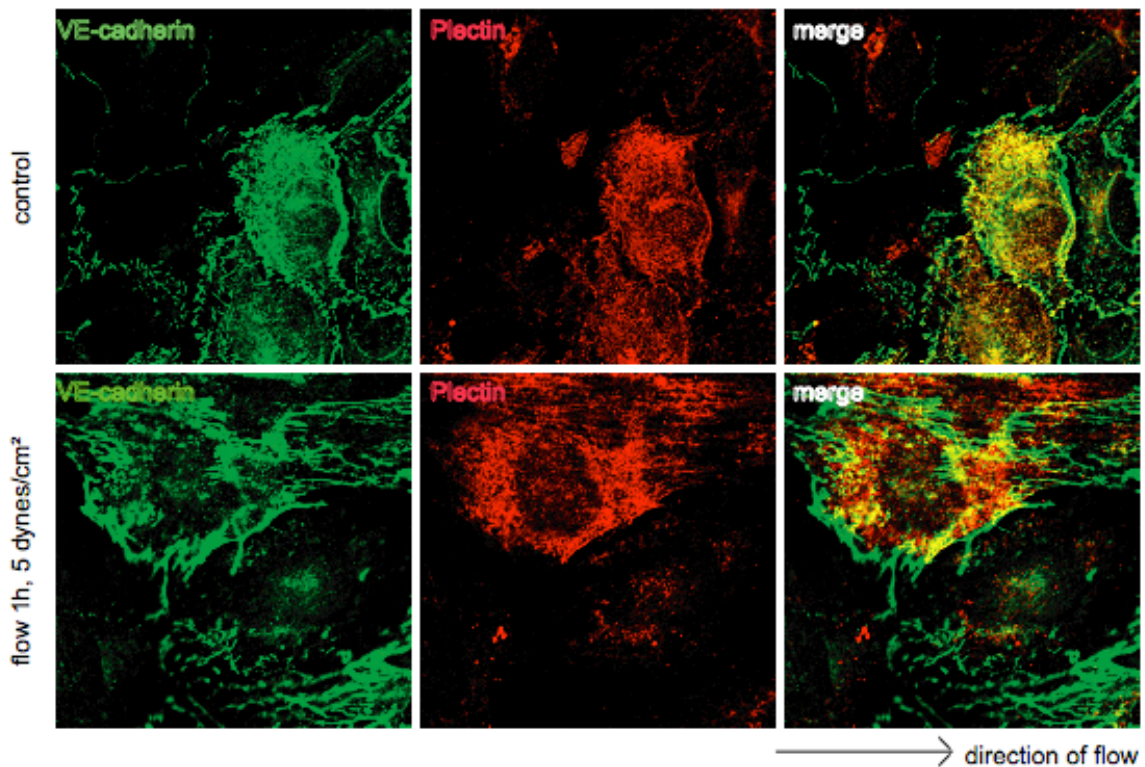


Fig. 29. Immunofluorescence microscopy of VE-cadherin and plectin in plectin<sup>+/+</sup> and plectin<sup>-/-</sup> DH-1 mixed cultures under static conditions and after 1 h of fluid shear stress (5 dynes/cm<sup>2</sup>). Magnification x 100

#### 4.9.4. Effects of shear stress analyzed by immunoblotting

After exposure to laminar shear stress, cells were lysed and protein expression was checked by immunoblotting using tubulin as loading control.

eNOS expression was checked in lysates of both pT Endo and DH-1 cells. eNOS levels were higher in plectin<sup>+/+</sup> pT Endo cells in comparison to plectin<sup>-/-</sup> cells under no-flow conditions. After exposure an up-regulation of eNOS protein levels was found in plectin<sup>+/+</sup> cells but no or very little up-regulation was found in plectin<sup>-/-</sup> pT Endo cells (Fig. 30). These results confirm immunofluorescence data of pT Endo cells (compare with Fig. 22).

Lysates of flow-stressed DH-1 cells showed contrary results compared to immunofluorescence microscopy. These preliminary data revealed, as expected, reduced eNOS levels in plectin<sup>-/-</sup> DH-1 cells under static conditions (Fig. 31B).

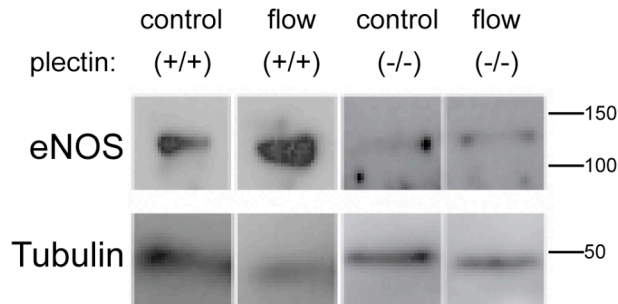


Fig. 30. eNOS protein levels in pT Endo cells. Plectin<sup>+/+</sup> and plectin<sup>-/-</sup> control and flow-stressed were lysed and analysed by immunoblotting using specific eNOS antibodies.

However, upon 1 and 6 h of flow eNOS levels were up-regulated in plectin<sup>+/+</sup> DH-1 cells. An up-regulation of eNOS was also twice observed in plectin<sup>-/-</sup> DH-1 cells after 1 hour of fluid shear stress (Fig. 31B). After 6 h of laminar shear eNOS levels did not change in shear-stressed plectin<sup>-/-</sup> cells in comparison to control plectin<sup>-/-</sup> cells. Due to the fact that there was no tubulin as a loading control it is very difficult to analyze these blots and make a definite statement.

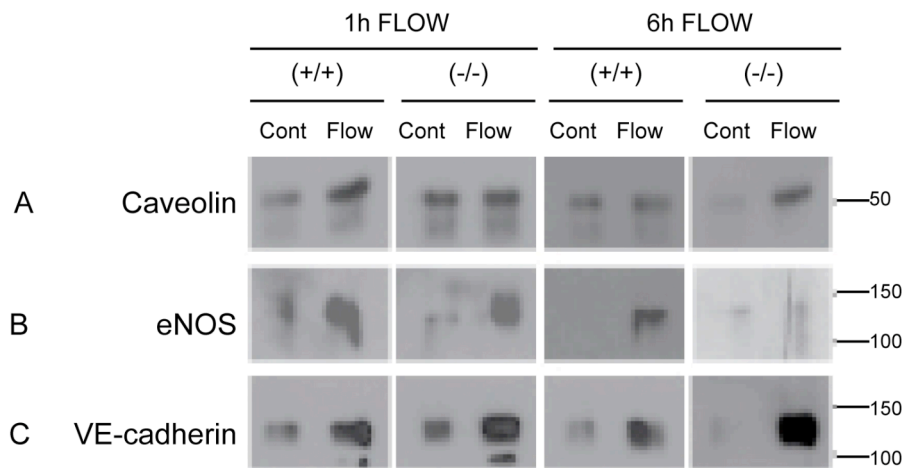


Fig. 31. Caveolin (A), eNOS (B) and VE-cadherin (C) protein levels in DH-1 cells. Plectin<sup>+/+</sup> and plectin<sup>-/-</sup> control and flow-stressed DH-1 cells were lysed and analysed using monoclonal antibodies.

Lysates of control and flow-stressed cells analyzed by immunoblotting showed that caveolin expression was slightly reduced in plectin<sup>-/-</sup> DH-1 cells in comparison to plectin<sup>+/+</sup> DH-1 cells under static conditions. After exposure to fluid shear stress for 1 hour caveolin was up-regulated in both plectin<sup>+/+</sup> and plectin<sup>-/-</sup> DH-1 cells confirming results from immunofluorescence microscopy (compare with Fig. 27). After 6 h of laminar shear immunoblotting revealed a

higher up-regulation of caveolin levels in plectin<sup>-/-</sup> cells in comparison to plectin<sup>+/+</sup> DH-1 cells (Fig. 31A).

Cell lysates, obtained from control and flow-stressed cells were tested for VE-cadherin expression using immunoblotting. Lysates from DH-1 cells showed more or less equal levels of VE-cadherin in plectin<sup>+/+</sup> and plectin<sup>-/-</sup> under static conditions. Upon onset of fluid shear stress higher levels of VE-cadherin were found in both plectin<sup>-/-</sup> and plectin<sup>+/+</sup> DH-1 cells (Fig. 31C). These data supported immunofluorescence data of mixed plectin<sup>+/+</sup> and plectin<sup>-/-</sup> cells that revealed no or very slight differences in the protein levels of VE-cadherin. Immunoblots of lysates from pT Endo cells revealed contrary results. In pT Endo cells no or only slight differences of VE-cadherin expression were detected under static conditions and after exposure to fluid shear stress (Fig. 32).

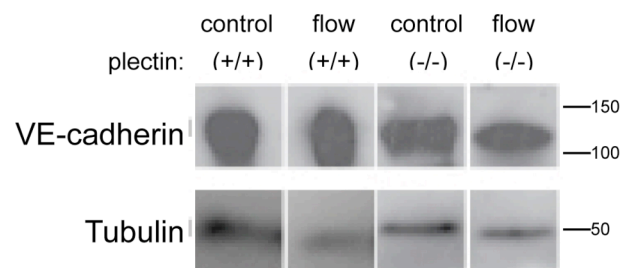


Fig. 32. VE-cadherin protein levels in pT Endo cells. Plectin<sup>+/+</sup> and plectin<sup>-/-</sup> control and flow-stressed pT Endo cells were lysed and analysed by immunoblotting using specific VE-cadherin and tubulin antibodies.

Taken together, the results did not completely confirm that eNOS was up-regulated in plectin<sup>+/+</sup> but not in plectin<sup>-/-</sup> pT Endo and DH-1 cells after exposure to fluid shear stress. VE-cadherin up-regulation in pT Endo and DH-1 cells in response to fluid shear stress could not be confirmed. Furthermore, immunoblotting revealed an up-regulation of caveolin in both plectin<sup>+/+</sup> and plectin<sup>-/-</sup> DH-1 cells after 1 hour of shear stress, reinforcing the immunofluorescence data.

## 5. Discussion

ECs form the permeable barrier between the blood and the vessel wall and play a role in cell remodelling, migration, apoptosis, and proliferation. Furthermore, ECs control the vascular homeostasis by secreting biochemical substances like NO, ROS or glutathione. The flow of blood results in mechanical stresses acting on the vessel wall influencing EC structure, growth and functions. Cell membrane proteins, ion-channels, caveolae and alterations of the cellular cytoskeleton are candidates for mechanosensors in ECs that sense changes in fluid shear stress (Fisher et al., 2001). Due to plectin's subcellular distribution and the vast variety of its binding partners plectin is supposed to be a scaffolding platform for signalling molecules. These facts let us suggest that plectin might play a role in sensing and / or responding to fluid shear stress in ECs. In this thesis the role of plectin in two different endothelial cell lines, pT Endo and DH-1, was investigated. Immunofluorescence microscopy and immunoblotting of cell lysates revealed that these cell lines expressed endothelial specific markers eNOS, van Willebrand factor and VE-cadherin.

eNOS is localized within plasma membrane invaginations called caveolae and the Golgi apparatus. In response to cell stimulation eNOS is shuttling between different intracellular compartments (see review Fleming and Busse, 2003). Although eNOS was detected in the cytosol and in association with the cytoskeletal cell fraction in some ECs the intracellular localization of this enzyme is still controversial. Immunoblottings showed that total levels of eNOS were reduced in plectin<sup>-/-</sup> ECs in comparison to plectin<sup>+/+</sup> cells. Cell fractionation experiments revealed an increase of the membrane fraction of eNOS in plectin<sup>-/-</sup> compared to plectin<sup>+/+</sup> pT Endo and DH-1 cells, with a corresponding reduction in the cytoskeleton fraction. These findings suggest an association of eNOS with the cytoskeleton via plectin as a linker. It is therefore conceivable that in the absence of plectin an accumulation of eNOS occurs at the cell periphery due to the lack of its cytoskeletal docking site. This mislocalization might in turn lead to increased eNOS degradation and thus to reduced total levels of this protein in the absence of plectin.



Altered localization and reduced levels of eNOS in plectin<sup>-/-</sup> ECs might affect the activity of the enzyme and thus NO production. Indeed, DAF-based assays (Räthel et al., 2003) showed that the amounts of NO produced in untreated and PMA-stimulated DH-1 cells were reduced in plectin<sup>-/-</sup> cells compared to plectin<sup>+/+</sup> cells. An inhibitor of eNOS, L-NAME, (Hibbs et al., 1987) led to a complete depletion of NO production in both cell types. These results are consistent with the observations obtained in plectin<sup>-/-</sup> pT cells (Spurny, 2006). It must be noted, however that already in untreated state a reduction in NO production was observed in pT Endo cells. This might be due to a high passage number at which pT Endo were used. Prolonged PMA incubation used in this assay most probably acts in two ways. First, it is known that it leads to an enhanced eNOS expression (Huige et al., 1997; Shu-Ching et al., 1999). Second, it enhances eNOS activity by causing a down-regulation of protein kinase C (PKC). Down-regulation of PKC most likely further activates eNOS since PKC phosphorylates Thr<sup>495</sup> (Michell et al., 2001) known as a negative regulatory site of eNOS (see review Fleming and Busse, 2003). Plectin might also directly influence PKC since it is known, however, from another cell system that the activity of PKC $\delta$  is strongly elevated in plectin<sup>-/-</sup> fibroblasts (Osmanagic-Myers and Wiche, 2004). Since PKC inhibits eNOS activity by Thr<sup>495</sup> phosphorylation the reduced eNOS activity in plectin<sup>-/-</sup> ECs might be caused by a stronger PKC signalling. It has been shown that some PKC family members (PKC $\alpha$ , PKC $\epsilon$ ) can phosphorylate eNOS also at Ser<sup>1177</sup> (Partovian et al., 2005; Zhang et al., 2004) supporting the theory that down-regulated PKC signalling reduces eNOS activity in plectin<sup>-/-</sup> ECs.

In addition to Thr<sup>495</sup> another major phosphorylation site through which eNOS activity is regulated by is Ser<sup>1177</sup>. Multiple stimuli like shear stress, estrogen or insulin activate Akt-kinase and cAMP-dependent protein kinase (PKA) that phosphorylate Ser<sup>1177</sup> which leads to a two- to threefold increase of NO production. Immunoblotting using specific antibodies against phospho-Thr<sup>497</sup> and phospho-Ser<sup>1177</sup> eNOS showed a significantly higher phospho-Thr<sup>497</sup>-specific signal eNOS and a slightly lower phospho-Ser<sup>1177</sup>-specific signal in plectin<sup>-/-</sup> cells compared to plectin<sup>+/+</sup> ECs. Thus, both assays implicate reduced activity of eNOS in plectin<sup>-/-</sup> cells in comparison to plectin<sup>+/+</sup> cells.

Shear stress can potentially activate eNOS enzyme by increasing intracellular calcium leading to Ser<sup>1177</sup> phosphorylation of eNOS within seconds. Prolonged exposure to fluid shear stress leads to an increase of eNOS mRNA and protein levels depending on cSrc-kinase and a MAP-kinase pathway involving Ras, Raf, MEK and Erk 1/2 (Harrison et al., 2006). After 1h of shear stress eNOS expression remains elevated, due to prolonged stabilization of eNOS mRNA mediated by cSrc-kinase (Harrison et al., 2006). Exposure to shear stress of plectin<sup>+/+</sup> and plectin<sup>-/-</sup> DH-1 and pT Endo cells revealed an up-regulation of eNOS plectin<sup>+/+</sup> but no or only a slight increase in plectin<sup>-/-</sup> cells. The reduced responsiveness of plectin<sup>-/-</sup> cells to shear stress stimuli regarding eNOS up-regulation might be due to several reasons: (i) Mislocalization of eNOS due to the lack of plectin as a cytoskeletal docking site; (ii) Significant differences of the actin filament system in plectin<sup>+/+</sup> and plectin<sup>-/-</sup> ECs in response to shear stress. Whereas, in plectin<sup>+/+</sup> cells shear stress induced the accumulation of cortical F-actin associated with adherens junctions, in plectin<sup>-/-</sup> DH-1 cells stress fibers predominated, especially after prolonged flow exposure. Su and colleagues found a co-localization of eNOS and actin within caveolae. Furthermore, they observed that a disruption of the actin filament network led to an increase in eNOS activity (Su et al., 2003). Hence, stress fibers might hinder eNOS in its activation. (iii) Elevated PKC signalling in plectin<sup>-/-</sup> cells as already mentioned above.

It has already been shown that eNOS localize in plasmalemmal caveolae (Garcia-Cardena et al., 1996). A variety of signalling molecules are concentrated within these flask-shaped structures present on the membrane among them is caveolin-1, the major coat protein of caveolae (Gratton et al, 2004). Caveolae have also been proposed to be shear stress mechanosensors in ECs (Fisher et al., 2001). Surprisingly, we found reduced levels of caveolin-1 in plectin<sup>-/-</sup> ECs compared to plectin<sup>+/+</sup> cells. Furthermore, a drastic increase of caveolin-1 in membrane fraction at the expense of the cytoskeleton fraction was observed in plectin<sup>-/-</sup> cells compared to plectin<sup>+/+</sup> cells using cell fractionation experiments. Mundi and co-workers proposed that the caveolar membrane system consists of three caveolin-1-containing compartments. These include caveolae that are kept at the cell surface by actin filaments, the peri-

centrosomal caveosomes and caveolar vesicles that move constitutively and bi-directionally along microtubules between the cell surface and caveosomes (Mundi et al., 2002). From the literature little is known about a connection between caveolin and IFs and their role in caveolin trafficking and localisation. Since plectin is an important IF-binding protein (Wiche and Baker, 1982) it is conceivable that the IF connection is impaired in plectin<sup>-/-</sup> ECs. We suggest that caveolin-1 is bound via plectin to the cytoskeleton. It remains to be investigated whether plectin connects caveolin with actin, microtubules or IFs. In the absence of plectin, the link between caveolin and the cytoskeleton might be abolished and caveolin therefore translocated to the membrane. Again, similar to eNOS, altered localization might lead to partial degradation of excess caveolin and thus reduced levels of this protein in the absence of plectin.

Exposure to shear stress increases caveolae density and alters caveolin expression and distribution. Furthermore, caveolar-residing proteins like eNOS, caveolin-1 or mitogen-activated kinases (Erk 1/2) are significantly up-regulated in response to fluid shear stress (Rizzo et al., 2002). We observed an up-regulation of caveolin in response to fluid shear stress in plectin<sup>+/+</sup> and plectin<sup>-/-</sup> cells although caveolin levels were still reduced in plectin<sup>-/-</sup> cells.

Based on the results obtained, the following working model can be proposed: In plectin<sup>-/-</sup> cells eNOS and caveolin accumulate at the membrane with a corresponding reduction in the cytoskeleton. This suggests that plectin either directly or indirectly is sequestering both proteins to the cytoskeleton. It is known that the putative caveolin scaffolding domain (amino acids 82 – 101) in caveolin-1 inhibits eNOS activity by reducing NADPH-dependent electron flux from its reductase to the oxygenase domain, thereby reducing NO release from cells (Gratton et al., 2004). A surplus of both proteins at the membrane fraction of plectin<sup>-/-</sup> cells might result in an enhanced inhibition of eNOS caused by the stronger interaction with caveolin. This would fit to our findings that eNOS activity and NO production were reduced in plectin<sup>-/-</sup> cells in comparison to plectin<sup>+/+</sup> ECs.

Plectin<sup>-/-</sup> mice die on the second day after birth developing large blisters often accompanied by bleedings, particularly at their extremities (Andrä et al., 1997). This type of bleeding might indicate a possible perturbation of the vas-

cular system. The establishment of monolayer integrity is regulated by VE-cadherin, a unique member of the cadherin family, specifically expressed in ECs (Venkiteswaran et al., 2001). VE-cadherin is known to play a role in adhesion of ECs and regulation of their growth, survival, migration and proliferation (Venkiteswaran et al., 2001). VE-cadherin deficient embryos develop severe vascular defects and die at day 11,5 of embryonic development. (Carmeliet and Collen, 2000). ECs from these embryos show increased apoptosis, due to an inability of VE-cadherin-deficient cells to respond to the survival signal of vascular endothelial growth factor (VEGF) (Carmeliet and Collen, 2000).

In comparison to plectin<sup>+/+</sup> cells, plectin<sup>-/-</sup> ECs showed a down-regulation of VE-cadherin on the first two days of cultivation as revealed by immunoblottings of the corresponding lysates. When cells became confluent the levels of VE-cadherin were equal. Cell fractionation experiments revealed an increase of VE-cadherin in membrane fraction at the expense of the cytoskeleton in plectin<sup>-/-</sup> cells compared to plectin<sup>+/+</sup> cells. Furthermore, by immunofluorescence microscopy, more zipper-like VE-cadherin structures were observed in subconfluent plectin<sup>+/+</sup> cultures in comparison to plectin<sup>-/-</sup> cultures (Osmanagic-Myers, unpublished data). Ukropec and colleagues proposed that these zipper-like structures result from overlapping regions of membranes on apposed ECs (Ukropec et al., 2002). These findings and the fact that VE-cadherin and plectin co-localized at the immunofluorescent level (Osmanagic-Myers, unpublished data) suggest a role of plectin in regulating VE-cadherin function. The absence of plectin might lead to a discontinuous border of loosely connected ECs.

Upon onset of shear stress the intracellular cadherin complexes seemed to broaden and stain more intensively (Ukropec et al., 2002). In response to fluid shear stress we observed an increase of VE-cadherin expression and clustering in both cell types, but cluster formation and expression levels seemed reduced in plectin<sup>-/-</sup> cells. The zipper-like character of VE-cadherin complexes in plectin<sup>+/+</sup> was most pronounced after 6 and 24 hours of fluid shear stress. In plectin<sup>+/+</sup> cells these structures coincided nicely with more pronounced cortical actin compared to plectin<sup>-/-</sup> cells implicating increased contractility of plectin<sup>+/+</sup> cells. For this reason, it would be conceivable that plectin<sup>+/+</sup> cells are able to withstand higher shear stress forces compared to plectin<sup>-/-</sup> cells. Thus, shear

stress induced changes of ECs junctions might have important implications for the control of the endothelial permeability barrier and other aspects of endothelial cell function. Since cluster formation and VE-cadherin levels were reduced in plectin<sup>-/-</sup> ECs the endothelial barrier function might be impaired in these cells.

Shear stress leads to a re-orientation of the cell parallel to the direction of flow. All three cytoskeletal networks adapt their structure in response to hemodynamic forces (Helmke, 2005). After exposure to laminar shear stress vimentin filaments are known to elongate and re-orientate parallel to the direction of flow (Garcia-Cardena et al., 2001). Under static conditions a more disorganized vimentin network was observed in plectin<sup>-/-</sup> ECs compared to plectin<sup>+/+</sup> cells. In response to shear stress plectin<sup>+/+</sup> ECs appeared as if trying to re-orientate in the direction of fluid shear stress, although DH-1 cells did not manage to re-orientate completely. However, the vimentin network of plectin<sup>-/-</sup> pT Endo and DH-1 cells did not show drastic changes. This might be due to the fact that very modest flow-related cytoskeletal reorientations occur in post-confluent cultures (Noria et al., 2004). Furthermore, the rate of cytoskeletal remodelling is significantly slowed in cells grown on gelatine (Helmke, 2005).

Taken together these results show the important role of plectin in regulating EC functions. It will be interesting to explore in more detail the exact mechanism by which plectin influences eNOS activity. Further studies involving the characterization of the endothelium-specific plectin deficient mice might open interesting aspects of plectin's potential role in the development of typical vascular diseases, such as atherosclerosis, vascular dilation, and aneurysm or hypertension.

## 6. References

- Andrä K.**, B. Nikolic, M. Stocher, D. Drenckhahn, G. Wiche. 1998. Not just scaffolding: plectin regulates actin dynamics in cultured cells. *Genes Dev.* 12: 3442 – 3451
- Andrä K.**, H. Lassmann, R. Bittner, S. Shorny, R. Fässler, F. Propst, G. Wiche. 1997. Targeted inactivation of plectin reveals essential function in maintaining the integrity of skin, muscle, and heart cytoarchitecture. *Genes Dev.* 11: 3143 – 3156
- Brown A.**, G. Bernier, M. Mathieu, J. Rossant, R. Kothary. 1995. The mouse dystonia musculorum gene is a neural isoforms of bullous pemphigoid antigen1. *Nat Gen.* 10: 301-306
- Buijsrogge J. J. A.**, de Jong M. C. J. M., Meijer H. J. Dijk F., Jonkman M. F., Pas H. H. 2005. Inflammatory epidermolytic bullous pemphigoid with coexistent IgA antibodies to plectin. *Clin. Exper. Dermatol.* 30: 531 – 534
- Calkins C. C.**, B. L. Hoepner, C. M. Law, M. R. Novak, S. V. Setzer, M. Hatzfeld, A. P. Kowalczyk. 2003. The armadillo family protein p0071 is a VE-cadherin- and desmoplakin-binding protein. *J. Biol. Chem.* 278, 1774-1783
- Carmeliet P. and D. Collen.** 2000. Molecular basis of angiogenesis: role of VEGF and VE-Cadherin. *Annals N. Y. Acad. Sci.* 902: 249 - 264
- Chien S.** 2006. Mechanotransduction and endothelial cell homeostasis; the wisdom of the cell. *J. Physiol. Heart Circ. Physiol.* 10: 1 – 64
- Coulombe P. A.**, M. B. Omary. 2002. 'Hard' and 'soft' principles defining the structure, function and regulation of keratin intermediate filaments. *Curr. Opin. Cell Biol.* 14: 110-122
- Dang M.**, L. Pulkkinen, F. J. Smith, W. H. McLean, J. Uitto. 1998. Novel compound heterozygous mutations in the plectin gene in epidermolysis bullosa with muscular dystrophy and the use of protein truncation test for detection of premature termination codon mutations. *Lab. Invest.* 78: 195 – 204
- Eger A.**, A. Stockinger, G. Wiche, R. Foisner. 1997. Polarisation-dependent association of plectin with desmoplakin and the lateral submembrane skeleton in MDCK cells. *J. Cell Sci.* 110: 1307 – 1316
- Elliott C. E.**, B. Becker, S. Oehler, M. J. Castanon, R. Hauptmann, G. Wiche. 1997. Plectin transcript diversity: Identification and tissue distribution of variants with distinct first coding exons and rodless isoforms. *Genomics.* 42: 115 – 125
- Fisher A. B.**, S. Chien, A. I. Barakat, R. M. Nerem. 2001. Endothelial cellular response to altered shear stress. *J Physiol. Lung Cell Mol. Physiol.* 281: L529 – L 533
- Fleming I.** and Busse R. 2003. Molecular mechanisms involved in the regulation of the endothelial nitric oxide synthase. *J. Physiol. Regul. Integr. Comp. Physiol.* 284: R1 – R12
- Foisner R.** and G. Wiche. 1987. Structure and hydrodynamic properties of plectin molecules. *J. Mol. Biol.* 198: 515 – 531
- Foisner R.**, F. E. Leichtfried, H. Hermann, J. V. Small, D. Lawson, G. Wiche. 1988. Cytoskeleton-associated Plectin: In situ localization, in vitro reconstitution, and binding to immobilized intermediate filament proteins. *J. Cell Biol.* 106: 723 – 733

- Foisner R.**, N. Malecz, N. Dressel, C. Stadler, G. Wiche. 1996. M-phase-specific phosphorylation and structural rearrangement of the cytoplasmic cross-linking protein plectin involve p34cdc2 kinase. *Mol. Biol. Cell.* 7: 273 – 288
- Foisner R.**, P. Traub, G. Wiche. 1991. Protein kinase I and protein kinase C-regulated interaction of plectin with lamin B and vimentin. *Proc. Natl. Acad. Sci. U S A.* 88: 12 – 6
- Folkman J.**, C. Haudenschild. 1980. Angiogenesis in vitro. *Nature.* 288: 551 – 556
- Fuchs P.**, M. Zörer, G. A. Reziniczek, D. Sparzierer, S. Oehler, M. J. Castanon, R. Hauptmann, G. Wiche. 1999. Unusual 5' transcript complexity of plectin isoforms: novel tissue-specific exons modulate actin binding activity. *Human Molecular Genetics.* 8: 2461 – 2472
- Fujiwara S.**, et al. 1996. Identification of a 450-kDa human epidermal autoantigen as a new member of the plectin family. *J. Invest. Dermatol.* 106: 1125-1130
- Fujiwara S.**, N. Takeo, Y. Otani, D. A. D. Parry. 2001. Epiplakin, a novel member of the plakin family originally identified as a 450-kDa human epidermal autoantigen. *J. Biol. Chem.* 276: 13340-13347
- Gache Y.**, S. Chavanas, J. P. Lacour, G. Wiche, K. Owaribe, G. Meneguzzi, J. P. Ortonne. 1996. Defective Expression of Plectin/HD1 in Epidermolysis bullosa simplex with muscular dystrophy. *J. Clin. Invest.* 97: 2289 – 2298
- Galbraith C. G.**, R. Skalak, S. Chien. 1998. Shear stress induces spatial reorganization of the endothelial cell cytoskeleton. *Cell Mot. Cytosk.* 40: 317–330
- Garcia-Cardena G.**, Oh P., Jiu J., Schnitzer J. E., Sessa W. C. 1996. Targeting of nitric oxide synthase to endothelial cell caveolae via palmitoylation: implications for nitric oxide signalling. *Proc. Natl. Acad. Sci. U S A.* 93: 6448 - 6453
- Garcia-Cardena G.**, J. Comander, K. R. Anderson, B. R. Blackman M. A. Gimbrone. 2001. Biomechanical activation of vascular endothelium as a determinant of its functional phenotype. *PNAS.* 98: 4478 – 4485
- Gedde-Dahl T. Jr.** 1990. Management of Blistering Diseases, 897 – 903
- Goldsmith S. C.**, N. Pokala, W. Shen, A. A. Fedorov, P. Matsudaira, S. C. Almo. 1997. The structure of an actin –crosslinkin domain from human fimbrin. *Nat. Struct. Biol.* 4: 708 – 712
- Gory-Fauré S.**, M. H. Prandini, H. Pointu, V. Roullot, I. Pignot-Paintrand, M. V. Philippe Huber. 1999. Role of vascular endothelial-cadherin in vascular morphogenesis. *Develop.* 126: 2093 - 2102
- Gratton J. P.**, P. Bernatchez, W. C. Sessa. 2004. Caveolae and caveolins in the cardiovascular system. *Circ. Res.* 94: 1408 - 1417
- Green K. J.**, C. A. Gaudry. 2000. Are desmosomes more than tethers for intermediate filaments?. *Nat. Revs. Mol. Cell Biol.* 1: 208-216
- Green K. J.**, D. A. D. Parry, P. M. Steinert, M. L. A. Virata, R. M. Wagner, B. D. Angst, L. A. Nilles. 1989. Structure of human desmoplakins. *J. Biol. Chem.* 265: 2603-2612
- Gregor M.**, A. Zeöld, S. Oehler, K. Andrä Marobela, P. Fuchs, G. Weigel, D. G. Hardie, G. Wiche. 2006. Plectin scaffolds recruit energy-controlling AMP-activated protein kinase (AMPK) in differentiated myofibres. *J. Cell Sci.* 119: 1864 – 1875.

- Guo L.**, L. Degenstein, J. Dowhling, Q. C. Yu, R. Wollman, B. Perman, E. Fuchs. 1995. Gene targeting of BPAG1: abnormalities in mechanical strength and cell migration in stratified epithelia and neurologic degeneration. *Cell*. 81: 233-243
- Gurubhagavatula I.**, Y. Amrani, D. Pratico, F. L. Ruberg, S. M. Albelda, R. A. Panettieri. 1998. Engagement of human PECAM-1 on human endothelial cells increases intracellular calcium ion concentration and stimulates prostacyclin release. *J Clin. Invest*. 101: 212 – 222
- Harrison D. G.**, J. Widder, I. Grumbach, W. Chen, M. Weber, C. Searles. 2006. Endothelial mechanotransduction, nitric oxide and vascular inflammation. *J. Intern. Med*. 259: 351 – 363
- Helmke B. P.** 2005. Molecular control of cytoskeletal mechanics by hemodynamic forces. *Physiol*. 20: 43 – 53
- Herrmann H.** and G. Wiche. 1986. Plectin and IFAP-300K are homologous proteins binding to microtubule-associated proteins 1 and 2 to the 240-kilodalton subunit of spectrin. *J. Biol. Chem*. 262: 1320 – 1325
- Hibbs J. B.**, R. R. Taintor, Z. Vavrin. 1987. Macrophage cytotoxicity: role for L-arginine deiminase and imino nitrogen oxidation to nitrite. *Science*. 235: 473 – 476
- Huige L.**, S. A. Oehrlein, T. Wallerath, I. Ihrig-Biedert, P. Wohlfart, T. Ulshöfer, T. Jessen, T. Herget, U. Förstermann, H. Kleinert. 1998. Activation of protein kinase C $\alpha$  and/or  $\epsilon$  enhances transcription of the human endothelial nitric oxide synthase gene. *Mol. Pharmacol*. 53: 630 – 637
- Iyer S.**, D. M. Ferreri, N. C. DeCocco, F. L. Minnear, P. A. Vincent. 2003. VE-Cadherin-p120 interaction is required for maintenance of endothelial barrier function. *J. Physiol. Lung Cell Mol. Physiol*. 286: L1143 – L1153
- Karakesisoglou I.**, Y. Yang, E. Fuchs. 2000. An epidermal plakin that integrates actin and microtubule networks at cellular junctions. *J Cell Biol*. 149: 195-208
- Koss-Harnes D.**, B. Hoyheim, I. Anton-Lamprecht, A. Gjest, R. S. Jorgensen, F. Jahnsen, B. Olaisen, G. Wiche, T. Gedde-Dahl. 2002. A site-specific plectin mutation causes dominant Epidermolysis bullosa simplex Ogna: Two identical de novo mutations. *J. Invest. Dermatol*. 118: 87 – 93
- Koss-Harnes D.**, F. L. Jahnsen, G. Wiche, E. Soyland, P. Brandtzaeg, T. Gedde Dahl Jr. 1996. Plectin abnormality in epidermolysis bullosa simplex ogna: Non-responsiveness of basal keratinocytes to some anti-rat plectin antibodies. *Exp. Dermatol*. 6: 41-48
- Leung C. L.**, D. Sun, M. Zheng, D. R. Knowles, R. K. H. Liem. 1999. Microtubule actin cross-linking factor (MACF): A hybrid of dystonin and dystrophin that can interact with the actin and microtubule cytoskeleton. *J. Cell Biol*. 147: 1275-1285
- Leung C. L.**, K. J. Green, R. K. H. Liem. 2002. Plakins: a family of versatile cytolinker proteins. *Trend Cell Biol*. 12: 37 – 45
- Leung C. L.**, M. Zheng, S. M. Prater, R. K. H. Liem. 2001. The BPAG1 locus: alternative splicing produces multiple isoforms with distinct cytoskeletal linker domains, including predominant isoforms in neurons and muscles. *J. Cell Biol*. 154: 691-697
- Liu C. G.**, C. Maercker, M. J. Castanon, R. Hauptmann, G. Wiche. 1996. Human plectin: Organization of the gene, sequence analysis, and chromosome localization (8q24). *Proc. Natl. Acad. Sci*. 93: 4278 -4283



- Lunter P. C.** and G. Wiche. 2002. Direct binding of plectin to Fer kinase and negative regulation of its catalytic activity. *Biochem. Biophys. Res. Com.* 296: 904 – 910
- Määttä A.,** C. Ruhrberg, F. M. Watt. 2000. Structure and regulation of envoplakin gene. *J. Biol. Chem.* 275: 19857 – 19865
- MacKenzie S.,** I. Fleming, M. D. Housay, N. G. Anderson, E. Kilgour. 1997. Growth hormone and phorbol esters require specific protein kinase C isoforms to activate mitogen-activated proteins kinases in 3T3-F442A cells. *Biochem. J.* 324: 159 – 165
- Markowitz D.,** S. Goff, A. Bank. 1988. A safe packaging line for gene transfer: Separating viral genes on two different plasmids. *J. Virol.* 62: 1120 – 1124
- McLean W. H.,** L. Pulkkinen, F. J. Smith, E. L. Rugg, E. B. Lane, F. Bullrich, R. E. Burgeson, S. Amano, D. L. Hudson, K. Owaribe, J. A. Mc Grath, J. R. McMillan, R. A. Eady, I. M. Leigh, A. M. Christiano, J. Uitto. 1996. Loss of plectin causes epidermolysis bullosa with muscular dystrophy: cDNA cloning and genomic organization. *Genes & Dev.* 10: 1724- 1735
- Mellerio J. E.,** F. J. Smith, J. R. McMillan, W. H. McLean; J. A. McGrath, G. A. Morrison, P. Tierney, D. M. Albert, G. Wiche, I. M. Leigh, J. F. Geddes, E. B. Lane, J. Uitto, R. A. Eady. 1997. Recessive epidermolysis bullosa simplex associated with plectin mutations: infantile respiratory complications in two unrelated cases. *Br. J. Dermatol.* 137: 898 – 906
- Michell B. J.,** Z-P. Chen, T. Tiganis, D. Stapleton, F. Katsis, D. A. Power, A. T. Sim, B. E. Kemp. 2001. Coordinated control of endothelial nitric-oxide synthase phosphorylation by protein kinase C and the cAMP-dependent protein kinase. *J Biol Chem.* 276: 17625 – 17628
- Mundi D. I.,** T. Macheidt, Y. S. Ying, R. G. Anderson, G. S. Bloom. 2002. Dual control of caveolar membrane traffic by microtubules and the actin cytoskeleton. *J Cell Sci.* 115: 4327 – 4339
- Nakamura H.,** D. Sawamura, M. Goto, H. Nakamura, J. R. McMillan, S. Park, s. Kono, S. Hasegawa, S. Paku, T. Nakamura, Y. Ogiso, H. Shimizu. 2004. Epidermolysis bullosa simplex associated with pyloric atresia is a novel clinical subtype caused by mutations in the plectin gene (Plec1). *J. Mol. Diagn.* 7: 28 – 35
- Nakatsubo N.,** H. Kojima, K. Kikuchi, H. Nagoshi, Y. Hirata, D. Maeda, Y. Imai, T. Irimura, T. Nagano. 1998. Direct evidence of nitric oxide production from bovine aortic endothelial cells using new fluorescence indicators: diaminofluoreseins. *FEBS Lett.* 427: 263 – 266
- Nikolic B.,** E. Mac Nulty, B. Mir, G. Wiche. 1996. Basic amino acid residue cluster within nuclear targeting sequence motif is essential for cytoplasmic plectin-vimentin network junctions. *J. Cell Biol.* 134: 1455 – 1467
- Noria S.,** D. B. Cowan, A. I. Gotlieb, B. L. Langille. 1999. Transient and steady-state effects of shear stress on endothelial cell adherens junctions. *Circ. Res.* 85: 504 - 514.)
- Noria S.,** F. Xu, S. McCue, M. Jones, A. I. Gotlieb, B. L. Langille. 2004. Assembly and reorientation of stress fibers drives morphological changes to endothelial cells exposed to shear stress. *Am. J. Pathol.* 164: 1211 - 1223
- Osmanagic-Myers S.** and G. Wiche. 2004. Plectin-RACK1 (receptor of activated C kinase 1) scaffolding. *J. Biol. Chem.* 279: 18701 – 18710

- Osmanagic-Myers S.**, M. Gregor, G. Walko, G. Burgstaller, S. Reipert, G. Wiche. Plectin-controlled keratin cytoarchitecture affects MAP kinases involved in cellular stress response and migration. *J. Cell Biol.* 174: 557 – 568
- Partovian C.**, Z. Zhuang, K. Moodie, M. Lin, N. Ouchi, W. C. Sessa, K. Walsh, M. Simons. 2005. PKC activates eNOS and increases arterial blood flow in vivo. *Circ. Res.* 97: 482-487
- Räthel T. R.**, J. F. Leikert, A. M. Vollmar, V. M. Dirsch. 2003. Application of 4,5-diaminofluorescein to reliably measure nitric oxide released from endothelial cells in vitro. *Bio. Proced. Online.* 5: 136 – 142
- Reipert S.**, F. Steinböck, I. Fischer, R. E. Bittner, A. Zeöld, G. Wiche. 1999. Association of mitochondria with plectin and desmin intermediate filaments in striated muscle. *Exp. Cell Res.* 252: 479 – 491
- Rezniczek G. A.**, J. M. De Pereda, S. Reipert, G. Wiche. 1999. Linking Integrin  $\alpha_6\beta_4$ -based cell adhesion to the intermediate filament cytoskeleton: Direct interaction between the  $\beta_4$  subunit and plectin at multiple molecular sites. *J. Cell Biol.* 141: 209 – 225
- Rizzo V.**, C. Morton, N. DePaola, J. E. Schnitzer, P. F. Davies. 2003. Recruitment of endothelial caveolae into mechanotransduction pathways by flow conditioning in vitro. *J. Physiol. Heart Circ. Physiol.* 285: H1720 – H1729
- Rouan F.**, L. Pulkkinen, G. Meneguzzi, S. Laforgia, P. Hyde, D. U. Kim, G. Richard, J. Uitto. 2000. Epidermolysis bullosa: novel and de novo premature termination codon deletion mutations in the plectin gene predict late-onset muscular dystrophy. *J. Invest. Dermatol.* 114: 381 – 387
- Ruhrberg C.**, M. A. N. Hajibagheri, D. A. D. Parry, F. M. Watt. 1997. Periplakin, a novel component of cornified envelopes and desmosomes that belongs to the plakin family and forms complexes with envoplakin. *J. Cell Biol.* 139: 1835-1849
- Sadler J. E.** 1998. Biochemistry and genetics of von willebrand factor. *An. Rev. Biochem.* 67: 395-424
- Schmelz M.**, W. W. Franke. 1993. Complexus adhaerentes. A new group of desmoplakin-containing junctions in endothelial cells, the syndesmos connecting retothelial cells of lymph nodes. *Eur. J. Cell Biol.* 61, 274-289
- Shu-Ching S.**, A. Mullen, K. Abrams, D. Mukhopadhyay, K. P. Claffey. 1999. Role of protein kinase C isoforms in phorbol ester-induced vascular endothelial growth factor expression in human glioblastoma cells. *J. Biol. Chem.* 274: 15407 – 15414
- Slomianka L.** School of Anatomy and Human Biology - The University of Western Australia URL: <http://www.lab.anhb.uwa.edu.au/mb140/CorePages/Vascular/Images/VesWall.jpg>.
- Speidel C. C.** 1933. Studies of living nerves II. Activities of ameboid growth cones, sheath cells, and myelin segments, as revealed by prolonged observation of individual nerve fibers in frog tadpoles. *Am. J. Anat.* 52: 29–79
- Stappenbeck T. S.**, E. A. Bornslaeger, C. M. Corcoran, H. H. Luu, M. L. A. Virata, K. J. Green. 1993. Functional analysis of desmoplakin domains: Specification of the interaction with keratin versus vimentin intermediate filament networks. *J. Cell Biol.* 123: 691-705
- Steinböck F. A.**, B. Nikolic, P. A. Coulombe, E. Fuchs, P. Traub, G. Wiche. 2000. Dose-dependent linkage, assembly inhibition and disassembly of vimentin and cy-

- okeratin 5/14 filaments through plectin's intermediate filament-binding domain. *J. Cell Sci.* 113: 483 – 491
- Steinböck F. A.**, Wiche G. 1999. Plectin: a cytolinker by design. *J. Biol. Chem.* 380: 151 – 158
- Su Y.**, S. Edwards-Bennett, M. R. Bubb, E. R. Block. 2003. Regulation of endothelial nitric oxide synthase by the actin cytoskeleton. *Am. J. Physiol. Cell Physiol.* 284: C1542 – C1549
- Urkopec J. A.**, M. K. Hollinger, M. J. Woolkalis. 2002. Regulation of VE-Cadherin linkage to the cytoskeleton in endothelial cells exposed to fluid shear stress. *Exp. Cell Res.* 273: 240 – 247
- Venkiteswaran K.**, K. Xiao, S. Summers, C. C. Calkins, P. A. Vincent, K. Pumiglia, A. P. Kowalczyk. 2001. Regulation of endothelial barrier function and growth by VE-Cadherin, plakoglobin and  $\beta$ -catenin. *J. Physiol. Cell Physiol.* 283: C811 – C821
- Wyatt A. W.**, J. R. Steinert, G. E. Mann. 2004. Modulation of the L-arginine/nitric oxide signaling pathway in vascular endothelial cells. *Biochem. Soc. Symp.* 71: 143 – 156
- Wiche G.** and M. Baker. 1982. Cytoplasmic network arrays demonstrated by immunolocalization using antibodies to a high molecular weight proteins present in cytoskeletal preparations from cultured cell. *Exp. Cell Res.* 138: 15 – 29
- Wiche G.** 1998. Role of plectin in cytoskeleton organization and dynamics. *J. Cell Sci.* 111: 2477 – 2486
- Wiche G.**, B. Becker, K. Luber, G. Weitzer, M. J. Castanon, R. Hauptmann, C. Stratowa, M. Stewart. 1991. *J. Cell Biol.* 114: 83 – 99
- Williams R. L.**, S. A. Courtneidge, E. F. Wagner. 1988. Embryonic lethality and endothelial tumors in chimeric mice expressing polyoma virus middle T oncogene. *Cell.* 52: 121 – 131
- Yang Y.**, J. Dowling, Q. C. Yu, P. Kouklis, D. W. Cleveland, E. Fuchs. 1996. An essential cytoskeletal linker protein connecting actin microfilaments to intermediate filaments. *Cell.* 86: 655-665
- Zhang J.**, C. P. Baines, N. C. Zong, E. M. Cardwell, G. Wang, T. M. Vondriska, P. Ping. 2004. Functional proteomic analysis of a three tier PKC $\epsilon$ -Akt-eNOS signaling module in cardiac protection. *Am. J. Physiol. Heart Circ. Physiol.* doi: 10.1152/ajpheart.00756.2004

# CURRICULUM VITAE

## Daniela Halak

**Adresse** Forchtenau 202, 4971 Auroldmünster, Österreich  
**Geburtsdatum** 21.08.1983  
**Geburtsort** Ried im Innkreis, Österreich  
**Telefon** +43 - 650 - 58 54 760  
**E-mail** daniela.halak@univie.ac.at  
**Staatsbürgerschaft** Österreich

---

### AUSBILDUNG

Jänner 2007 – Diplomarbeit  
Plectin's role in cytoskeletal remodeling in endothelial cells  
Institut für molekulare Zellbiologie  
Leitung: Dr. Gerhard Wiche,  
Universität Wien, Österreich

Oktober 2002 - Diplomstudium der Molekularen Biologie  
Universität Wien, Österreich  
Schwerpunktfächer: Zellbiologie, Immunologie , Neurobio-  
logie

1994 – 2002 Matura  
Handelsakademie, Ried im Innkreis, Österreich

---